Design and Engineering of Low-Cost Centimeter-Scale Repeatable and Accurate Kinematic Fixtures for Nanomanufacturing Equipment Using Magnetic Preload and Potting

by

Adrienne Watral

S.M. Mechanical Engineering
Massachusetts Institute of Technology, 2010

Submitted to the Department of Mechanical Engineering
in Partial Fulfillment of the Requirements for the Degree of
Master of Science in Mechanical Engineering

at the

Massachusetts Institute of Technology

December 19, 2010
[February 2011]

Signature of Author.....
Department of Mechanical Engineering
December 19, 2010

Certified by.....
Martin L. Culpepper
Associate Professor of Mechanical Engineering
Thesis Supervisor

Accepted by.....
David E. Hardt
Professor of Mechanical Engineering
Graduate Officer

Design and Engineering of Low-Cost Centimeter-Scale Repeatable and Accurate Kinematic Fixtures for Nanomanufacturing Equipment Using Magnetic Preload and Potting

by

Adrienne Watral

Submitted to the Department of Mechanical Engineering
on December 19, 2010 in Partial Fulfillment of the
Requirements for the Degree of Master of Science in
Mechanical Engineering

ABSTRACT

This paper introduces a low-cost, centimeter-scale kinematic coupling fixture for use in nanomanufacturing equipment. The fixture uses magnetic circuit design techniques to optimize the magnetic preload required to achieve repeatability on the order of 100 nanometers. The fixture achieves accuracy to within one micrometer via an adjustable interface composed of UV curing adhesive between the mating kinematic coupling components. The fixture is monitored by a micro-vision system and moved by a six-axis nanopositioner until proper alignment is achieved, at which point the fixture position is permanently set by UV light. This thesis presents design rules and insights for design of a general accurate and repeatable kinematic fixture and presents a case study of fixtures used for tool exchange on dip pen nanolithography machines. A prototype fixturing assembly was fabricated and tested for repeatability and stability in six degrees of freedom. The test results concluded that the fixture has a 1-σ 3-D translational repeatability of 87 nanometers and a 3-D stability of 344 nanometers over 48 hours. This is an order of magnitude improvement on past low-cost accurate and repeatable fixture designs. This optimized accurate and repeatable kinematic fixture will enable repeatable, accurate, quick, and elegant tool change, thus advancing the manufacturing capabilities of nanofabrication techniques.

Thesis Supervisor: Martin L. Culpepper
Title: Associate Professor of Mechanical Engineering

ACKNOWLEDGEMENTS

First and foremost, I would like to thank my thesis advisor, Professor Martin Culpepper. He has been a wonderful mentor to me and has taught me mechanical design at a very deep level. I greatly appreciate all his help through the course of this thesis. Marty was supportive of me during a very difficult year and picked up my slack after I broke my back and was unable to do much hands-on work for a few months. Thanks for everything, Marty.

I would like to thank NanoInk for providing me the financial support for the first two semesters of my Master's program. NanoInk also provided the functional requirements and constraints for the project and allowed me to use their DPN 5000 machine on multiple occasions.

I would like to thank all of my friends and family who supported me during the course of my Master's program. Thanks to my fellow PCSL students, especially Maria Telleria. You were a great group of people to work with. I would like to thank my parents for their continual support for all of my endeavors.

I would like to thank Bill Buckley of the Laboratory for Manufacturing and Productivity for always being happy to help out in the machine shop.

Finally, I would like to thank Ian Wolfe. Ian has done more for me the past year and a half than anyone, and I would not have been able to finish this thesis without his love and support.

CONTENTS

Contents

FIGURES

TABLES

CHAPTER

1

INTRODUCTION

1.1 Introduction to Research

The purpose of this research was to generate the knowledge, technology, and methods required to engineer potted joints that yield cm-scale fixtures with 1 micron accuracy and 100 nanometer repeatability. This research includes the design and fabrication of an adjustable kinematic fixturing system, the construction of a micro vision system that identifies alignment errors in each fixture and automatically adjusts them for proper alignment, and the development of a specific UV cure potting process to permanently set the fixture in an accurate, calibrated, and stable position. Additionally, this thesis provides the general design rules and methods necessary to create small scale kinematic fixtures with desired accuracy and repeatability. Figure 1.1 shows the fabricated kinematic fixture, and Figure 1.2 shows an exploded CAD model.

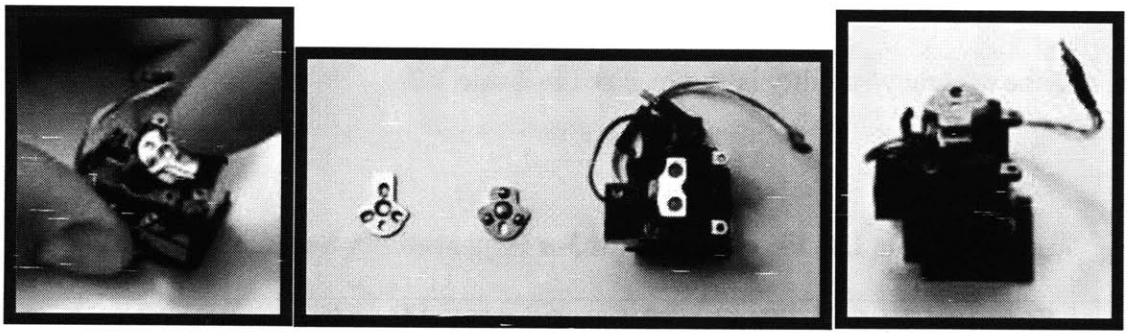

Figure 1.1: Accurate and repeatable kinematic fixture prototype mounted to a universal scanner mount of a DPN machine

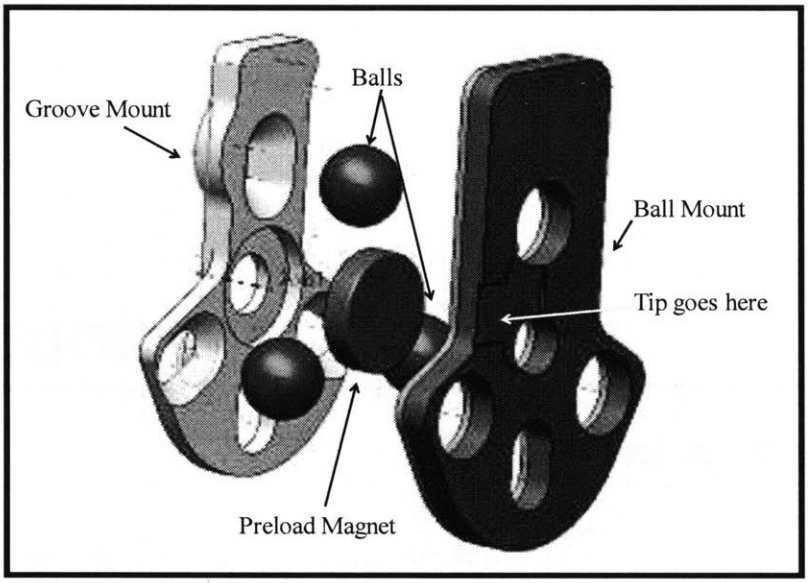

Figure 1.2: Accurate and repeatable kinematic fixture CAD model exploded view

The fixture was measured to have a 1- σ three-dimensional translational repeatability of 93 nanometers. The accuracy of the fixture was measured by a stability test since the fixture was individually calibrated and positioned; error in accuracy then come primarily from displacement of the adjustable fixture interface, which is measured by displacement over time. The stability of the fixture was monitored over a 48 hour time period and the total displacement after 48 hours was measured. The greatest error occurs in the z direction and was measured to be 876 nanometers. The fixture repeatability is summarized in Table 1.1 below, and the accuracy/stability is summarized in Table 1.2.

Table 1.1: Fixture 1-σ and 3-σ Repeatability Summary

	X(μm)	Y(μm)	Z(μm)	θ_x(μrad)	θ_y (μrad)	θ_z (μrad)	3D(μm)
σ	0.107	0.092	0.120	10.3	22.0	11.0	0.093
3σ	0.321	0.276	0.360	30.8	66.0	33.2	0.279

Table 1.2: Fixture 48-Hour Stability Summary

	X(μm)	Y(μm)	Z(μm)	θ_x(μrad)	θ_y (μrad)	θ_z (μrad)
Displacement after 48 hr	0.082	0.073	0.876	21.1	9.07	4.33

1.1.1 Motivation

This work is important because it allows for a low-cost means to align parts and tools in instruments and equipment for nano-scale research and nanomanufacturing. Reliability, rate, cost, quality, and flexibility of a manufacturing process depends on the ability to effectively position tools and parts with the exact location of such tools and parts being known. Fixturing technology enables a fabrication process to become a manufacturing process by enabling rapid, frequent positioning and part and tool changeovers. Accurate, repeatable, and quick interchange of parts within various nanomanufacturing systems is important, as it allows for improved alignment and positioning of parts and tools with respect to relevant equipment, thus improving reliability, rate, quality, cost, and flexibility.

In order to practice lean manufacturing, a manufacturing business must be able to rapidly and accurately changeover machines and equipment. The most effective way of doing this is by reducing machine set-up time. Indexable tools and fixturing technologies have greatly simplified and improved the changeover process (1).

Upcoming manufacturing processes at the small scale require fixturing capabilities that are beyond the limits of conventional coupling methods. Achieving better precision at a lower cost

has posed a challenge, and so far there is not a fixturing system that can achieve the strict repeatability requirements that small-scale manufacturing processes call for. Various mechanical couplings exist with their distinct advantages and disadvantages compared later in this chapter; however, none of these couplings sufficiently meet all of the requirements of nanomanufacturing processes on their own. Thus a new fixturing technology is necessary.

The impact of this research is a general technology that improves (i) rate, cost, quality, and flexibility in nanomanufacturing & (ii) quality and speed of measurement in instruments and research. The impact of this research will be to fill the fundamental gap – fixturing technology – that would block the adaptation of small scale fabrication equipment to manufacturing applications. Additionally, this fixturing technology will improve rate and reliability in current low volume fabrication processes, therefore advancing research in the area of small-scale manufacturing.

The specific fixturing technology developed in this thesis, shown in Figure 1.1, was built to be integrated into a dip pen nanolithography (DPN) machine. The fixture is used on the machine to enable rapid accurate and repeatable tool placement and exchange. Chapter 5 presents a case study which evaluates the need for the fixture in the current DPN tool changing process, lays out the specific customer requirements for the fixture in combination with the machine, as well as detailing the use of the fixture with the DPN machine.

Past research has been done with the goal of accurate and repeatable kinematic fixtures (see Chapter 1.3), however the solution of this research is unique. The accuracy and repeatability of

the fixture designed in this thesis are achieved via the distinct combination of potting and magnetic preload, which will be discussed in detail in Chapters 3 and 4, respectively.

Achieving accuracy with a kinematic coupling requires calibration. The calibration will be achieved by the design and fabrication of a micro-vision and micropositioning system that will allow for errors between actual and desired probe tip position to be identified and corrected. After adjusting any misalignment, the fixture will be permanently set by a UV-curing epoxy in an accurate, stable, and calibrated position. An accurate and repeatable alignment and fixturing system allows for improvements in rate, quality, and reliability of accurately attaching tools to relevant equipment. It also establishes limits for alignment capacity, as well as accuracy and repeatability limits for tool change fixtures. Additionally, this research helps determine a relationship between fixture design, added cost, quality of alignment, and tool change rate. The general kinematic coupling fixturing design can be used to generate custom fixtures, calibration equipment, and calibration processes. Such a fixturing system will advance the automation in small scale manufacturing processes, thus leading to benefits in cost, rate, quality, and flexibility.

In addition to solving the problem of accuracy in kinematic couplings, this research is also unique in that the kinematic fixtures designed are at a small scale. Research in fixture design at the small scale must be directed toward the inherent differences in the engineering science and implementation at the small scale from those at the macro scale. Large-scale principles and practices do not necessarily work at the small scale due to differences in the dominant physics, thermal and material considerations, and manufacturing capabilities. Due to these differences, there must be a shift in the way machines and processes are thought about at the small scale,

including the engineering design principles and analysis, as well as the practical manufacturing and use considerations.

In order for a manufacturing process to succeed it is necessary to be able to move tools and relevant equipment with respect to each other and to know their exact location. This requires highly repeatable precision fixturing technologies. In large-scale machine design, the engineering and physics are well-known; however, very few precision engineers work on the engineering principles and practices at the small scale, thus current fixturing technologies are not sufficient for small-scale machines and processes. In order to progress in the field of small-scale manufacturing, further knowledge about the differences between large and small-scale machines is required. This includes investigation into the differences in the dominant physics at the micro and nano scales from the macro scale, fabrication and manufacturing considerations, as well as concerns arising from thermal variations. Large-scale design principles cannot necessarily be applied to small-scale machines. This research provides insight and design rules pertaining to how to design fixtures for small-scale processes, allowing the reader to better understand the philosophical and practical differences between large and small-scale design.

The fixturing technology developed in this thesis can be implemented in a variety of small-scale fabrication or manufacturing systems as a method of improving rate, quality, cost, and flexibility. This thesis is based on a fixture designed for use in DPN, which is currently a low-volume fabrication process. The addition of accurate and repeatable fixturing technology allows the possibility for DPN to become a high-volume manufacturing process.

1.2 Thesis Organization

The first chapter in this thesis provides the reader with a brief history and comparison of common mechanical fixturing methods. This is important information for selecting the best method for the small scale accurate and repeatable fixtures developed in this thesis. The second chapter introduces the reader to the dip pen nanolithography process that these fixtures were designed to work with, as well as detailing the need for a new fixturing method. Chapter two goes on to describe the design requirements of the fixture and how these were met and an overview of the kinematic fixture design. The third chapter addresses the importance of repeatability and how repeatability is achieved in this fixture via exact constraint design, magnetic preload, and manufacturing techniques for surface finish. The fourth chapter discusses the need for accuracy and how potting can be used to achieve accuracy on the order of 1 micron. Chapter 4 discusses the chemistry and curing process of the adhesive used in the potting and the characteristics based upon which it was selected as a method of achieving accuracy. The fifth chapter presents a case study of the fixture that was designed specifically for use with NanoInk's DPN machines as a method of improving rate and reliability in low to moderate volume DPN experiments. Chapter 5 also provides the reader with validation of the fixture design with repeatability and stability testing results. The thesis concludes with a discussion of future work and future applications.

1.3 Knowledge and Technology Gap

Many methods of alignment and fixturing exist, all with various advantages and disadvantages. None of which by themselves are sufficient to meet the requirements of accuracy and repeatability in small scale manufacturing applications. The following section discusses a number of these fixturing techniques, including design principles, how they work, and potential benefits as well as shortcomings in the category of accurate and repeatable fixturing for small scale manufacturing.

1.3.1 Comparison of Common Fixturing Methods

The pin-in-hole alignment method is a non-exact constraint method frequently used for low-cost and easy alignment. Two parts are mated together by pins that fit into corresponding holes or slots. Though the pin-in-hole method is simple and low-cost, it is not sufficient for precision fixturing. These joints are generally sized on the order of inches, with repeatability on the order of tens of microns (2) (3) (4). The performance of pin-in-hole joints is unpredictable, as it is dependent on a number of geometric variables, including the diameters, straightness, parallelism, cylindricity, and distance between the pins and holes. If clearance exists between the diameter of the pin and hole, the location of each component relative to the other is not exactly defined, thus reducing the repeatability. For precision applications, this clearance has to be strictly controlled, thus leading to additional manufacturing costs and increased difficulty in assembly. Pin-in-hole joints are highly susceptible to wedging and jamming, leading to increased assembly time and

damaged parts, thus reducing productivity and increasing costs. The pin-in-hole approach is non-deterministic and repeatability and stiffness are difficult to analyze or predict, so these parameters must be measured experimentally. There are many drawbacks to the pin-in-hole method: tight manufacturing tolerances, binding and jamming, holes slightly larger than pins reduces repeatability and stiffness (2).

Elastic averaging is another common alignment method. Common fixturing methods based on elastic averaging include tapers, rail and slots, collets, and press fits. This method is useful in applications that require high joint stiffness and load capacity and well as in applications where sealing interfaces are necessary. Elastic averaging is based on geometrically over-constraining the mating parts. This over-constraint leads to problems with repeatability, specifically that the tight fit is usually disrupted after repeated use as the surface wears away. Thus repeatability decreases with increased use and surface wear (3).

Kinematic couplings are a reliable, simple, and inexpensive means of linking systems with high repeatability. The design of a kinematic coupling is deterministic in that for every degree of freedom to be constrained there is a point of contact (4) (5) (6) (7). The potential for repeatability on the order of tens of nanometers makes the kinematic coupling a principal candidate for precision applications. Traditionally, kinematic couplings have been made with three balls that contact six points which restrict motion in six degrees of freedom. These contact points can either be in the form of three grooves or one groove, one tetrahedral socket, and one flat surface. These six contact points create high Hertzian stresses at each point, so care must be taken to

ensure that the contact surfaces can withstand the high stresses and to prevent brinelling beneath the surface of the contacts. A traditional kinematic coupling is shown in Figure 1.3 (4).

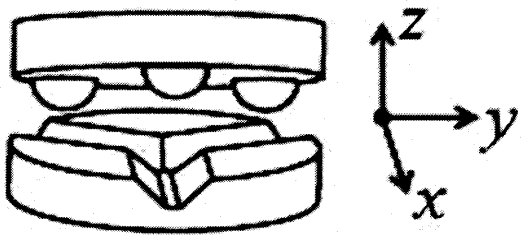

Figure 1.3: Traditional three groove kinematic coupling

The traditional passive kinematic coupling can be modified to enable certain performance characteristics. These modifications include the compliant kinematic coupling, which uses compliant members, i.e. flexures or cantilevers, to allow for controlled motion in specific degrees of freedom. The compliant kinematic coupling is not economical in high volume due to the cost of manufacture and assembly of the compliant members. They have shown to be repeatable to approximately 5 microns (4) (5).

Quasi-kinematic couplings bring an elastic averaging approach to kinematic couplings. Instead of spheres mating with grooves, a quasi-kinematic coupling consists of three convex elements that fit into three corresponding concave elements, thus creating six arcs of contact rather than six points of contact that are present in a kinematic coupling. Since they are not exact constraint mechanisms, they can only achieve repeatability on the order of 250 nanometers (3).

Active kinematic couplings have been made by adding adjustable components to either the balls or the grooves to actively control the position of the coupling elements. This active position control allows for accuracy as well as repeatability (8) (9). A major drawback to active kinematic couplings is that the position control elements are expensive to manufacture. Additionally, the active components reduce the repeatability of the coupling to approximately 1 micron. Therefore, in applications where better than 100 nanometer repeatability is desired, the performance of the active kinematic coupling is not sufficient.

One of the major risks to using kinematic couplings in small-scale precision processes is that friction has a large negative impact on repeatability (6). Reducing the impact of friction has a great effect on improving the repeatability of the coupling. The effect of friction is reduced by lubrication, cleansing of surfaces, improved surface finish, or modification of the contacting components, for example adding elastic hinges to the grooves (5), though this increases manufacturing time and reduces joint stiffness.

Kinematic couplings have traditionally been used in macro-scale manufacturing, and the design and performance of small-scale kinematic couplings has not been studied in detail at this point. The average kinematic coupling is repeatable to approximately 500 nanometers, with repeatability to 100s of nanometers observed with best practices (4) (5). However, additional research is necessary to meet the 100 nanometer repeatability requirement for certain nanomanufacturing processes. The discussed fixturing mechanisms are compared in terms of achievable repeatability and relative cost in Figure 1.4.

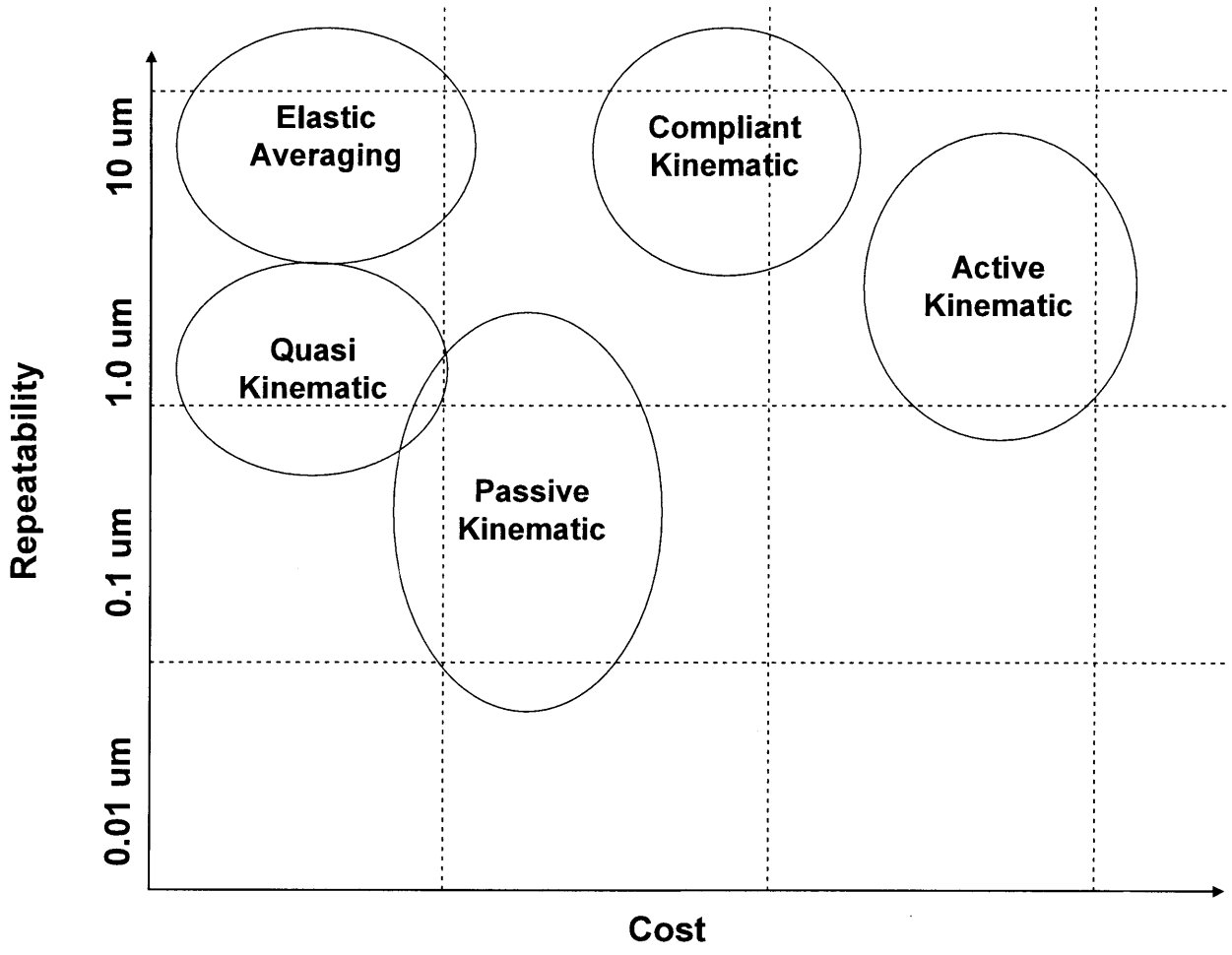

Figure 1.4: Cost vs. repeatability comparison of coupling technologies

1.3.2 Historical Perspective on Accurate and Repeatable Fixturing

Kinematic couplings are frequently used in applications where repeatable fixturing is necessary due to their potential for high repeatability with low cost. General design guidelines have been developed for standard kinematic couplings (7) (10) (6). A common area of interest in kinematic coupling research involves improving the achievable repeatability. KC repeatability may be improved by adding flexural elements to the ball (11) or groove (5) surfaces. Flexures have been

shown to improve the repeatability of a KC by a factor of 10. A flexure-enabled KC is shown in Figure 1.5, with flexures added to the ball side of the KC. This design was measured to have a repeatability of approximately 35 nm. The repeatability of a KC is also affected by friction at the contact interface. The effects of friction on repeatability have been studied (12), and it has been proven that reducing friction at the coupling interface improves repeatability of the KC.

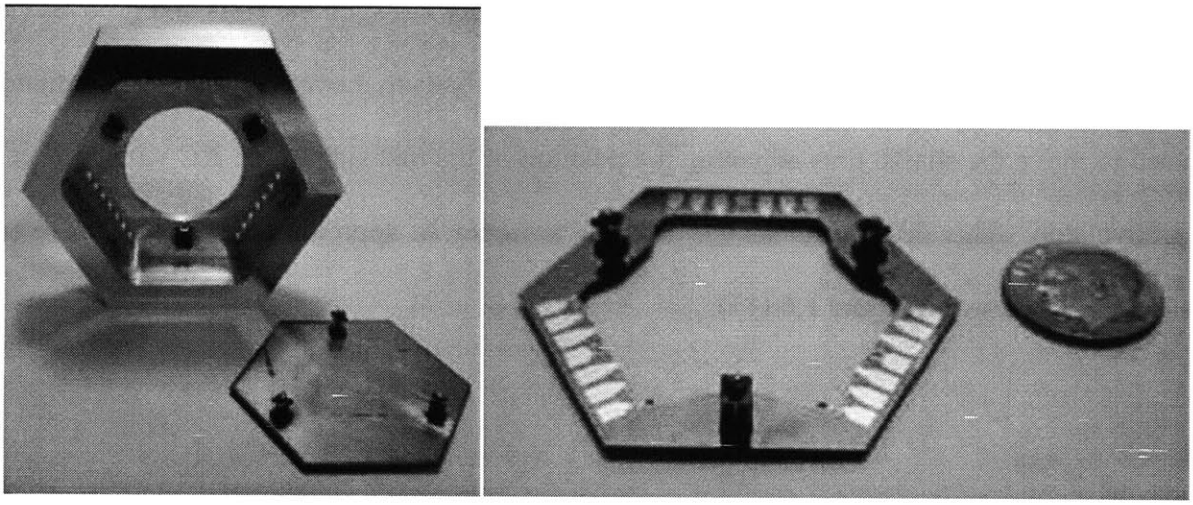

(a) (b)

Figure 1.5: KC modified with flexural hinges on the ball side to improve the repeatability by reducing friction. The entire KC is shown in (a), and a close up of the ball flexures are shown in (b).

Achieving accuracy is not a problem a traditional kinematic coupling can solve. The traditional KC design guidelines have been modified in order to design KCs with an accuracy requirement. Achieving accuracy with a KC requires calibration. Taylor and Tu developed an accurate and repeatable micropositioning stage based on the KC that uses 2-D motion control for accurate

positioning (8). The most advanced micropositioning units are capable of position control to 1 nanometer by using piezoelectric stacks. The KC based micropositioning system consists of a base plate with 3 vee-grooves and 3 balls on the other half. One of the balls is fixed while the other two are maneuverable within slots via linear actuators. This particular system is applicable to light load applications in microelectronics manufacturing. However, this method is expensive and therefore cost-prohibitive for manufacturing applications.

Accurate KCs have been designed via an adjustable interface between the balls and grooves (13) (14), where the balls are attached to a shaft that allows the balls to move eccentrically. Actuators are used to move the shafts, thus adjusting the position of the ball side of the KC with respect to the groove side. This design has shown to allow accuracy to approximately 2-3 micrometers. This method is shown in Figure 1.6 (15).

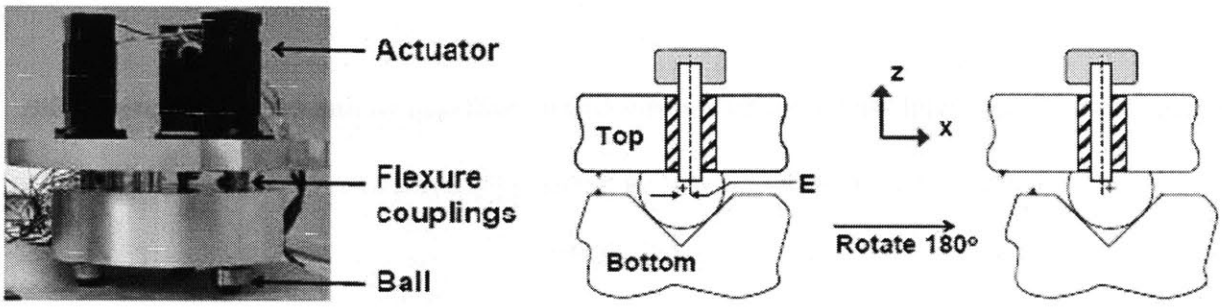

(a) **(b)**

Figure 1.6: a. Prototype (groove side removed for clarity). b. Adjustable KC joint

1.4 Chapter Summary

The fixtures designed in this thesis are to be used for tool changing of dip pen nanolithography machines. The functional requirements and constraints of these fixtures are presented in Table 1.3.

Table 1.3: Functional Requirements and Constraints

Probe tip placement accuracy	1000	nm
Fixture centroid repeatability	100	nm
System incremental cost per probe or tool	50	$
Fixture load capacity	1	N
Fixture change-out time	15	s
Calibration time	60	s

The functional requirements and constraints are difficult to achieve by the common fixturing methods described earlier in this chapter. Pin-in-hole alignment does not meet the cost requirements due to the tight manufacturing tolerances that would be necessary to meet the repeatability requirements, does not meet the accuracy or repeatability requirements due to the unpredictable performance due to clearance and straightness errors in manufacturing, and does not meet the size constraints necessary to be used on nanomanufacturing equipment.

Elastic averaging does not meet the repeatability requirements due to the geometric over-constraint that the elastic averaging method is based on. Traditional kinematic couplings have the most promise of historical fixturing methods in achieving all of the functional requirements and constraints but still do not meet the accuracy or repeatability requirements. Quasi-kinematic

couplings do not meet the repeatability requirements due to their elastic averaging aspect and the fact that they are not exact constraint mechanisms. Active kinematic couplings do not meet the cost requirement since they require expensive position control elements, and they are not as repeatable as necessary due to these active components.

Not only is there a need for improved fixturing technologies at the small scale, but there is also a need for a low cost fixturing technology that embodies accuracy as well as repeatability. Kinematic couplings have the most promise of currently available fixturing techniques with respect to being able to achieve the repeatability required to make high precision products at the small scale; however, the kinematic couplings available to date are not sufficient for applications that require accuracy. The accurate and repeatable kinematic fixture developed in this thesis satisfies the needs for accuracy, repeatability, and low cost that are important for small scale manufacturing processes.

Kinematic couplings are inherently repeatable but not accurate. Repeatability is important for precision fixtures, but not sufficient for all applications. Kinematic couplings have been used for years in applications requiring precision fixturing, and numerous methods for improving the functionality of kinematic couplings have been studied, though this research is the first to achieve repeatability on the order of 100 nanometers and accuracy on the order of a single micron using the low cost methods of magnetic preload and potting used in this thesis. Additionally, all of the research that has been done on achieving accuracy and high repeatability with kinematic couplings has been on large scale devices and most use costly methods. The focus of this thesis is low-cost, small-scale fixtures that are both accurate and repeatable.

CHAPTER

2

DESIGN REQUIREMENTS

2.1 Dip Pen Nanolithography

Dip Pen Nanolithography (DPN) is a method of nanofabrication in which materials are deposited onto a solid-state substrate through an atomic force microscope (AFM) tip. It can be thought of as the nano-scale equivalent of a quill pen, in which the AFM tip acts as the "pen," which is coated with a chemical compound acting as the "ink," which is delivered to the substrate, the "paper," via capillary transport (16). A schematic representation of DPN is illustrated in Figure 2.1 below.

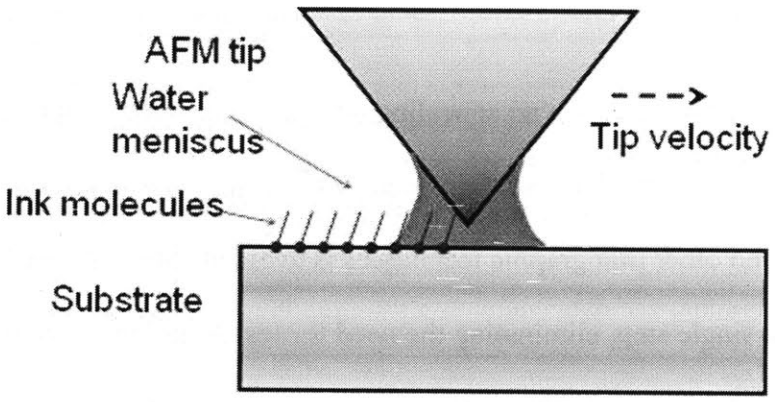

Figure 2.1: DPN Schematic: molecules are transported from the AFM tip to the substrate via capillary transport

DPN can be used for drug printing, customized drug delivery, creating nanostructures relevant to current technology, as well as for a variety of experimental processes in surface patterning and parallel writing. DPN is a flexible process as far as nanofabrication goes and has many features that make it appealing for nanomanufacturing, including resolution, speed, material flexibility, and cost. The features and highlights of DPN are summarized in Table 2.1 below.

Table 2.1: DPN Features and Highlights

Resolution	• Writes features as small as 14 nm • Reads features as small as 1 nm
Material Flexibility	• Wide range of inks can be deposited onto wide range of surfaces
Speed	• Scalable speed allowed by multiple tip arrays • Most time spent on set-up and tool changing
Cost	• Low start up and maintenance costs
Multiplexing	• Multiple inks may be deposited onto the same substrate
Operation Space	• Operates in ambient conditions • Isolation chamber for humidity and temperature control • No clean room needed

The above features of DPN make it an appealing alternative to standard lithographic techniques. A clean room is not necessary for operation because the risk of contamination that exists in photolithography and other lithographic techniques is avoided. DPN allows the creation of nanostructures in a single step, eliminating the need for resists and multiple time consuming processes. DPN can achieve very high resolution features, with linewidths as small as 14 nm and imaging down to 1 nm possible (17). One of the most unique characteristics of DPN is that the

same device is used to both read and write a pattern, so patterns of multiple inks can be formed or aligned on the same substrate.

The ability of DPN to achieve such high resolution depends of proper alignment of the tip. If the tip is not correctly aligned the written features will not be positioned accurately with respect to the substrate or accompanying features. Aligning the tip is currently a difficult and time consuming process; the majority of the time spent using the machine is spent on tip alignment in the initial setup of the machine and tip alignment during tool changes. The addition of an accurate and repeatable tool fixture will eliminate much of the setup time, therefore greatly improving the rate and reliability of the process.

The current tip mounting process used by NanoInk, a company that builds and sells DPN machines, for their machines is time consuming and involved. The goal of the kinematic fixture is to reduce the time and effort required to mount the tips in addition to improving the accuracy and repeatability of the tip position. Preparing the tip for proper alignment involves first mounting the tip into a probe holder that positions the tip in the correct orientation with the DPN machine and holds the tip in place while DPN operations are performed. If the tip is not properly mounted in the probe holder the success of the DPN operation is compromised. The probe holder is shown in Figure 2.2.

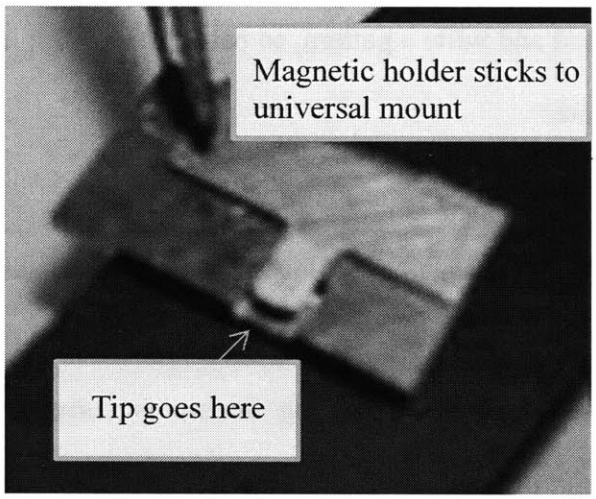

Figure 2.2: Probe holder used for positioning the tip onto the DPN machine

A mounting block is used to facilitate the process of mounting the tip in the holder. The mounting block includes a flat indent the probe holder fits into as well as an alignment area where the tip is aligned to the probe holder. The mounting block is shown with the cover in both the open and closed positions in Figure 2.3.

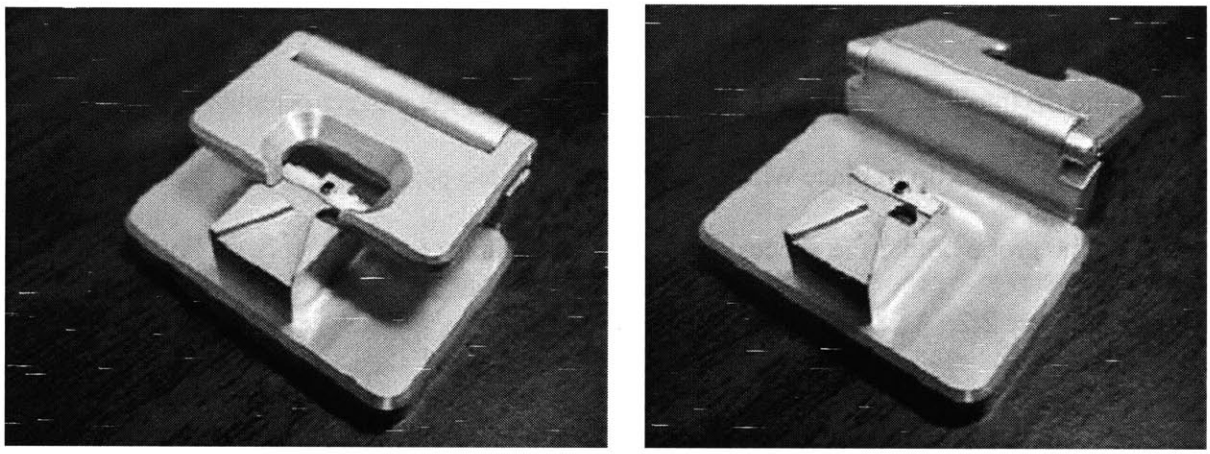

(a) **(b)**

Figure 2.3: Mounting block used for securing tip into probe holder in closed (a) and open (b) positions

The probe holder is first inserted into the mounting block and secured by pressing the cover closed. Then the tip is placed on the mounting block and lined up by eye to the center of the probe holder. The tip is sandwiched into the probe holder and held in place. Figure 2.4 shows the tip being inserted into the probe holder.

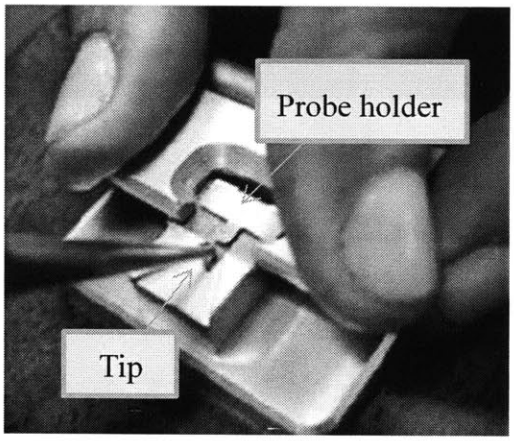

Figure 2.4: Mounting of tip into probe holder

Once the tip is mounted in the probe holder, it must be installed onto the DPN machine. The probe holder attaches to the machine scanner head assembly via the two small magnets. The alignment is done by lining up the flat sides of the probe holder with the two flat alignment guides on the scanner head assembly universal mount. The universal mount is shown in Figure 2.5.

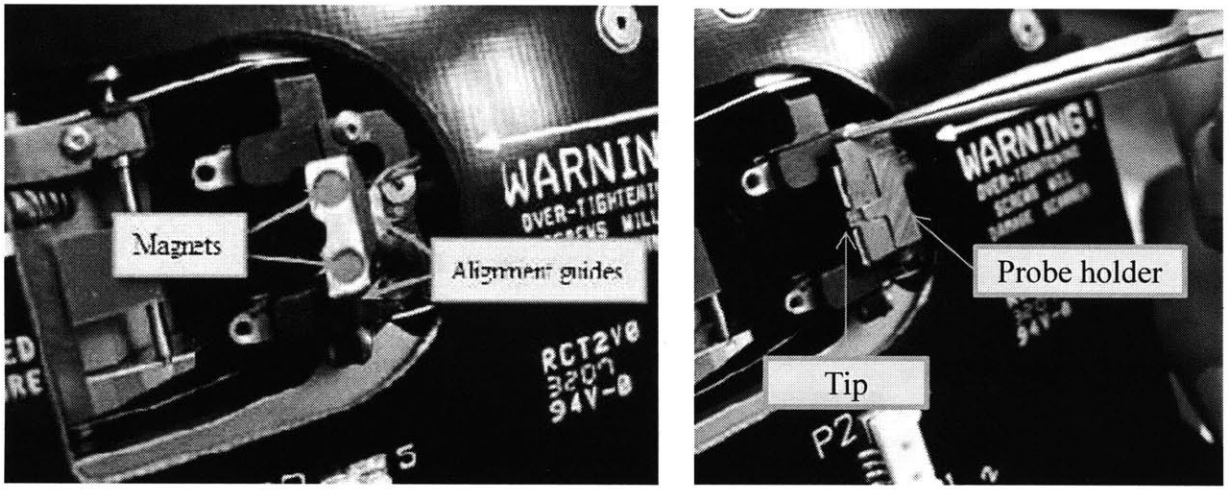

(a) (b)

Figure 2.5: Universal mount on DPN machine, used for alignment of tip assembly. Magnets and alignment guides are shown (a) as well as the tip assembly placement (b)

After mounting the tip into the probe holder and mounting the probe holder to the machine, the tip must be aligned with respect to the machine. Currently a laser is used to align the tip. The tip is moved around very slowly, three microns at a time until the tip is located by the laser. This process can take approximately 45 minutes of repetitively moving the tip. The objective of the accurate and repeatable kinematic fixture is to eliminate the probe holder and the process of laser alignment for each tip. The groove side of the fixture will be mounted directly to the machine, and the tip will be mounted directly to the ball side of the fixture, so the tip will be accurately and repeatably located by the fixture to the machine.

An accurate and repeatable kinematic fixture would allow for the tip to be placed in a matter of seconds with accuracy and precision, thus removing the need for the current arduous and time consuming alignment process.

2.2 Design Requirements

The design requirements are defined foremost by understanding the problem and the need for accurate and repeatable fixturing. The problem is that small-scale fabrication processes do not meet the requirements in rate, quality, cost, and flexibility in order to become manufacturing processes. Current fixturing technologies allow for high repeatability at low cost at the large scale, but have not yet met accuracy, repeatability, and cost requirements for small-scale processes.

Specific functional requirements and constraints of the fixtures designed in this thesis were defined by the customer for a specific application, DPN. These requirements include accuracy of the probe tip location, repeatability of the fixture centroid, incremental cost of the system per probe or tool, fixture load capacity, tool change out time, and fixture size or envelope. The functional requirements and constraints for the fixture for DPN applications are summarized in Table 2.2.

Table 2.2: Functional Requirements and Constraints

Probe tip placement accuracy	1000	nm
Fixture centroid repeatability	100	nm
System incremental cost per probe or tool	50	$
Fixture load capacity	1	N
Fixture change-out time	15	s
Calibration time	60	s
Fixture envelope	1.5 x 1.5 x ¼	cm^3

The functional requirements and constraints allow the fixturing technology to be easily adapted into standard DPN machines and other nanomanufacturing equipment. The accuracy and repeatability requirements ensure accurate and repeatable tool placement, thus greatly reducing tool change-out time and improving the overall rate of the process. It is important to achieve a balance of cost and performance with this fixture design; it is not necessary to design the most repeatable KC ever made, but it is necessary to have a low-cost fixture that meets the performance requirements as well as the cost requirements. The fixture envelope is also important, as customers are not likely to use a fixture on their machines if they must reconfigure the whole machine in order to allow space for the fixture. Most nanomanufacturing equipment does not have significant free space in which to add additional elements, so it is important to keep envelope in mind when designing a fixture.

2.3 Kinematic Fixtures: General Concept

The fixtures in this thesis were designed to be accurate and repeatable. The repeatability is achieved via exact constraint design methods, and the accuracy is achieved via calibration. The fixture is a traditional three ball, three groove passive kinematic coupling. The fixture is shown in Figure 2.6. The groove side mounts to the desired equipment, and the tool is mounted to the ball side, thus repeatably and accurately attaching the tool to the machine.

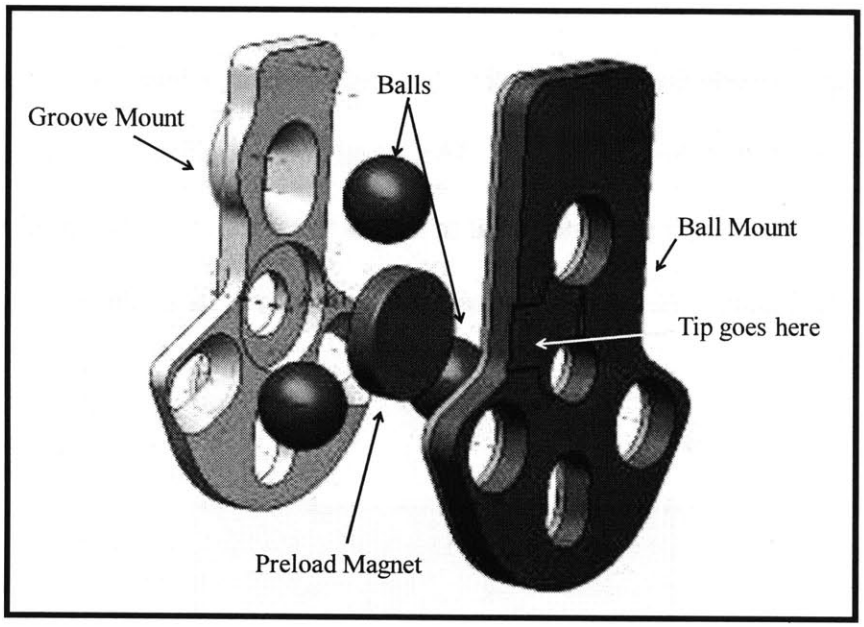

Figure 2.6: Accurate and repeatable kinematic fixture CAD model exploded view

The calibration is achieved by an adjustable interface on the ball side of the kinematic coupling. The ball side of the fixture includes three holes for the balls to be placed into. The three holes are 152.4 micrometers larger than the balls, allowing the position of each ball to be adjusted within the constraints of the hole. The ball side of the KC is shown in Figure 2.7.

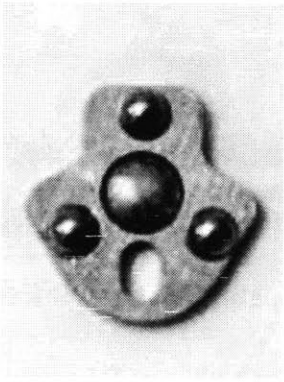

Figure 2.7: Ball side of the KC, showing the clearance between the balls and the holes to allow for position adjustment

After the balls are set into the oversized holes, the holes are filled with a UV curing epoxy, which fills the gap between the ball and hole. This epoxy is in a liquid state until subjected to UV light, at which point it becomes solid. The kinematic coupling is set up on an assembly station that includes a microvision system that monitors the position of the coupling. The fixture assembly station, including the vision system, nanopositioner, and ultraviolet light set-up is shown in Figure 2.8.

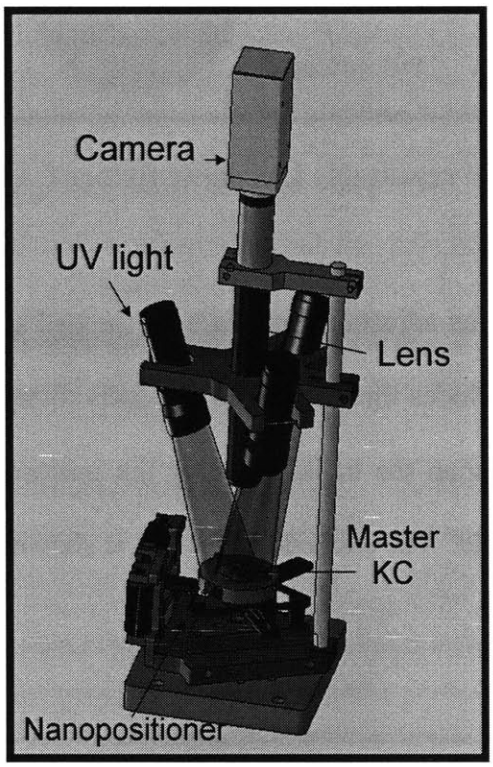

Figure 2.8: Assembly station CAD model, including vision system, nanopositioner, UV lights, and master KC fixture

The vision system is used to measure the error in position of the kinematic coupling and informs a nanopositioner of that error. The nanopositioner is then instructed to correct for the error in alignment, at which point the vision system is used to verify the corrected position of the

coupling. Once the alignment is correct, the area is flooded with UV lights and the position of the balls is set in the UV cure epoxy. This allows accuracy while taking advantage of the passive KC's repeatability characteristics.

CHAPTER

3

REPEATABILITY

3.1 Definition and Importance of Repeatability

Repeatability is a measure of variation among repeated measurements. Though repeatability and accuracy are often thought to have the same meaning, they have very different meanings in the context of precision engineering. Measurements are accurate when they agree with the true value of the quantity being measured. They are repeatable when individual measurements of the same quantity agree. A measurement is accurate only if the measurement is correct. A measurement is repeatable if the results are essentially the same each time a measurement is made. Measurements are therefore repeatable, but not necessarily accurate, when they are reproducible.

Figure 3.1 (4) below illustrates an analogy explaining repeatability and accuracy using targets. Accuracy is a measure of how close the arrow comes to the center of the target, and repeatability is a measure of how tightly the arrows are clustered together.

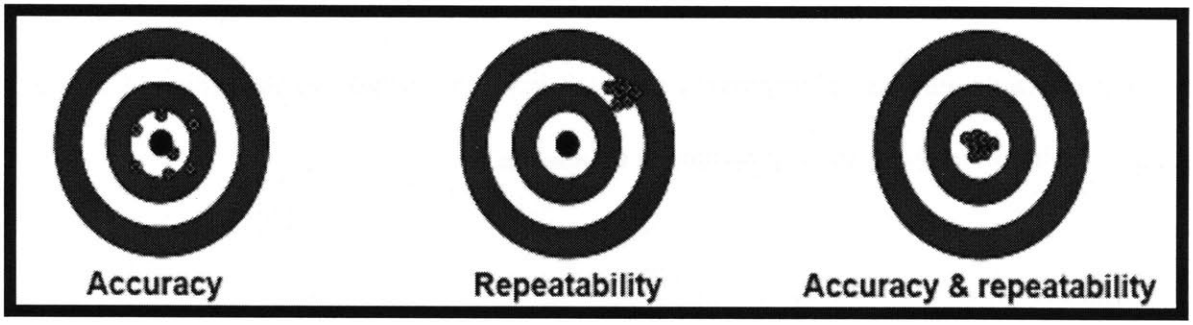

Figure 3.1: Target analogy for repeatability and accuracy

Repeatability is especially important in small-scale manufacturing for tool changing and part locating. It is necessary to know the exact location of your tool and part. As the repeatability of the system improves, so does the likelihood that you know the location of the tool and part.

Repeatability of tool placement requires a repeatable coupling interface. Common coupling methods include elastic averaging, passive kinematic couplings, active kinematic couplings, compliant kinematic couplings, and quasi-kinematic couplings. These mechanisms are discussed in detail in Chapter 1. Typical alignment mechanisms are compared in Figure 3.2 (3) in terms of cost and achievable repeatability. Kinematic couplings are inherently highly repeatable due to their exact constraint design; the number of constraints is equal to the number of degrees of freedom constrained. However, repeatability within 500 nanometers is extremely difficult to achieve with a traditional passive kinematic coupling design due to friction, surface finish, stability of materials, and compliance errors. Friction between the contact surfaces is the most significant contributor to nonrepeatability, which can be minimized by improving surface finish at the coupling interface, adding flexures to the coupling interface, or by changing the groove angle. Improving repeatability is a common research interest in the field of fixture design,

specifically in kinematic couplings. In addition to reducing friction at the coupling interface, one of the most effective methods of improving repeatability is by increasing the preload force on the coupling. Preload will be discussed further in Chapter 3.2.

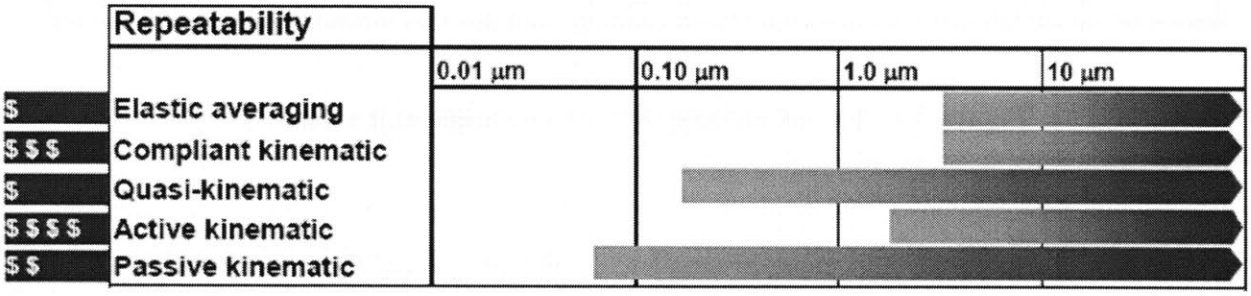

Figure 3.2: Cost and repeatability comparison for alignment mechanisms

With two major functional requirements being repeatability and cost, the fixture design was based on the passive kinematic coupling. The $50 incremental system cost per tool specified in the functional requirements discussed in the previous chapter is possible with a passive kinematic coupling design. The 100 nanometer repeatability requirement proves to be a more difficult problem. With a standard passive kinematic coupling design, it is customary to achieve repeatability of approximately 500 nm. The customer requirements of this fixture demanded an improvement of one order of magnitude on previously available kinematic coupling designs.

3.2 Kinematic Coupling Design

The functional requirements of a kinematic coupling are as follows:

- it connects two parts or assemblies
- can be separated and rejoined on demand
- fine repeatability
- some level of accuracy
- some level of stiffness
- is cost appropriate

The intrinsic flaws of kinematic couplings are that they (i) can have high stress concentrations at the contact points, (ii) do not permit sealed joints, and (iii) usually offer moderate stiffness and load capacity.

The first design to consider is a three-ball, three-groove design, shown in Figure 3.3 (13). The advantages of the three-groove design are that it is symmetric and therefore more evenly distributes the contact forces and is also less expensive and easier to manufacture. This design allows for better centering and is not sensitive to thermal expansion, as it tends to expand about a center point. Its disadvantages are that the six point contacts create high stress concentrations and this design usually has low stiffness and load carrying capacity in comparison to other designs.

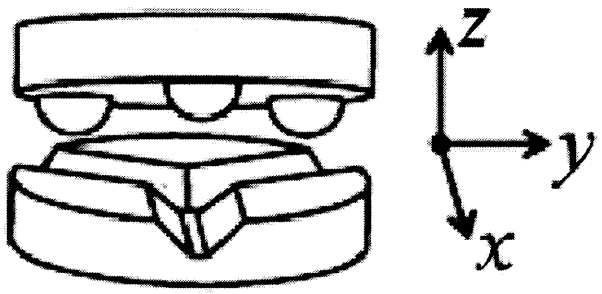

Figure 3.3: Three-groove kinematic coupling

The three-groove design may be compared with the Kelvin model: a tetrahedral socket, groove, and flat, as shown in Figure 3.4 (4). The tetrahedral socket of this model adds a natural pivot point for angular adjustment, but it still contains six contact points, therefore still incorporating the same high stress concentrations. For high cycle applications it is best to use hardened corrosion resistant materials (e.g., ceramics or hardened steel) for contact surfaces to prevent nonrepeatability due to high contact stresses. Countermeasures to the high stress concentrations and low stiffness and load capacity in both the three-groove and the tetrahedral-groove-flat designs include modifying the point contacts so they become line contacts (for example, turning the tetrahedral socket into a conical socket) or by increasing the area of contact by substituting gothic arches for the grooves or canoe-shaped balls for the traditional spheres.

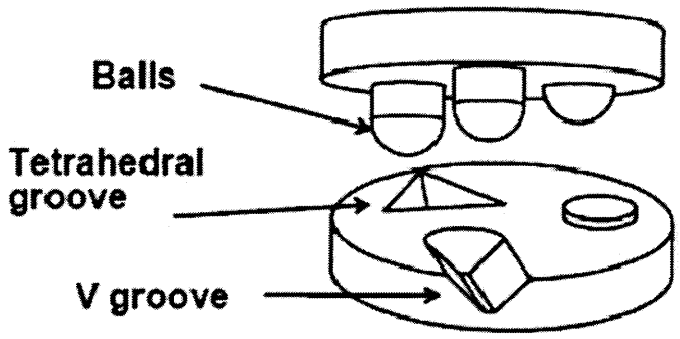

Figure 3.4: Kelvin kinematic coupling

The symmetry inherent in a three-groove KC model aids in reducing manufacturing costs, and the use of grooves for all contact regions minimizes the overall stress state in the KC; therefore it is generally best to use a three-groove design for fixturing applications. Once the basic KC ball and groove layout is determined, the orientation of the grooves must be optimized. In order to guarantee stability in a 3-groove kinematic coupling, the normal vectors to the contact forces should bisect the angles between the balls. Additionally, the contact force vectors should intersect the plane of coupling action at a 45 degree angle to balance stiffness in all directions, therefore implying a 90 degree angle groove (18). A stable 3-groove kinematic coupling layout is shown in Figure 3.5 below. The angle bisectors intersect at a point that is also the center of the circle that can be inscribed in the coupling triangle; this point is referred to as the coupling centroid, and is only coincident with the coupling triangle's centroid when the coupling triangle is an equilateral triangle (19).

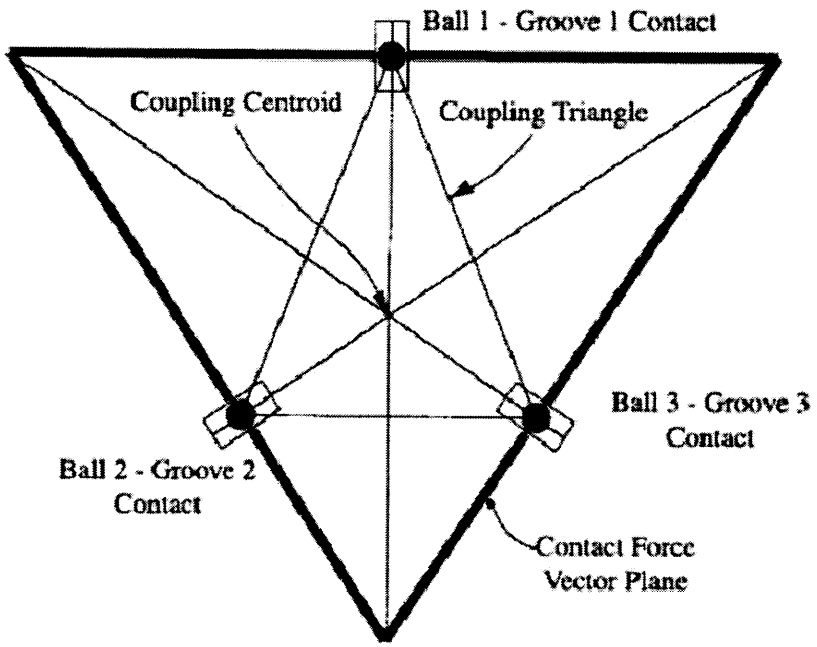

Figure 3.5: Ball and groove layout for optimal stability (18)

3.3 Error

Systematic errors influence the accuracy but not the repeatability. It is possible to get measurements that are consistently the same but systematically wrong. Random errors influence both the accuracy and repeatability of the measurement. Systematic errors can be reduced by improving the accuracy of the tools and equipment used or by decreasing human error of the individual making the measurement. Random errors can be reduced by averaging the results of many measurements of the same quantity (20).

3.3.1 Friction

Friction plays an important role in determining the performance of a kinematic coupling. Friction between the coupling surfaces is the most influential source of repeatability error in a KC. When a KC is fully engaged, it settles into a position where potential energy is minimized; that is, the balls slide down into the grooves as far as is possible. Friction between the balls and grooves prevents the KC from settling into this minimum energy state. Even though the contacting surfaces may appear to be smooth, they may contain micrometer scale asperities, so for applications requiring nanometer scale repeatability the surfaces actually seem rough. Only the surface asperities really touch each other. Friction is due to the interaction between the asperities of the ball and groove surfaces. The ball catches on surface asperities on the groove surface and sits in an unstable position. The ball may likely slide off of a particular catching asperity and the coupling position will move. This is illustrated in Figure 3.6 (4).

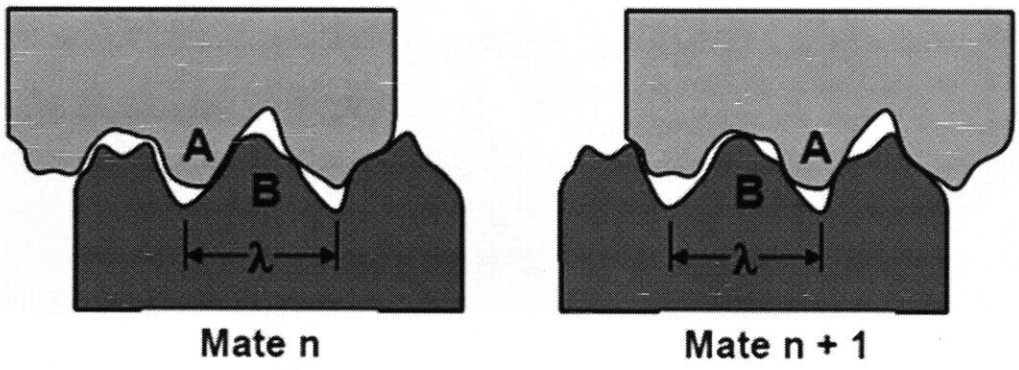

Figure 3.6: The effect of surface asperities on coupling

The friction at the coupling interface depends on the surface finish of the balls and grooves. Therefore, achieving good surface finish is one of the most important parts of KC design. Ball and groove surface finish should be specified in the design and can be achieved by optimizing

machining feeds and speeds, polishing, or brinelling the surface. Brinelling is a permanent deformation in the surface of the material caused by contact stress that exceeds the material elastic limit. The result is a permanent shiny dent in the surface. Brinelling the surface destroys the asperities, thus smoothing the area of contact and reducing friction.

Friction can also be mitigated by lubrication at the contact interfaces using high pressure grease or by adding flexures to the KC (11) (5). Adding flexural hinges to the ball side of the KC has been shown to improve the repeatability by a factor of 10, from repeatability on the order of hundreds of nanometers to repeatability of approximately 30 nanometers. This concept is exemplified by the flexure-enabled KC shown in Figure 3.7 below. The KC designed by Schouten, et al with flexures added to the grooves is shown in Figure 3.8.

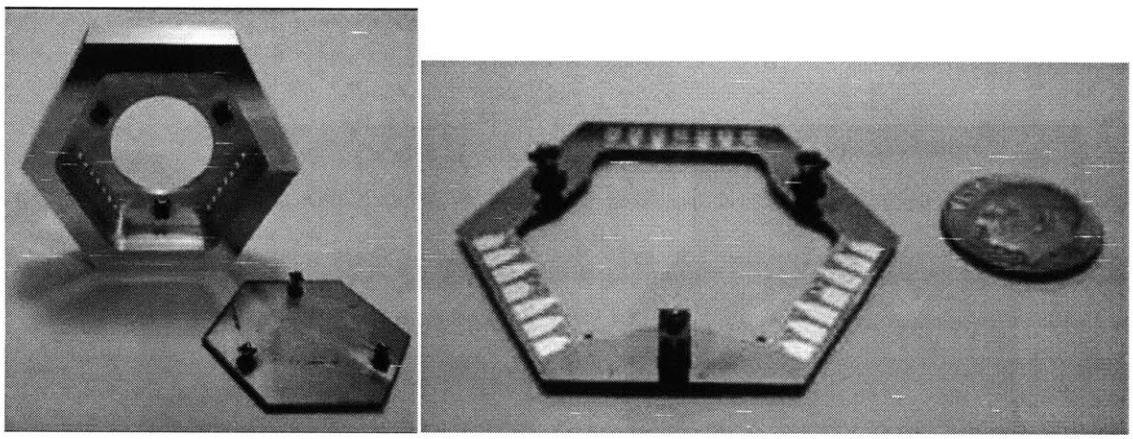

(a) **(b)**

Figure 3.7: KC modified with flexural hinges on the ball side to improve the repeatability by reducing friction. The entire KC is shown in (a), and a close up of the ball flexures are shown in (b).

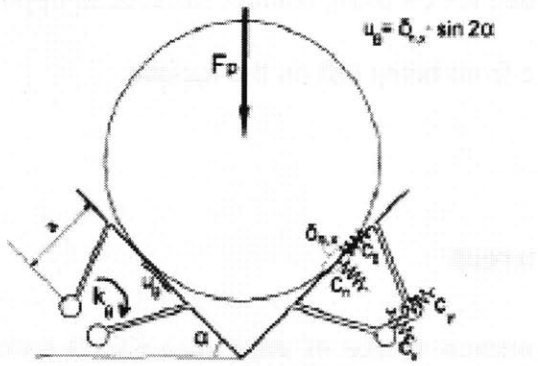

Figure 3.8: Ball in KC vee-groove modified with elastic hinges

For low-cost, small-scale fixtures, such as those in this thesis, adding flexures may not be an option, thus friction at the coupling interface must be controlled via surface finish and lubrication. Polished and hardened surfaces of ceramics or stainless steel are good options. Surface finish can also be controlled in manufacturing by optimizing the cutting speed and feed rate. Optimal feeds and speeds for various materials can be calculated based on the material of the work being cut, the material of the cutting tool, the economical life of the tool, and other cutting conditions. Cutting speeds and feeds can also be looked up in reference books, charts, or tables (21) but are always subject to change depending on the cutting conditions. At the small scale, controlling the surface finish to the specified roughness is often difficult, so additional steps beyond manufacturing may need to be taken. Post-manufacturing options for surface finish include polishing or brinelling the contact surfaces to remove surface asperities, or lubricating the contact surfaces with wax or high pressure machine grease to fill in the asperities.

The coupling surface must also be thoroughly cleaned because debris is another source of additional friction. Double sided tape may be used to remove any obvious debris, and compressed air or an oil mist may be used to clean the ball and groove surfaces. Compressed air

or an oil mist is recommended for cleaning contact surfaces as opposed to rags or paper towels in order to prevent any residue from being left on the surface.

3.3.2 Other Error Sources

After friction, the most common source of error in a KC is temperature variation over time, which causes thermal growth and shrinkage in the structural loop, including the tool, tool holder, machine elements, work holder, and work piece. Therefore, though the tool and work piece might be repeatably fixtured, if the fixture itself is sensitive to thermal variations the repeatability of the system will be compromised.

Since any deviation in temperature results in displacements due to thermal expansion, it is wise to utilize symmetry in the design of a kinematic coupling to increase repeatability. Symmetry was incorporated into the design of the fixtures presented in this thesis so that in the event of thermal expansion the coupling center would remain undistorted. In addition to using the advantages of a symmetric fixture design, material selection is important in mitigating error due to thermal expansion. Choosing materials with low coefficients of thermal expansion will help reduce geometric changes in the design due to temperature changes.

Of course, one way to alleviate error due to variations in temperature is to control the ambient temperature in which the fixture is used. The specific fixtures in this thesis are to be used in a temperature-controlled environment. Temperature control is the most effective method of mitigating thermal error since if the temperature remains constant, thermal expansion does not

occur; however, in many applications, the environmental temperature may not be able to be controlled, so in such cases it is best to design accurate and repeatable fixtures using symmetry.

For applications requiring better than 100 nm repeatability, errors due to hysteresis become a problem. Hysteresis is the difference between the coupling compression when the preload increases and the compression when the preload decreases. The effects of hysteresis can be decreased by increasing the hardness of the grooves (6) or by minimizing frictional forces at the contact surfaces, which can be done by adding a flexural element that allows the grooves to self adjust (5). However, adding flexures into the grooves decreases the stiffness of the coupling and is very difficult to do at the small scale due to constraints in manufacturing.

3.4 Preload

Preload force is the force required to keep the coupling components engaged and to prevent tipping. A greater preload force results in greater repeatability. In order for a kinematic coupling to be positionally stable it must be preloaded by some mechanical means. The most common and simplest method of achieving preload force is by gravity, or simply the weight of the kinematic coupling. Gravitational preload is, however, not an option in numerous small scale manufacturing applications since the kinematic coupling assemblies are often not perpendicular to gravitational force. Additional weight may also be applied as a preload force. Adding weight as a preload force requires the space necessary to hold that added weight, which in small scale manufacturing technologies is not always available.

A magnetic force may be used as a preload force. Magnetically preloaded kinematic couplings are cost efficient, space efficient, and have been successfully used in applications where the preload force is oriented perpendicular to the gravitational force (22). Magnetic preload force can be very strong relative to the size of the kinematic coupling, which allows for increased repeatability.

Additional methods of preload include clips, double sided tape, springs, levers, and positive gas pressure or a vacuum. All of these methods were examined and proved to be too expensive, too complicated, too large and bulky, not strong enough, difficult to adjust, or short-lived for the desired application. These several different methods of preload are compared in Table 3.1 below. The most important parameters (cost, preload strength, and envelope) are starred. After careful evaluation of all of these methods, magnetic preload was chosen as the optimal preload technique for these kinematic fixtures.

Table 3.1: Pugh Chart Comparison of Preload Concepts

Preload Concept	Gravity	External Load	Magnetic	Clips	Tape	Spring	Lever	Positive Gas Pressure or Vacuum
Cost*	+	+	+	+	+	-	-	-
Complexity	+	+	0	0	0	0	-	-
Strength*	-	0	+	0	-	0	+	+
Envelope*	+	-	+	-	0	-	-	-
Flexibility	-	0	+	-	-	-	-	-
Lifetime	+	+	0	0	-	0	0	+
Total	**+2**	**+2**	**+4**	**-1**	**-2**	**-3**	**-3**	**-2**

3.4.1 Magnetic Preload

After evaluating the above methods of preload, magnetic force was selected as the optimal choice for this application. Though a more intuitive choice would have been an external weight, the limited space available did not allow for any additional components to be added. A magnetic preload is cost efficient, strong, and able to be optimized for the ideal preload force without adding too many additional components or requiring extra space. Additionally, magnetic preloading was a good choice for this application because the universal mount on the DPN machine that the tips must be mounted to already includes two small Alnico magnets. Utilization of these two preexisting magnets removed the need to add additional magnets, which would require extra space. The strength of the magnetic preload is easily adjustable without making substantial changes to the design of the coupling. The strength of a magnetic field varies as the square of the distance between the two interacting magnetic materials; therefore, the force between the two parts varies substantially with very small changes in their separation.

It is not only important to apply a sufficient preload force, but to apply the correct preload force. If the preload is not strong enough the coupling will not sit together well and the repeatability of the coupling is compromised. However, if the preload force is too great the coupling is at risk of failure due to high Hertzian stress at the contact points.

3.4.2 Contact Mechanics

Understanding contact mechanics is critical for kinematic coupling design. Most problems in contact mechanics can be solved via Hertzian contact analysis developed by Hertz in 1880.

Hertzian contact stress is a description of normal contact stress between two mating elastic solids. It gives the contact stress as a function of the normal contact force, the radii of curvature of both surfaces, and the modulus of elasticity of each contact material. The contact stresses in KCs are cyclic and over time lead to sub-surface fatigue cracks, so it is important to design with these stresses in mind to prolong the life of the KC.

The following assumptions are made in Hertzian contact analysis:

- the strains are small and within the elastic limit
- the area of contact is much smaller than the characteristic radius of the body
- the surfaces are continuous
- the surfaces are frictionless

A spreadsheet was designed in order to calculate the contact forces, contact stresses, deflections at the contact points, and the error motions of any KC based on the user inputs of the ball diameters, groove radii of curvature, contact point locations, contact force directions, preload force locations and magnitudes, applied force locations and magnitudes, and material properties. The spreadsheet uses force and moment balance equations as well as the Hertz equations for elliptical contact to calculate the outputs. The spreadsheet can be viewed in Appendix A, the force and displacement calculations in Appendix B, and the Hertz equations in Appendix C.

3.5 Magnetic Circuit Design

Magnetic circuit design techniques were used to optimize the preload force for maximum repeatability. The groove side of the fixture attaches to the universal mount of the DPN machine via two small Alnico embedded magnets. A magnet was embedded into the ball side of the kinematic coupling for added preload force. The universal mount and ball and groove sides of the KC, including the Alnico mount magnets and the preload magnet, can be seen in Figure 3.9.

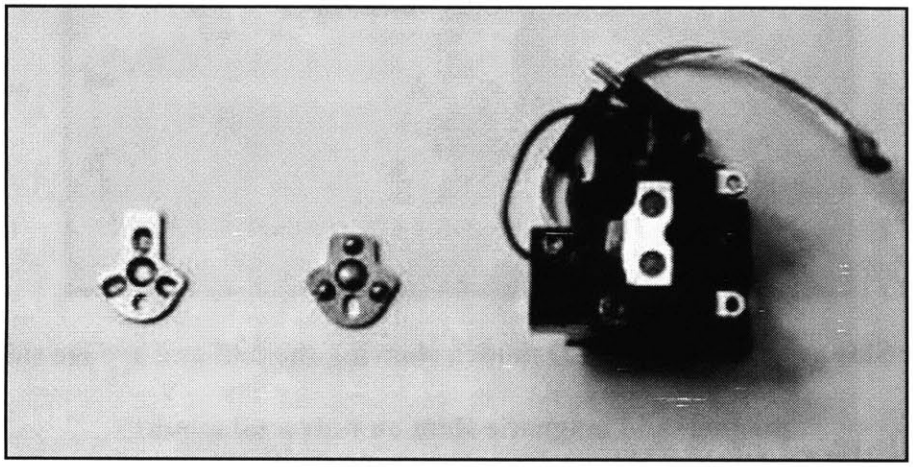

Figure 3.9: KC fixture ball and groove components aside DPN machine universal mount. The groove side of the KC is held onto the universal mount by the two small Alnico magnets in the mount

The magnetic flux flows from the preload magnet in the ball side of the KC through the air gap that separates the ball side of the KC from the universal mount, and into embedded universal mount magnets. This path was optimized and the air gap reduced by the addition of a steel shim that was added to increase the magnetic holding force of the fixture onto the universal mount. Figure 3.10 shows a side view of the layers of the fixture, including the preload magnet and the

steel shim. The embedded magnets are located inside of the universal mount, which sits below the KC.

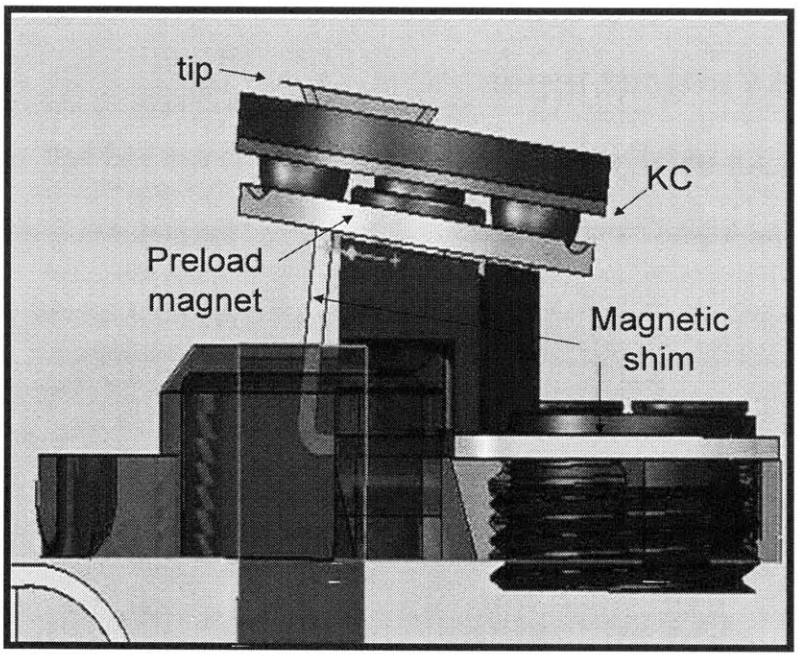

Figure 3.10: Side view of fixture CAD model, showing the ball and groove sides, preload magnet, and magnetic shim on universal mount

Using magnetic balls on the kinematic coupling was considered, however, this idea was rejected due to the fact that debris would easily stick to the balls, but more importantly, that the balls would be attracted to each other. This is a problem because they would not be rigidly attached in place until after the bonding had been completed. In order to prevent attraction between the balls and to eliminate any debris that might be attracted to the balls, stainless steel balls were selected.

3.5.1 Magnetic Circuit Mathematical Model

A magnetic circuit is comprised of one or more closed loop paths that contain a magnetic flux. The magnetic flux in this case is generated by the permanent magnets in the universal mount and the permanent magnet in the ball side of the kinematic coupling. The magnetic flux is confined to a path by magnetic cores. The magnetic circuit for the fixtures designed in this thesis is illustrated in Figure 3.11. There is one magnetic flux loop for each magnet. The flux travels easily through ferromagnetic materials and resists traveling through other materials like air. Air gaps add a resistance to the path, decreasing the amount of magnetic force. The largest resistance comes from the air gap as the flux travels from the groove side of the KC back to the universal mount magnet.

As the preload force, F1, increases, the coupling stiffness increases, the coupling accuracy increases, and the repeatability improves, so the maximum performance of the KC is achieved with the largest possible preload force. The holding force, F2, must be significantly greater than the preload force to prevent the KC from dismounting from the machine. This holding force is limited by the magnets already embedded into the universal mount, so the stiffness, accuracy, and repeatability of the KC is limited by the universal mount design. A shim was added into the magnetic circuit to increase the holding force, thus allowing the preload force to be increased and the performance of the KC to be optimized. The magnetic circuit with the addition of the shim is shown in Figure 3.12.

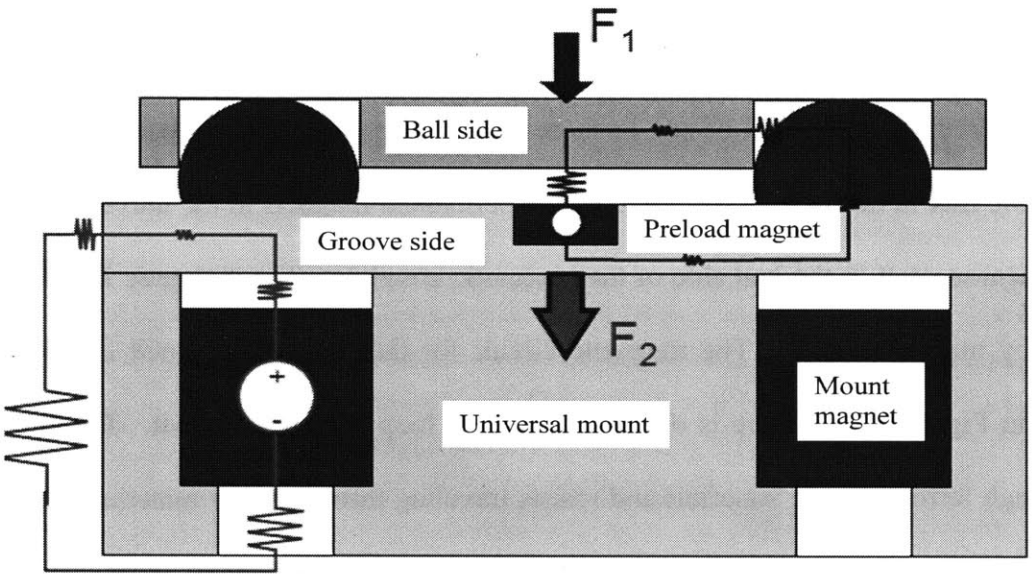

Figure 3.11: KC magnetic circuit model. The large air gap provides a large resistance in the flux loop that decreases the magnetic force.

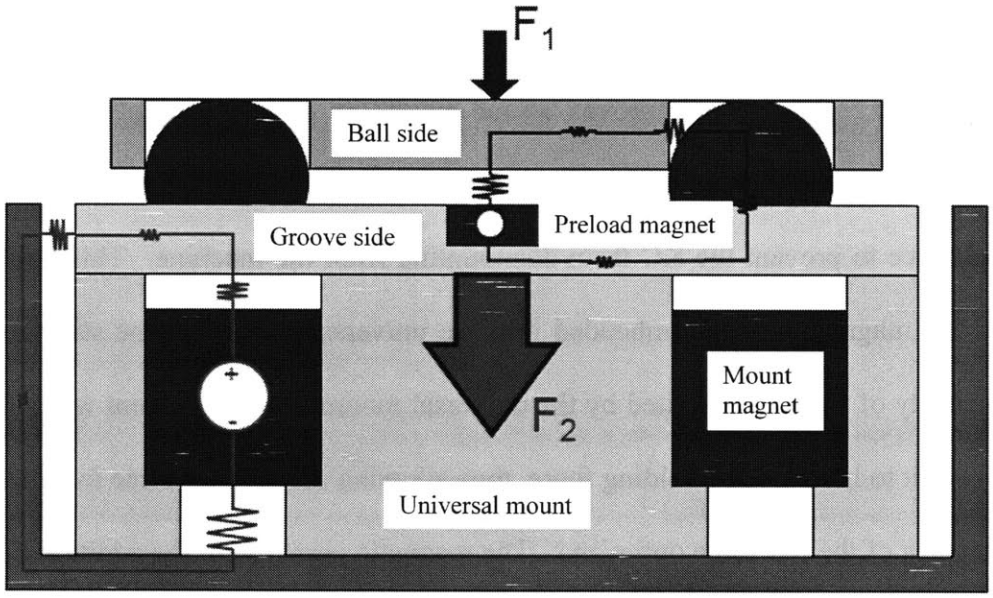

Figure 3.12: KC magnetic circuit model with shim. The air gap is reduced and the magnetic force increased

The ball sides of the kinematic coupling were manufactured from aluminum for cost and ease of manufacturing reasons, which diminished the magnetic flux path since the flux was required to

travel through aluminum instead of a ferromagnetic material. To improve the magnetic force, the flux path needed to be improved, thus it was important to understand magnetic circuit design.

The goal of this magnetic circuit was to have the groove side of the kinematic fixture be magnetically attached to the universal mount and to have the ball side of the fixture be magnetically attached to the groove side with sufficient magnetic preload. In order for the fixture to function properly, the physics behind the magnetic attraction must be understood.

The most fundamental equation to understand is Maxwell's pulling force formula (Equation 1), which describes the attractive force between two magnetized objects.

$$F = \frac{B^2 A}{2\mu_0} \qquad [1]$$

The force, F, between the groove side of the KC and the universal mount can be calculated by Equation 1, where B is the magnetic flux density, A is the cross-sectional area of the magnet, and μ_0 is the permeability of free space, 1.257×10^{-6} H/m. As Equation 1 shows, the magnetic force can be increased most efficiently by increasing the magnetic flux density, B, passing through the two objects. The magnetic flux can be calculated by Equation 2,

$$B = \mu_0 H \qquad [2]$$

Where H is the magnetic field strength. The magnetic field strength is closely related to flux density, but also depends on the material within the field; using the magnetic circuit designed in

this thesis, the material within the magnetic field is air, thus the permeability of free space, μ_0, is applied. The magnetic field strength can be calculated by Equation 3,

$$H = \frac{F_m}{l_e} \quad [3]$$

Where F_m is the magnetomotive force and l_e is the effective length in meters. Magnetomotive force is any force that produces magnetic flux and is measured in Amperes. The effective length is the distance which flux lines travel to make a complete circuit and can be measured by the physical geometry of the magnetic circuit. For the purposes of this thesis, the effective length is equal to the distance of the air gap, g.

Substituting Equation 3 into Equation 2, the flux density, B, can be calculated by

$$B = \frac{\mu_0 F_m}{g} \quad [4]$$

Substituting Equation 4 into Equation 1, the attractive force can be calculated by

$$F = \frac{\mu_0 (F_m)^2 A}{2g^2} \quad [5]$$

As shown in Equation 5, the attractive force varies as the gap length squared varies. Therefore, if the gap distance decreases, the force becomes exponentially stronger.

These five equations inform the design of the magnetic circuit for the fixture. Equation 1 shows that the magnetic force depends on the magnitude of the magnetic flux density squared. This shows that the magnetic force can most effectively be increased by increasing the magnetic flux density, which is achieved in this case by decreasing the resistance in the magnetic flux path by eliminating the air gaps. The air gaps are eliminated by the addition of a magnetic shim.

Equation 2 relates the magnetic flux to the magnetic field strength. The magnetic flux is calculated by the strength of the magnetic field multiplied by the permeability of the material within the magnetic field. This shows that the material within the magnetic field influences the strength of the magnetic flux. In the magnetic circuit designed for the purposes of this thesis, the material within the magnetic field is air, so the permeability of free space was used.

Equation 3 describes the relationship between the magnetic field strength and the effective length that the flux must travel to complete the magnetic circuit. The magnetic field strength is inversely proportional to the effective length, so in order to increase field strength, the effective length must be decreased. In this thesis, the effective length was equal to the distance of the air gap. In order to increase the magnetic field strength, the length of the air gap was reduced by adding a magnetic shim.

Equation 4 relates the magnetic flux density to the effective length or air gap, showing that as the length of the air gap decreases the magnetic flux density increases.

Equation 5 shows that the magnetic force is inversely proportional to the gap length squared. This demonstrates the importance of decreasing the length of the air gap in increasing the magnetic attractive force. By decreasing the length of the air gap with the magnetic shim, the attractive force exponentially increases.

3.5.2 Magnetic Circuit Modeling in FEMM

In order for the magnetic preload to work correctly, the correct preload force must be applied. Magnetic circuit design is complex, and computer software can be helpful in modeling the magnetic behavior. In the design of the fixture presented in this thesis, Finite Element Method Magnetics (FEMM) software was used in combination with the fundamental equations of magnetism to analyze and optimize the magnetic field produced by the preload magnets. FEMM is a finite element software package for solving low frequency magnetic and electrostatic problems in two dimensions (planar or axisymmetric).

In addition to allowing for the magnetic preload force and stick-on force to be approximated, FEMM analysis was used to determine the proper material to manufacture the groove side of the KC from. Aluminum allows for easier machining, which also means lower cost, but is not ferrous, which means the magnetic forces will be depleted as the flux travels through the aluminum. Steel is more difficult to machine, thus increasing cost, but is a ferrous material, therefore increasing both the magnetic preload and the holding force between the groove mount and universal mount. It is optimal to design the fixture such that the preload force is sufficient to achieve the desired repeatability requirements yet weaker than the magnetic stick-on force that holds the KC onto the universal mount to eliminate the possibility of the entire KC dismounting

(explained in 1.3.3). Numerous models were constructed and analyzed in FEMM with groove mounts of steel, aluminum, and combinations of the two. Figures 3.13 and 3.14 show flux density diagrams of the magnetic flux in two models, Figure 3.13 with aluminum grooves and Figure 3.14 with steel grooves. A summary of the analysis is displayed in Table 3.2.

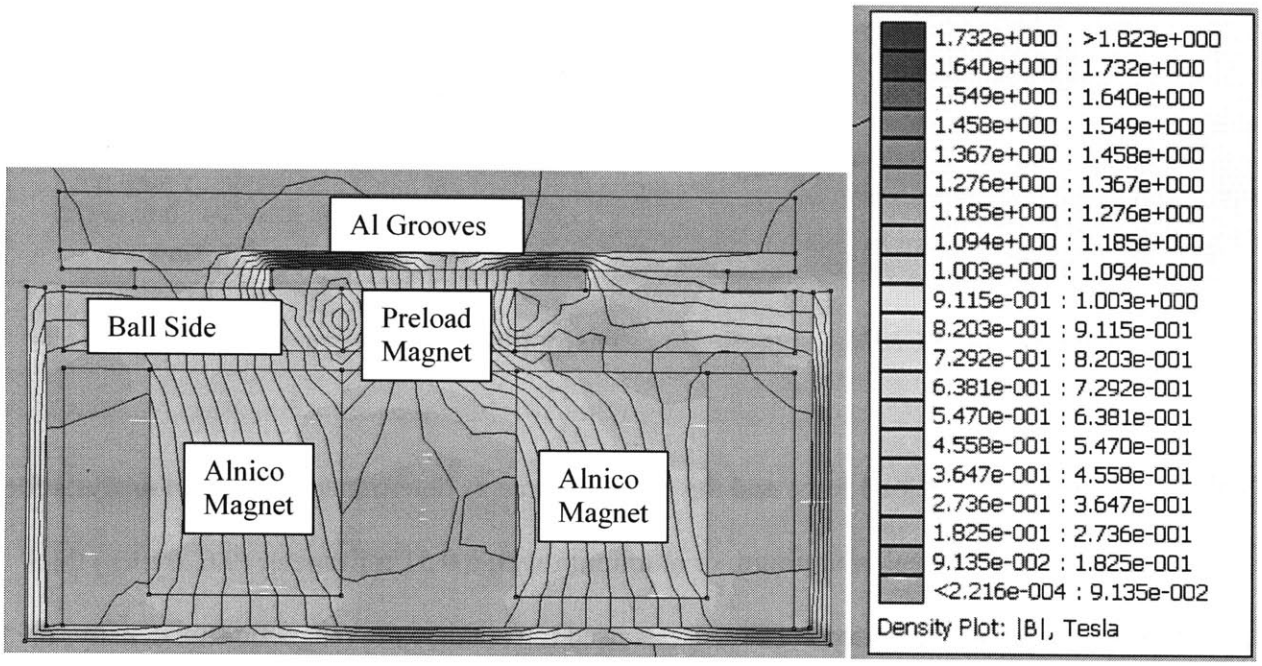

Figure 3.13: FEMM magnetic flux density plot for aluminum grooves model

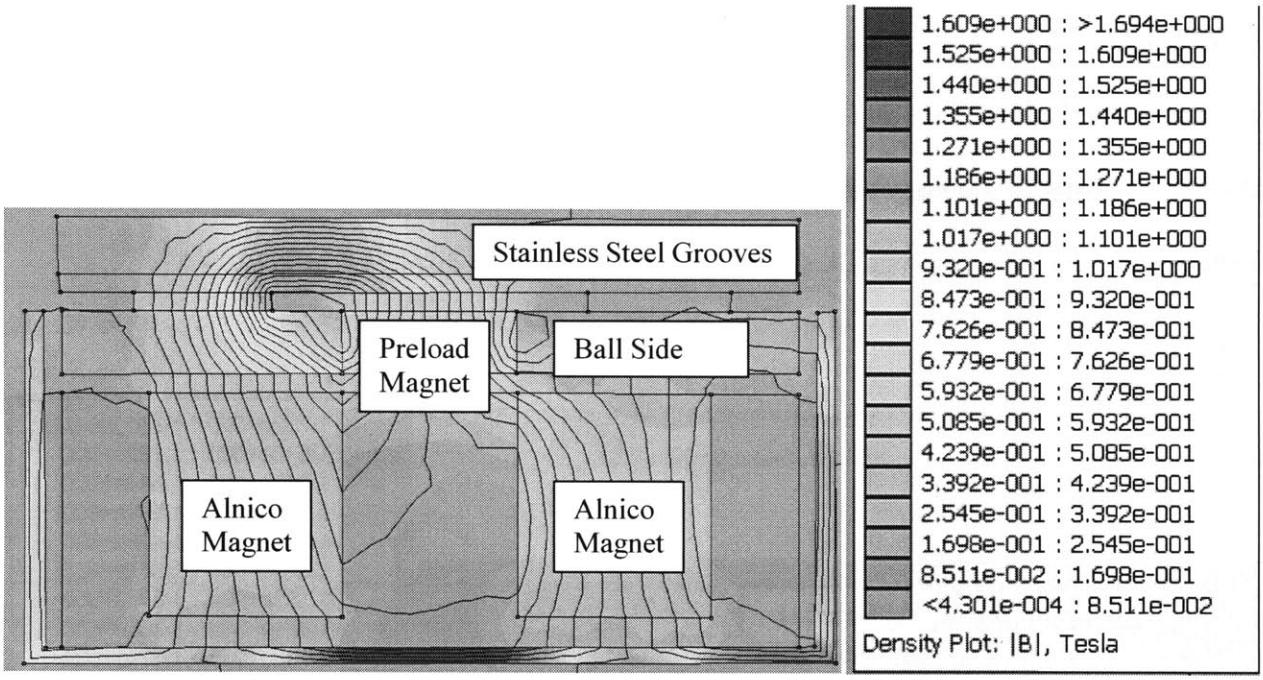

Figure 3.14: FEMM magnetic flux density plot for steel grooves model

Table 3.2 compares the preload force and the stick-on force as determined by FEMM analysis for a groove mount made of steel, aluminum, or aluminum with a 0.51 millimeter (0.020 inch) thick strip of steel attached to the bottom. FEMM was used to calculate the magnetic flux density, *B,* and the attractive force was calculated using Equation 1. All of the scenarios analyzed estimate the shape of the universal mount and the KC as rectangular layers of the same thickness and include a stainless steel shim of correct thickness. Each model is identical, other than the material of the groove mount. It was found that the steel groove mount led to a much higher preload force than the aluminum groove model or the aluminum with a 0.51 millimeter thick steel shim, but the stick-on force was only slightly higher than that of the aluminum groove model and slightly less than that of the aluminum with thin steel. Additionally, in the steel groove mount model, the preload force was more than double that of the stick-on force, which would lead to fixture dismounting. Thus the optimal material for the groove mount was

determined to be aluminum, in terms of ease of manufacture, cost, and magnetic preload and stick-on force optimization.

Table 3.2: Preload force and stick-on force compared for steel grooves, aluminum grooves, and aluminum grooves with a steel shim

	Steel Grooves	Al Grooves	Al Grooves +0.51 mm Steel
Preload Magnetic Field (T)	0.60	0.42	0.45
Stick-on Magnetic Field (T)	0.43	0.43	0.44
μ_0	7.9E-08	7.9E-08	7.9E-08
A (m^2)	1.0E-05	1.0E-05	1.0E-05
Preload Force (N)	23.2	11.4	13.3
Stick-on Force (N)	11.9	12.0	12.5

3.5.3 Magnetic Shim

The accuracy and repeatability of the kinematic fixture are only valid assuming the groove mount is held in place. In early iterations of the fixture it was found that the optimal preload force for the desired repeatability was greater than the holding force of the groove mount to the kinematic mount, causing the ball and groove sides of the kinematic coupling to stick together more strongly than the groove side and the universal mount. Thus, when the user attempted to remove the ball side of the KC in order to perform a tool change, the entire fixture would be removed.

In order for the fixture to work properly, the holding force between the universal mount and the groove mount must be greater than the KC preload force. This could be achieved by increasing

the attractive force between the groove mount and universal mount or by decreasing the preload force. In order to maintain the fine repeatability achieved by using the calculated necessary preload force, the fixture was modified to increase the magnetic force between the groove mount and universal mount. Due to size and manufacturing constraints, it was not feasible to place additional magnets between the groove mount and the universal mount. Therefore, a magnetic shim was designed.

The shim allows the holding force between the groove mount and universal mount to be increased via simultaneous magnetic and mechanical force. The shim includes two tabs that stick up along the side of the universal mount, thus reducing the air gap in the magnetic circuit and increasing the magnetic force; the tabs simultaneously apply a mechanical force to the side of the groove mount. With the addition of the shim, the vertical force required to displace the groove mount increased by a factor of 9.4, from 0.14 N to 1.29 N. Similarly the lateral force increased by a factor of 27.9, from 0.09 N to 2.45 N.

The shim sits between the universal scanning head and the universal mount on the DPN machine. The placement of the shim can be seen in the exploded diagram of the groove mount, universal mount, and universal scanning head assembly shown in Figure 3.15 below. The two tabs extending upward from the shim provide a mechanical preload force to the side of the groove mount, securing it in place, while also improving the magnetic force between the groove mount and the universal mount by reducing the air gaps in the magnetic circuit. The shim was fabricated from 0.020 inch thick 17-7 PH stainless steel machined and formed to optimize its performance.

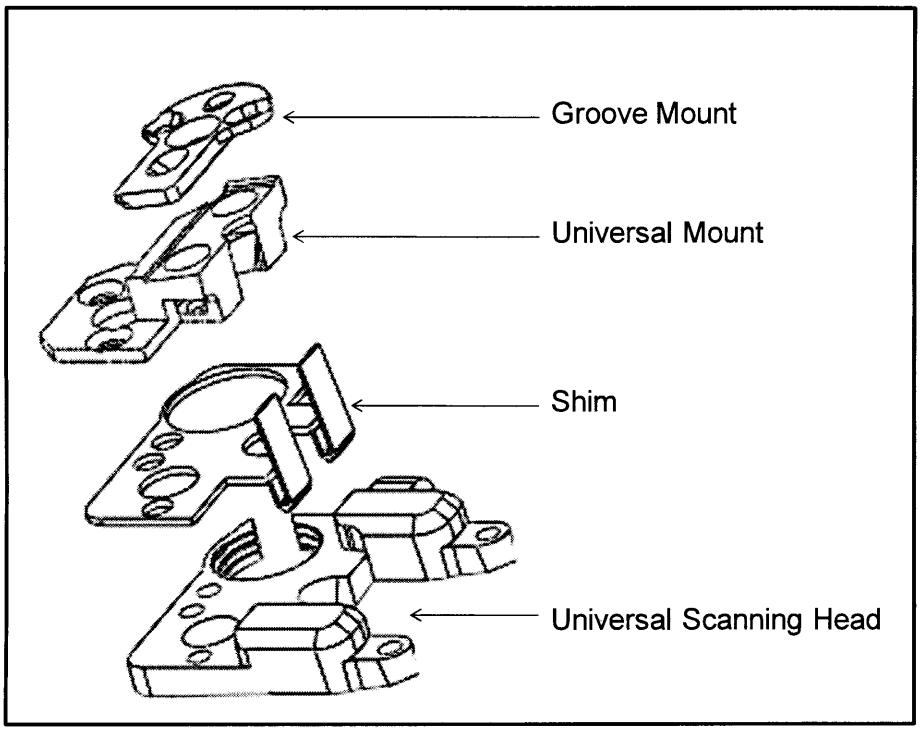

Figure 3.15: Exploded view of shim placement on universal mount

3.6 Lessons learned/design rules/insights

There are many factors that influence the repeatability of a kinematic coupling that must be considered. Understanding these factors and the effect each has on repeatability is important for optimizing KC design. The following design guidelines should generally be followed.

1. Faces of vee-grooves should make a 90 degree angle to optimize stiffness and load capacity. For balanced stiffness in all directions the contact force vectors should intersect the plane of coupling action at a 45 degree angle.

2. For stability, the normal vectors to the planes containing the contact force vectors should bisect the angles between the balls.
3. Symmetry is helpful for manufacturing, stability, and repeatability.
4. Contact stresses are usually high, so for high-cycle applications it is best to use corrosion-resistant materials for contact surfaces.
5. Choosing materials with low coefficients of thermal expansion will help reduce geometric changes in the design due to temperature changes.
6. Temperature control is the most effective method of mitigating thermal error since if the temperature remains constant, thermal expansion does not occur.
7. A greater preload force results in greater repeatability.
8. However, if the preload force is too great the coupling is at risk of failure due to high Hertzian stress at the contact points. Therefore, the highest preload force possible without inducing failure is optimal.
9. Friction at the coupling interface should be minimized to maximize repeatability.
10. Achieve the best surface finish possible by optimizing manufacturing feeds and speeds, polishing, and/or brinelling.
11. Compressed air or an oil mist is recommended for cleaning contact surfaces as opposed to rags or paper towels in order to prevent any residue from being left on the surface.
12. Lubricate grooves or use flexures to reduce friction at the contacts.
13. For magnetic preload, reduce the resistance in the magnetic flux path as much as possible to increase magnetic force. Eliminating air gaps is one way to do this.

CHAPTER

4

ACCURACY

4.1 Definition and Importance of Accuracy

Accuracy is the degree of proximity of a measurement to the true value of the quantity being measured. Accuracy is a function of repeatability, wear, tolerances, thermal and other errors. A system can be accurate but not repeatable or repeatable but not accurate, but accuracy of a system can only be as good as the repeatability of that system. It is not possible to achieve fine accuracy in a nonreapeatable system. This can be clearly explained with the target analogy referred to in Chapter 3, shown again in Figure 4.1. If the arrows are not grouped closely together near the target center (repeatable) then they cannot all be very close to the center (accurate). The average of the measurements might be accurate but each individual measurement can only be as accurate as it is repeatable.

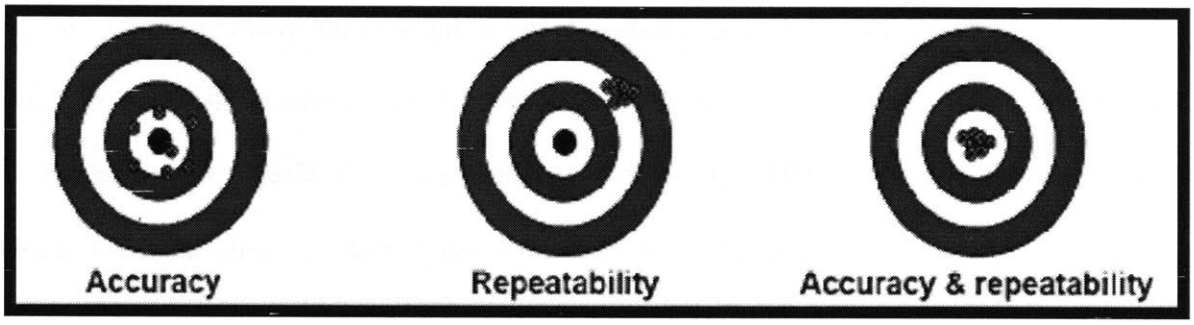

Figure 4.1: Accuracy and repeatability target analogy

Repeatability is necessary in precision fixturing applications but not sufficient. Precision fixturing applications, such as DPN, also require accuracy. Presently, a time consuming and labor intensive process is used to achieve alignment of the tip at the desired location before the process can be initiated. Part of this process can easily and inexpensively be eliminated by installing a kinematic coupling. Kinematic couplings themselves, however, are not inherently accurate. The accuracy of a kinematic coupling is affected by errors in the manufacturing and assembly of the components, such as errors in ball or groove size and placement, as well as other errors, such as poor surface finish and friction. Achieving accuracy with a kinematic coupling, therefore, requires calibration in order to compensate for any error. Calibration reduces alignment errors by adjusting the fixture position to match the desired position. Previous work in accurate kinematic couplings has consisted of small displacement adjustments in six degrees of freedom via actuated eccentric ball-shafts (9). This type of adjustable KC can provide accuracy on the order of micrometers. However, introducing adjustable components at the small scale studied in this thesis is difficult and expensive. Therefore, this thesis proposes an adjustable fixture design that requires no additional mechanical components to be added to the fixture itself.

An adjustable fixture design coupled with a complementary vision system will allow for fixturing errors to be corrected while the fixture is in an adjustable state. The adjustable state will be achieved by placing an adjustable interface between the ball and groove components of the KC. The fixture will not be set into its permanent state until its correct positioning has been verified. The vision system will (i) measure the current position of the fixture, (ii) command a nanopositioner to correct for any alignment error, and (iii) verify that the newly aligned fixture is in its proper configuration and trigger permanent setting of position. The vision system may then

be used to calibrate many fixtures. Each fixture may be interchanged between many nanomanufacturing machines while maintaining the desired accuracy. An overview of this concept can be seen in Figure 4.2.

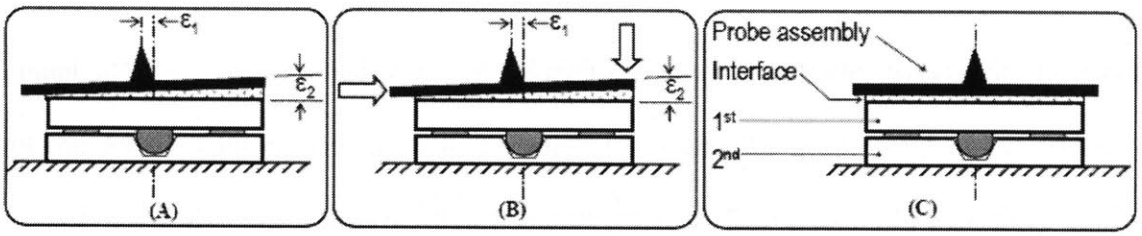

Figure 4.2 (Culpepper): Generic concept for adjustable interface in the context of a two-axis error calibration. The probe assembly was originally placed with translation error ε_1 and rotation error ε_2 (A). Probe tip error is measured via vision system and then adjusted via actuators (B). Improved alignment post calibration and fixation (C). The probe assembly is then ready for accurate alignment into machine.

4.2 Methods for achieving accuracy

The accuracy requirement that the fixture must meet is 1 micrometer. An adjustable interface exists between the ball and groove sides of the KC, such that the ball side is able to move with respect to a master groove fixture. A vision system is used to detect and measure the error between the actual and desired position of the fixture. After measuring the error, the vision system uses computer control to command the actuators of a nanopositioner to adjust the relative position of the ball side of the fixture with respect to the groove side. The vision system then verifies the correct positioning of the ball side and then initiates permanent assembly, securing

the adjustable interface in place. The adjustable interface is accomplished by one of three methods: (i) potting in ultraviolet (UV) curing adhesive, (ii) plastically deformed flexures, or (iii) adjustable coupling elements.

4.2.1 Potting in UV Curing Adhesive

The first concept for the adjustable interface is a thin layer of UV curing adhesive. The balls of the KC will be set in UV curing adhesive and therefore will be free to move until properly aligned. The calibrated alignment will be permanently fixed by curing the adhesive. Risks to consider in using this method include shrinkage of the adhesive during the curing process and long-term stability, which are assessed by manufacturers' specifications as well as careful in-house testing. If shrinkage is measured to be consistent for multiple tests, the positioning process may be adjusted such that the fixture obtains the correct position after the curing process. A variety of UV curing adhesives is commercially available with various shrinkage specifications, cure times, strengths, and costs.

4.2.2 Plastically Deformed Flexures

The second concept for the adjustable interface is plastically deformed flexures. Plastic deformation of metallic flexural elements has been used historically with great success to provide rapid and inexpensive precision alignment in numerous applications, including alignment of laser cavity components (23) (24) (25) (26), alignment of micro-optical components (27), photonics devices (28) (29) (30) (31) (32) (33) (34) (35), and automotive components (36) (37). This concept is more complex than the UV adhesive because it requires an additional metal

flexural component to be manufactured for each fixture, thus increasing manufacture time and cost of the system. The main risk to consider with plastically deformed flexures is how springback will affect proper alignment. Springback is the phenomenon that occurs when a force applied to a metal component causes the component to bend. Then when the force is removed the metal component recovers a portion of its original shape in elastic deformation. Therefore, it is necessary to bend the flexural components past their desired location to compensate for springback. If springback is properly calculated and compensated for, it has been proven possible to obtain sub-micron alignment using plastic deformation (15).

4.2.3 Adjustable Kinematic Coupling

Mechanically adjustable kinematic couplings have been designed with two axis adjustability in x and y (8), three axis adjustability in x, y, and θ_z (38), and with six axis adjustability (9) (39) (13). A fixture that is adjustable in six degrees of freedom is expensive, complicated, and difficult to manufacture at the small scale. Therefore, the adjustable kinematic coupling concept was discarded early in the selection process.

4.3 Chosen Method: System Overview

Potting in UV curing adhesive was the concept chosen to act as the adjustable interface between the ball and groove components of the KC due to its low cost, simplicity, and requirement of no additional space in the fixture. The three concepts are compared in Table 4.1.

Table 4.1: Comparison of Adjustable Interface Concepts

Concept	Potting	Plastic Deformation	Adjustable KC
Accuracy	+	+	+
Cost	+	+	-
Complexity	+	0	-
Envelope	+	0	-
Flexibility	-	0	+
Total	**+3**	**+2**	**-1**

The potting concept was selected based on its potential for high accuracy, low cost, low complexity, and small envelope. The UV potting method requires UV lights to cure the adhesive, a nanopositioner to adjust the position of the KC, and a micro vision system to monitor and verify the position adjustments. These components are all assembled into a fixture assembly station, shown in Figure 4.3.

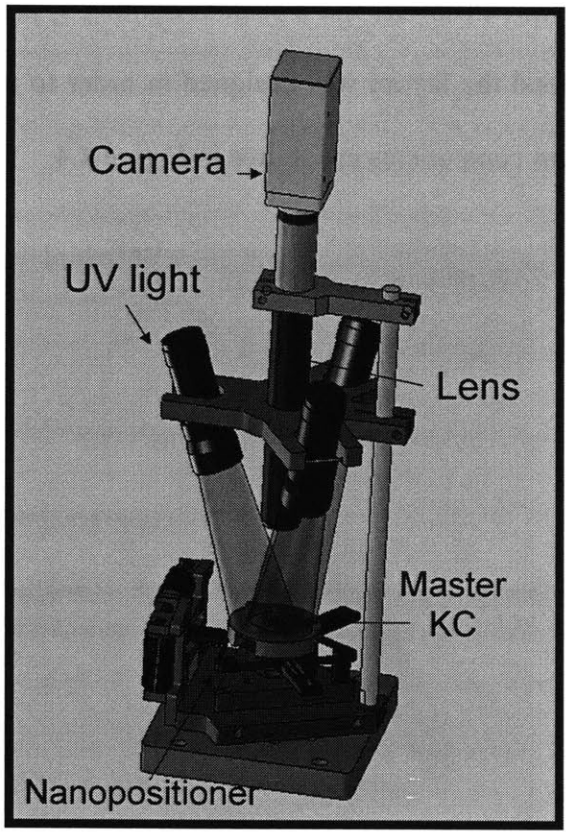

Figure 4.3: KC fixture assembly station

4.3.1 Vision System

A vision system will be used to identify and correct errors in the alignment of the fixture. Vision has been selected as opposed to other position sensors for its flexibility and ability to gather simultaneous information. The vision system is able to detect the position and alignment of the fixture and at the same time command a nanopositioner to adjust the positioning of the fixture. A vision system, therefore, outperforms any other single sensor of comparable cost. The vision system is used to (i) inspect the fixture, (ii) measure the alignment error, (iii) command a nanopositioner to provide the necessary correction, and (iv) verify the position after re-positioning before final assembly. The vision system consists of an objective microscope lens, a

5.0 megapixel high resolution camera, and a coaxial lighting system. The hardware components were carefully selected and the layout was designed in order to maximize the resolution of the system. The vision system components are shown in Figure 4.4.

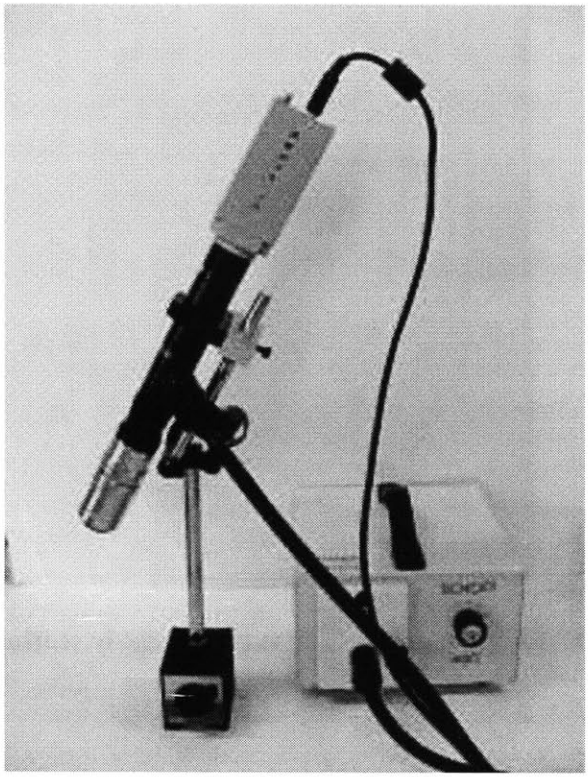

Figure 4.4: Vision system hardware components set-up

The camera is a CMOS USB from Pixelink with a resolution of 2529x1994 at 8 bit/pixel and 7 Hz. The high-end commercial objective lens is a Navitar model Precise Eye Ultra C-mount with Numerical Aperture 0.42 with 1x adapter and lighting. The working distance of the lens used is 20 mm respectively, and the lens has magnification of 20x. A coaxial lighting configuration was selected to optimize the direction and intensity of the lighting. With visible lighting, the vision system hardware has a resolution of approximately 200 nm. Labview image acquisition and image processing software is used to acquire and process the images automatically.

Communication between the software and the positioner directs the corrective actions of the positioner so as to move the tip into correct alignment.

4.4 Potting

Potting is the covering or encapsulation of a device with a liquid compound that turns to a solid plastic by a chemical reaction. Epoxy, silicone, polyester, acrylics, and polyurethane materials are described as thermoset plastics because the chemical reaction that they undergo when hardening is irreversible, as opposed to thermoplastics, which can be melted back into their liquid state. Very high heat (around 600°F) will cause thermoset plastics to burn but not melt. The chemical reaction that initiates the hardening of the potting compound may occur when the compound is mixed with a hardening compound or when heat or light is applied. Depending on the potting compound, the hardening reaction may occur at room temperature or it might require heating to up to 300°F.

4.4.1 Overview of Potting

A two-part potting system consists of the potting resin and a hardener material that are stored separately. When the two are mixed, the hardening reaction is initiated. A two-part system requires the resin and the hardener to be thoroughly mixed together in a proper ratio such that every resin molecule crosslinks with every hardener molecule, ensuring complete curing. Most two-part potting compounds develop adequate properties after 16 hours of hardening, but the

curing time can be adjusted by increasing or decreasing the temperature at which the two parts are mixed together.

In a one-part potting system, the hardener and resin come as one compound, previously mixed. The hardener is inactive until heat or UV light is applied and initiates the reaction. The advantages of a one-part system are that no mixing is required and no ratio measurement is needed. In order for curing to occur, heat or light must be added to the system. The hardening speed of a one-part system can be affected by increasing the temperature or the amount of light energy applied. One-part potting compounds generally do not have as large of a range of available properties as two-part systems.

The time to fully harden ranges from approximately 20 seconds to many days. The selection of hardeners and modification of the resin with accelerators determines the resulting hardening time. The system hardens by linking chains together in a three-dimensional structure and continues until the material has achieved its desired properties.

The crosslinking process is an exothermic reaction. Potting compounds harden when a chemical reaction occurs. During the chemical reaction heat is released as the chains crosslink. The faster the chemical reaction, the higher the internal temperature becomes since heat is not readily dissipated by the potting compound. Similarly, the hotter the potting compound becomes, the faster the crosslinking reaction occurs. This exothermic temperature can help to harden the polymer faster; however, it must be known and used carefully, especially in applications involving heat sensitive components, so as not to cause damage.

When the chemical reaction occurs, the potting compound shrinks in volume. This volume change ranges from approximately 0.2% to 4% of total volume, depending on whether the potting compound is made with filler, which will not shrink, or no filler. During the reaction, the polymer is heated but the heat is not transmitted quickly. Therefore, the outside edges of the polymer can dissipate heat but the middle cannot. This makes the middle react more and more quickly until it is fully cured and all shrinkage has occurred. Therefore, more shrinkage is apparent in the middle of the potted volume than the outsides. The speed of hardening also affects the shrinkage. The faster the cure time, the greater the shrinkage. Therefore, the ideal system cures very slowly and has no exothermic reaction. However, extremely slow curing is not always desirable when production speed is a priority. This balance of fast curing time and low shrinkage requirements is not intuitive and makes the selection of an ideal potting compound difficult.

4.4.2 Chemistry of Ultraviolet Adhesives

A material that cures upon being subjected to ultraviolet light was chosen as the ideal material for potting in the application of the accurate kinematic coupling. UV curing materials have a distinct quality in that they are able to remain in a liquid state until the exact moment that the user wants to harden the material and subjects it to UV light. UV curing adhesives do not have a finite time period within which they must be used before they become hard, as epoxies that harden at room temperature upon mixing do; therefore, UV curing adhesive allows the position of the kinematic coupling to be adjusted before being set. Most UV curing adhesives are single material epoxies and do not require mixing like typical epoxies do. This increases convenience

for the user as well as eliminating any error that arises from inconsistent mixing. Eliminating any variation in the consistency of the epoxy decreases variation between fixtures.

Ultraviolet light is a portion of the light spectrum ranging from approximately 200 nanometers to 400 nanometers in wavelength. Figure 4.5 shows where UV light falls on the light spectrum. Ultraviolet light is typically used in a variety of applications, including semiconductor lithography, sun tanning, water purification, as well as adhesive curing. Pure UV light is not visible to the human eye since its wavelength falls below the visible portion of the light spectrum. In addition to wavelength, the intensity of UV light is also an important measurement. The intensity of UV light is measured by a radiometer and is measured in terms of power per area (usually milliwats per square centimeter, mW/cm^2).

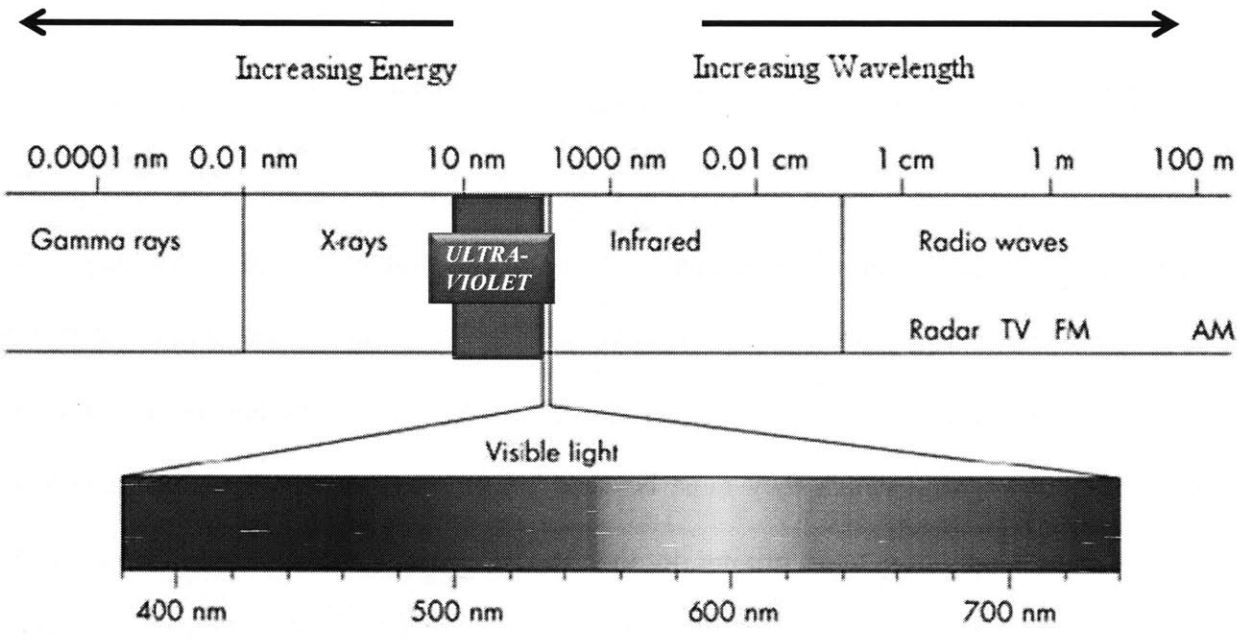

Figure 4.5: Light Spectrum. UV light ranges from approximately 200 to 400 nm in wavelength (40).

As mentioned before, UV curing adhesive is made of a single material; however, though only a single material is handled, there are two components within the material. The adhesive resin is already mixed with a second component called a photoinitiator. The photoinitiator and the adhesive resin do not react with each other under normal conditions. However, when the adhesive is placed under UV light, the photoinitiator absorbs the UV light and undergoes a chemical reaction. The by-products of this chemical reaction cause the adhesive resin to become hard. The photoinitiator does not react to exposure to any light; the light delivered must be of the correct wavelength and of sufficient intensity in order to produce the chemical reaction. Otherwise incomplete curing of the adhesive, if any at all, will occur.

4.4.3 Selecting a Light Source

Selecting the optimal light source for curing UV adhesives requires knowledge of how the light affects the curing process. A higher intensity (the light energy reaching the surface per time, measured in mW/cm^2) light used for curing will generally provide a faster curing time. The distance the light source is positioned from the adhesive affects intensity. Intensity decreases with increasing distance from the light. Intensity is also reduced when curing through substrates that transmit less than 100% of the light used for curing. Since light curing materials themselves absorb light, there is a maximum depth into the adhesive that curing can occur. For most adhesives, this maximum curing depth was determined to be between ¼ inch and ½ inch. The strength of the bond achieved with UV curing adhesives is at its maximum once the adhesive has completely cured. Curing has completed when the adhesive has changed completely from a liquid state to a solid state, or more accurately when further light exposure no longer improves

the properties of the adhesive. UV curing adhesives will not cure unless exposed to light of appropriate wavelength, intensity, and duration, thus the curing light source and UV curing adhesive should be selected as a pair. The recommended wavelengths, intensities, and curing duration for UV curing adhesives can be obtained from the adhesive manufacturer or distributer.

The light source for this application was selected based on the adhesive to be used. The light source selected is a combination of three small portable UV lights consisting of 21 LED's at a wavelength of 395 nanometers. The selected adhesive cures after approximately 20 seconds of exposure. This is a fast curing time compared to most adhesives. In general, the longer the adhesive cures, the stronger the bond; however, a fast-drying adhesive is desirable in applications where expediency is important, for example, for use in manufacturing. The three UV lights are arranged such that each light hits the fixture from a different angle, thus maximizing the curing area. The three UV lights can be seen in the assembly station pictured in Figure 4.6.

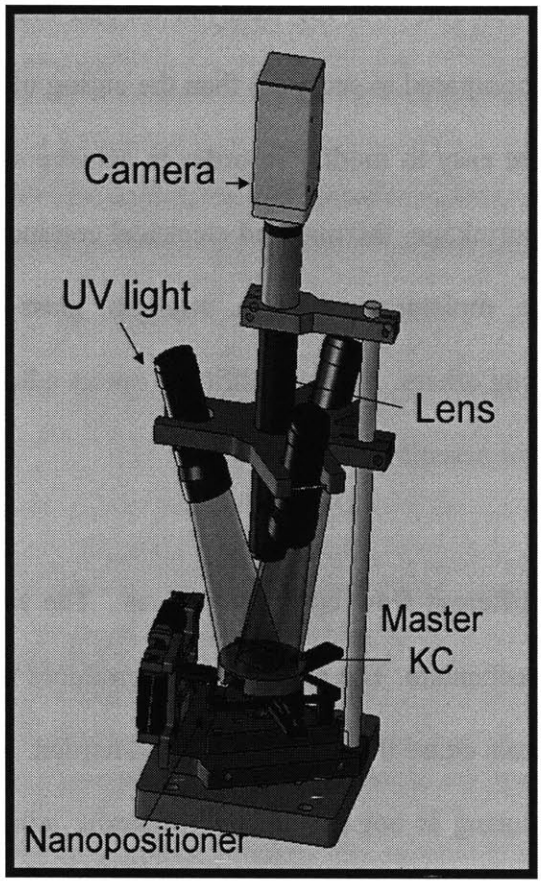

Figure 4.6: KC fixture assembly station. Three UV lights arranged to maximize area of adhesive exposed to light.

4.4.4 Types of UV Adhesives

Many varieties of UV curing adhesives are used, depending on the application. The two primary categories of UV curing adhesives typically used in product assembly, and specifically small scale product assembly, are epoxy adhesives and acrylic adhesives. Epoxy adhesives employ a catalytic curing mechanism. That is, the chemical reaction that occurs within the photoinitiator when UV light is delivered creates a catalyst by-product. This by-product, in turn, promotes the hardening of the adhesive resin. This property allows for material that was not directly exposed

to the UV light to cure by reaction with the catalyst, though this shadow curing takes much longer (on the order of days compared to seconds) than the curing of the portion that was directly exposed. Epoxy adhesives are easy to modify in order to achieve special properties. Additives are often used to adjust the shrinkage, thermal and electrical conductivity, thermal and electrical insulation, impact resistance, moisture resistance, strength, glass transition temperature, and adhesion characteristics, among others. The versatility of epoxy adhesives makes them a popular type of UV curing adhesive for assembly purposes.

Acrylic adhesives are very different from epoxy adhesives. The curing of acrylic adhesives is achieved via a free radical mechanism. The photoinitiator produces free radicals during exposure to UV light. These free radicals cause the adhesive resin to harden, but they are consumed in the curing process, so shadow curing is not possible with acrylic adhesives. Curing only occurs where the adhesive was directly exposed to UV light. This means that if two parts are being bonded by acrylic UV curing adhesive, at least one of the parts must be UV transparent in the areas that are being bonded. Modification of acrylic adhesives is not as simplistic as using additives, and can only be done at the chemical level by changing the chemical compounds of the base resin or photoinitiator.

Epoxy based adhesives were chosen as the optimal type of adhesive for the fixturing application. There are two types of UV cure epoxies. Acrylate urethane epoxies are the type that can reach into shadows. Cationic epoxies tend to be more rigid and have lower shrinkage.

In addition to the type of adhesive, optimal curing conditions are also highly important. It is important that cure conditions are suitable and consistent from one period to the next. Important parameters include wavelength of light, intensity of light, duration of exposure, and direction/angle of exposure.

4.4.5 Testing of Adhesives

With the requirement of 1 micron accuracy and 100 nanometer repeatability, low shrinkage of the adhesive is critical. Several different low shrinkage UV curing adhesives were purchased and tested to determine which would be the best for the application; specifically, they were tested for shrinkage or expansion, stabilization time, and long term stability. Additionally, 24 hour water absorption should be compared for each adhesive tested since water absorption affects growth of the adhesive, so lower water absorption is preferable. It is important to consider viscosity of the adhesive as well to make sure the adhesive will apply to the ball surfaces appropriately rather than wicking and coating the entire ball.

Each adhesive was tested for stability over 48 hours. For each adhesive tested, four drops of adhesive were applied to four corners of a thin plate of sheet metal steel that was being bonded to a block of aluminum. It was determined throughout this testing that less shrinkage occurs with less adhesive applied, so minimal adhesive was used to bond the plate to the block. UV light was applied at a wavelength of 395 nm for 20 seconds. The assembled test piece and curing process are shown in Figures 4.7 (a) and (b) below.

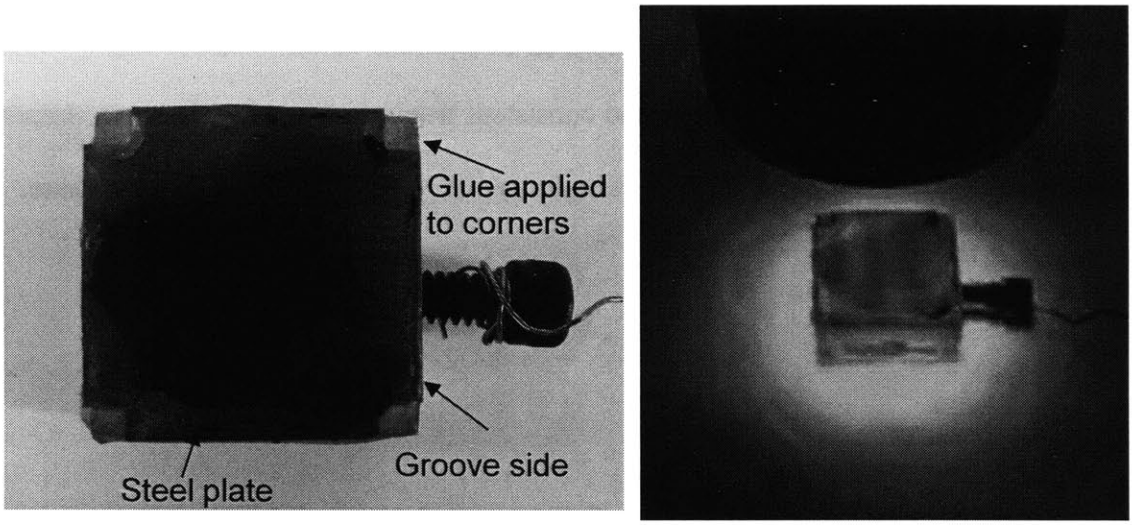

(a) (b)

Figure 4.7 Assembly configured to test various adhesives, consisting of a thin steel plate on top of an aluminum block. Adhesive was applied to each of four corners (a). The assembly is placed under UV light for curing (b).

The shrinkage or expansion of the adhesive was measured by recording the position of the plate continuously over 48 hours. Three capacitance probes were oriented over the plate to measure the vertical displacement of the plate. Three points define a plane, so by measuring the displacement of the plate at three points the position of the plate was accurately determined. The assembly was bolted to an air table to eliminate vibration. The system was electrically grounded via a copper wire attached to a bolt that was threaded into the aluminum block. The set-up was then covered with aluminum foil to further reduce electrical noise and placed in a plastic isolation chamber to reduce errors arising from thermal and electrical fluctuations in the testing area. The capacitance probe measurement set-up and the light and electricity isolation chamber are shown in Figures 4.8 (a) and (b).

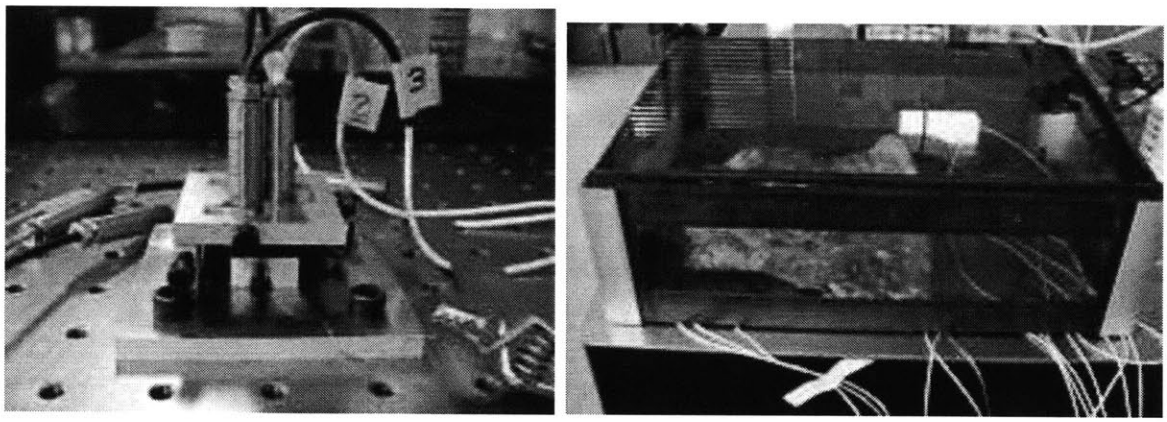

(a) (b)

Figure 4.8: Capacitance probe measurement set-up (a) and Light & electricity protection box (b)

It was found that the adhesive with the least shrinkage or expansion was from the Dymax fiber optical assembly OP-4-20632 series. It is an acrylate urethane adhesive with a reported 0.2% shrinkage after curing. The data sheet for the selected adhesive can be seen in Appendix D.

The measured displacement of this adhesive turned out to be in expansion rather than shrinkage and was measured to be approximately 600 nm of growth in the z-direction (vertical) over a time period of 48 hours. The measured z-axis data is shown in Figure 4.9 below. Growth in the z-direction was greater than the displacement in the x and y directions, thus the x and y data is not shown, but the displacement in the x and y directions was measured to be approximately 500 nanometers for both, which meets the customer requirements of 1 micron accuracy. The expansion was most likely due to humidity in the air being absorbed into the adhesive; the chosen adhesive has a reported 1% increase in weight when submerged in water for 24 hours. However, 600 nm of growth met the 1 μm accuracy requirement for this application. This

adhesive also exhibits high strength, which is necessary to withstand the required preload and applied forces.

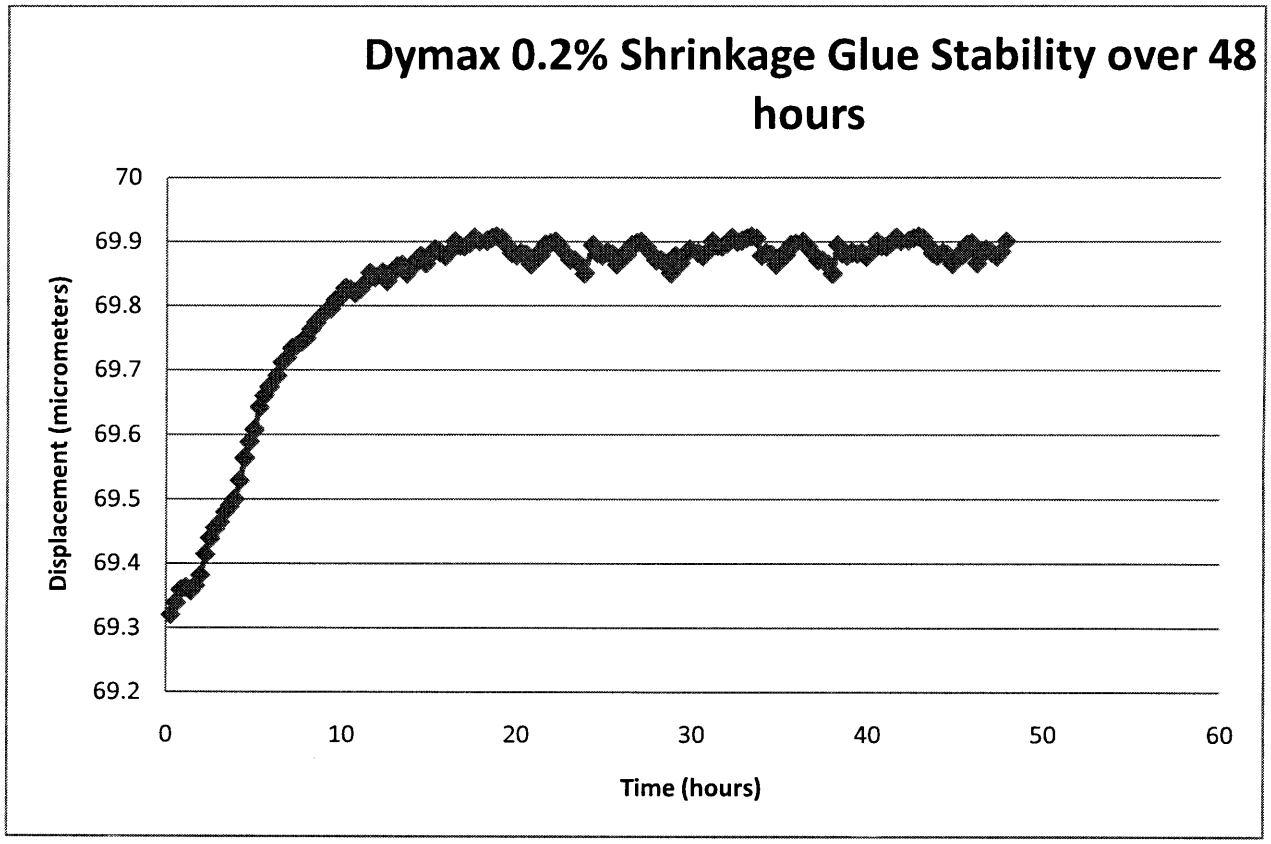

Figure 4.9: Dymax 0.2% shrinkage glue stability over 48 hours test results

4.4.6 Lessons learned/design rules/insights:

When designing an accurate KC with an adjustable interface via an UV adhesive, it is important to understand the chemistry of the adhesives and the bonding process to optimize the KC design. The following insights should be kept in mind:

1. Dispense adhesive as uniformly and minimally as possible. Minimize mass of epoxy to minimize expansion or shrinkage.
2. Apply adhesive symmetrically for best results.
3. With a fast hardening resin system the shrinkage is higher due to the exothermic heat given off during hardening and the fact that the reaction speeds up when the temperature is raised further increases the speed of hardening and more shrinkage. Therefore, to reduce shrinkage, lower the hardening temperature to minimize exotherm and slow the reaction to allow orderly flow in to shrinking areas. By reducing the mass of the potting compound less exotherm will develop which will help reduce the shrinkage.
4. The faster the cure time, the greater the shrinkage. Therefore, the ideal system cures very slowly and has no exothermic reaction. However, extremely slow curing is not always desirable when production speed is a priority.
5. To ensure proper bonding: apply a small bead of adhesive to one surface. Join surfaces with optimum surface to surface contact. Upon assembly, the bead of adhesive should spread to fill the joint. Cure the bonded joint under the appropriate light for selected adhesive for specified cure time, making sure that as much of the adhesive as possible is exposed to UV light.

CHAPTER

5

CASE STUDY: DIP PEN NANOLITHOGRAPHY TOOL CHANGING

5.1 Project Introduction

This chapter demonstrates the analysis, design, manufacturing, and verification of an accurate and repeatable kinematic fixture as used in a case study of DPN tool changing. The fixture was built for use in DPN machines made by NanoInk. NanoInk is a technology company that specializes in nanometer-scale fabrication and manufacturing applications. The kinematic fixtures manufactured over the course of this research were implemented into NanoInk's DPN 5000 desktop nanofabrication system. The fixture attached to the machine and mounted with the DPN tool, which is an atomic force microscope (AFM) tip, can be seen in Figure 5.1. Figure 5.2 shows the DPN 5000 machine. See Appendix E for a detailed DPN 5000 system product data sheet.

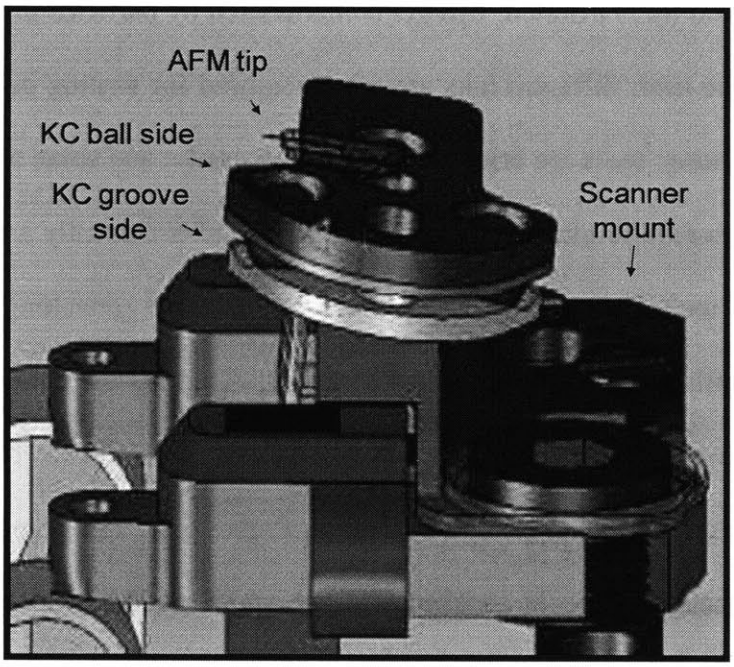

Figure 5.1: CAD model of fixture on scanner universal mount

Figure 5.2: NanoInk DPN 5000 machine

The need for the accurate and repeatable kinematic fixture is in reducing set-up time and tool changeover time. In DPN frequent tool changes are necessary. When the ink on one tip wears

out, a new freshly inked tip is inserted; tips get contaminated by particles in the environment, on the substrate, or by the user; different inks are often required for writing on different substrates or for variations in writing; tools are brittle and will break easily; and some applications require a single tip, while others require multiple tips. Changing a tool is currently a time consuming and involved process that includes inserting the tip into a probe holder, attaching the probe holder to the machine, and aligning the tip via laser and software. The tips are currently located by two flat edges on the universal mount and held in place by magnetic force. The universal mount, with the alignment edges and magnets can be seen in Figure 5.3. The objective of the accurate and repeatable kinematic fixture is to eliminate the probe holder and the process of laser alignment for each tip. The groove side of the fixture will be mounted directly to the machine, and the tip will be mounted directly to the ball side of the fixture, so the tip will be accurately and repeatably located by the fixture to the machine.

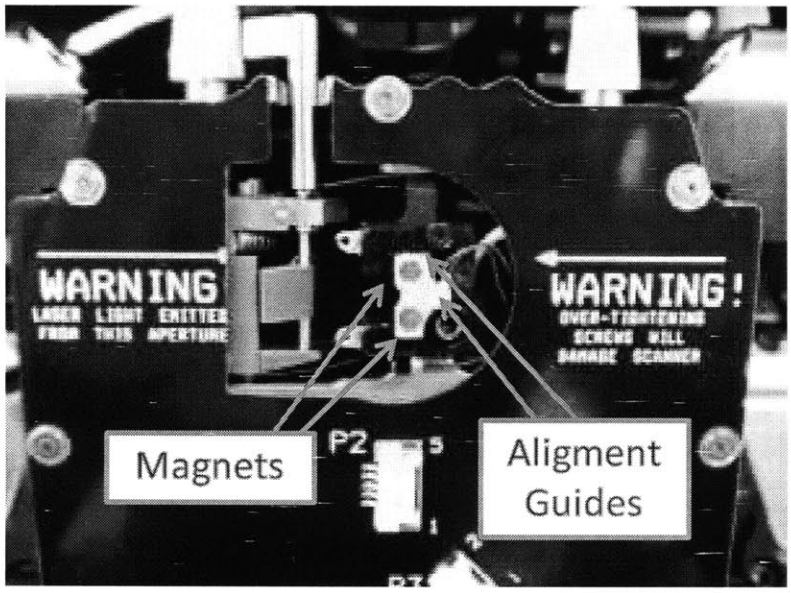

Figure 5.3: DPN 5000 scanner universal mount with magnets and alignment guides for mounting the tool

The tool changing process takes approximately 45 minutes. The purpose of adding the accurate and repeatable fixture to the DPN 5000 was to essentially eliminate all of the set-up time required for aligning the tool. Once the tool is mounted, the entire scanner head assembly that the universal mount is a part of is moved around until the tip is located by a laser. The accurate and repeatable fixture allows for the tip to be placed in the correct position every time, so this step is no longer necessary. Figure 5.4 shows the laser aligned to the tip after the tip was attached to the machine via the accurate and repeatable fixture. The laser is clearly set right at the tip within a few seconds of inserting the tool.

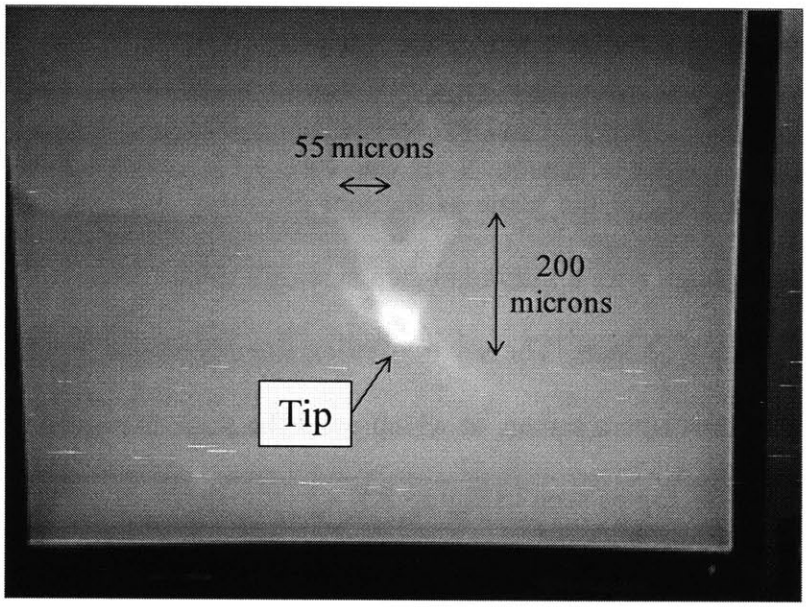

Figure 5.4: Laser positioned accurately on tip, verifying that the fixture provides accurate and repeatable alignment.

5.2 Current Procedure

The method used by NanoInk to align the tool after installation is currently a time consuming and inefficient procedure. After mounting the tool onto the probe holder as explained in Chapter 2, the probe holder must be mounted to the machine. The assembled probe holder is positioned onto the universal mount and is located by the two perpendicular edges. The probe holder is held in place by the two Alnico magnets embedded into the universal mount. The universal mount and its locating features can be seen in Figure 5.3.

After the assembled probe holder is roughly positioned onto the machine, the user turns on a low coherence laser that is used to align the tip of the tool. The laser is watched on a camera so the user can see what the laser is hitting. The DPN 5000 machine has three independently adjustable z axis motors that serve to level the plane of the tool assembly and two x-y stage translating motors to move the x-y stage with a minimum step size of 3 micrometers. The x-y stage has a maximum travel of 1 inch by 1 inch. The x-y translation stage is moved around blindly until the tip comes into view on the camera screen, at which point the stage is moved to center the tip of the tool on the laser spot, as can be seen in Figure 5.5.

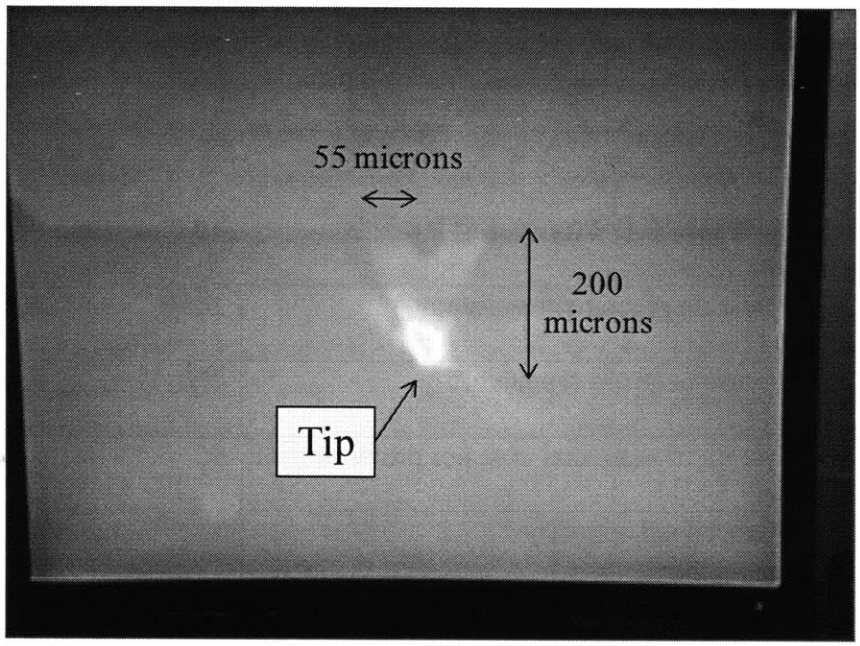

Figure 5.5: Laser spot locating the tip of the tool

NanoInk's current alignment procedure using manual positioning is inefficient and consumes the majority of the changeover time. Reducing this tool installation time is critical for the transition of DPN from nanometer-scale fabrication to manufacturing. The accurate and repeatable fixture reduces the tool installation time from 45 minutes to 15 seconds.

5.3 Overview of Fixture Design

5.3.1 Review of major requirements

The design requirements in this case study are defined by NanoInk for their DPN 5000 machine. The requirements include accuracy of the probe tip location, repeatability of the fixture centroid, incremental cost of the system per probe or tool, fixture load capacity, tool change out time, and

fixture size or envelope. The functional requirements and constraints for the fixture for DPN applications are reviewed in Table 5.1.

Table 5.1: Functional Requirements and Constraints

Probe tip placement accuracy	1000	nm
Fixture centroid repeatability	100	nm
System incremental cost per probe or tool	50	$
Fixture load capacity	1	N
Fixture change-out time	15	s
Calibration time	60	s
Fixture envelope	1.5 x 1.5 x ¼	cm^3

The accuracy and repeatability requirements ensure accurate and repeatable tool placement, thus greatly reducing tool change-out time and improving the overall rate of the process. It is important to achieve a balance of cost and performance with this fixture design so that the improved tool changing process is cost-effective enough that it can be implemented onto all DPN machines. The fixture envelope is critical, as the design of the universal mount is unable to be changed without an array of other intrusive design changes to the machine, so the fixture must fit into the current machine design without redesign of current components. The fixture is shown with the universal mount in Figures 5.6 and 5.7 below.

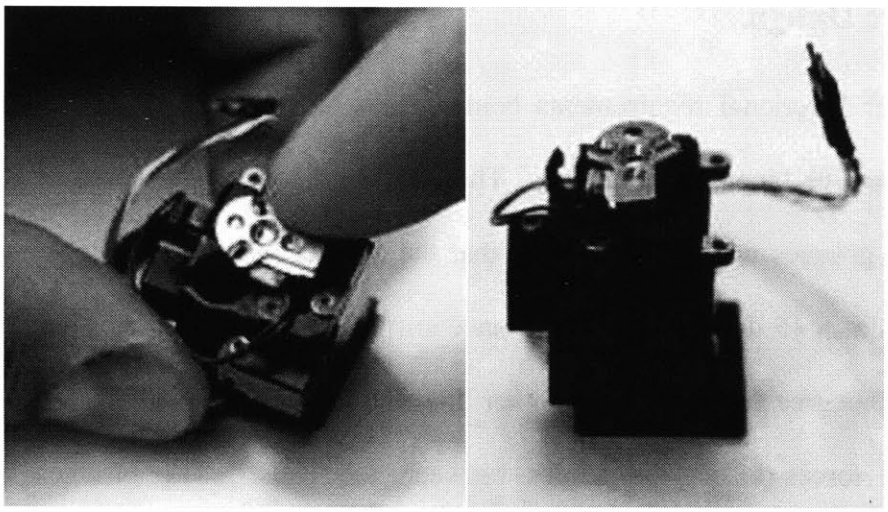

Figure 5.6: Fixture groove side mounted to DPN 5000 universal mount

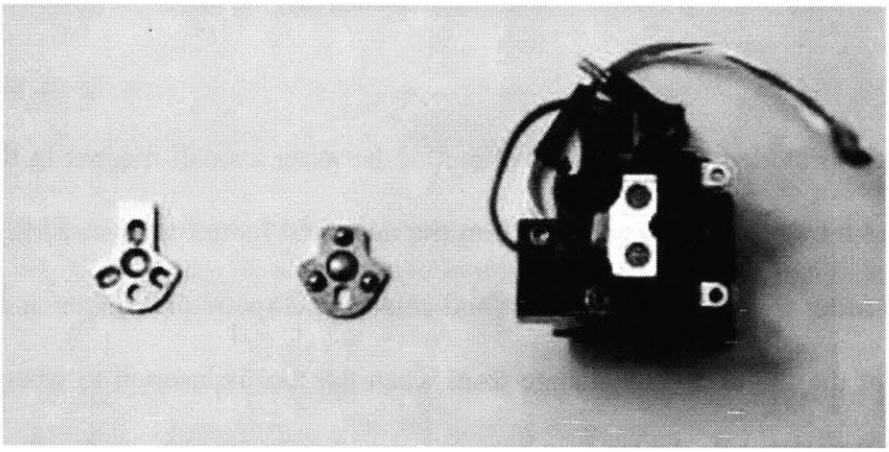

Figure 5.7: Fixture ball and groove sides with DPN 5000 universal mount

An additional consideration to keep in mind when designing NanoInk's fixture was that the DPN writing process may affect the fixture and that the fixture might affect the writing process. During the writing process the fixture would be subjected to severe environmental conditions, including high temperatures, high humidity, and ink vapors. The design must be such that the process does not negatively affect the fixture performance and that the modified mass and stiffness to the machine due to the addition of the fixture would not alter the DPN process.

5.3.2 Fixture Design

With two major functional requirements being repeatability and cost, the fixture design was based on the passive kinematic coupling. The design guidelines presented in Chapter 3 were followed. The grooves were oriented such that the contact force vectors intersect the plane of coupling action at a 45 degree angle to balance stiffness in all directions; therefore the groove faces are at a 90 degree angle from each other. In order to guarantee stability, the normal vectors to the contact forces bisect the angles between the balls. The grooves were arranged symmetrically so that in the event of thermal expansion the coupling center would remain undistorted.

Preload force was provided by a magnetic attraction between a small magnet in the ball side of the coupling and the groove side, which sits on the universal mount magnets. Magnetic preload was selected in order to satisfy the low-cost and small envelope requirements and also because the orientation of the fixture would change from when the tool is inserted to when the tool is in use. Additionally, magnetic preloading was a good choice for this application because the universal mount on the DPN machine provides access to two small Alnico magnets.

The preload force was optimized using the kinematic coupling design spreadsheet shown in Appendix A as well as by magnetic circuit design techniques. There are three magnetic circuits in the fixture design: magnetic flux is generated by the permanent magnet in the ball side of the KC used for preloading the fixture, and there are two identical flux paths that flow between each of the universal mount magnets and the groove side of the KC that provide the holding force to keep the KC mounted to the universal mount. There is a large air gap between the groove side of

the KC and the universal mount magnet, which diminishes the magnetic force that holds the fixture onto the universal mount. The holding force was increased by adding a magnetic shim to decrease the air gap. The magnetic circuit design for the fixture is discussed in detail in Chapter 3. The fixture's magnetic circuit is shown with and without the shim addition in Figures 5.8 and 5.9. Without the shim, the large air gap in the flux path between the universal mount magnet and the groove side of the KC creates a large resistance that decreases the magnetic attraction. With the addition of the shim the air gap, and therefore the resistance, is reduced so the magnetic force is strengthened by a factor of 9.4.

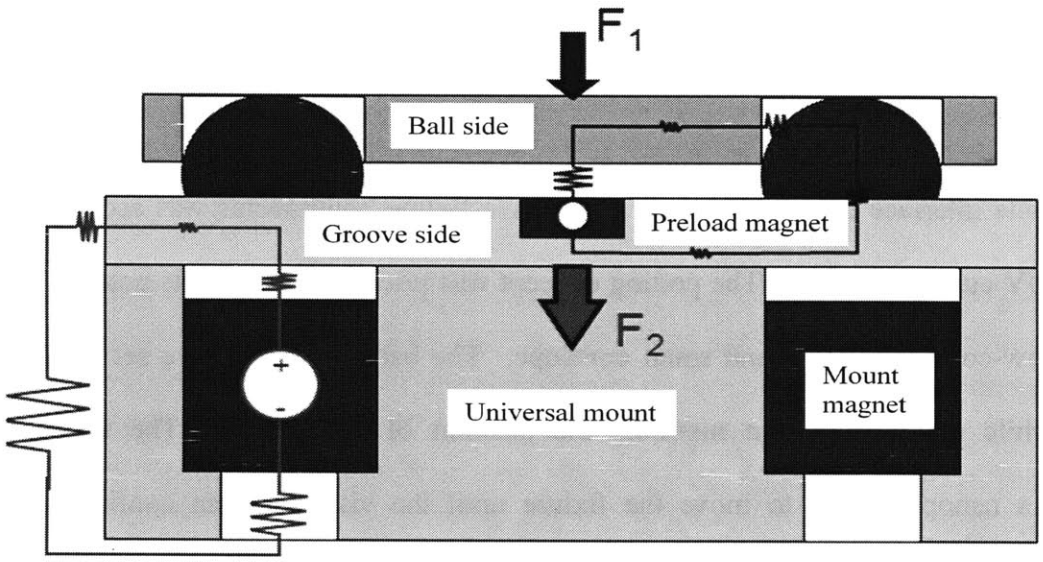

Figure 5.8: KC magnetic circuit model. The large air gap provides a large resistance in the flux loop that decreases the magnetic force.

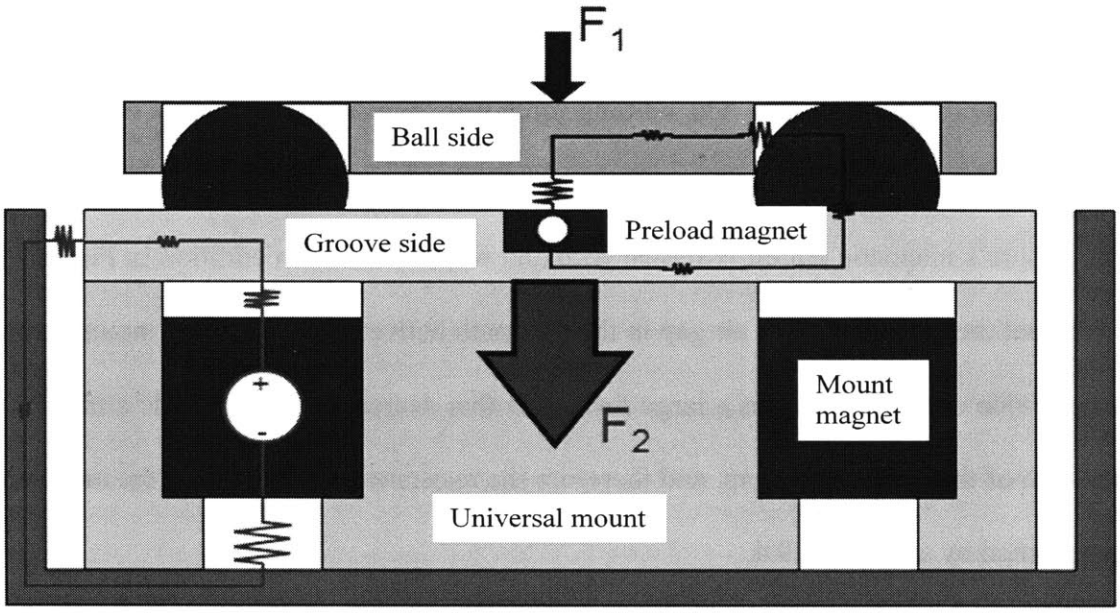

Figure 5.9: KC magnetic circuit model with shim. The air gap is reduced and the magnetic force increased

The adjustable interface between the ball and groove fixture components was accomplished by potting in UV curing adhesive. The potting concept was selected based on its potential for high accuracy, low-cost, simplicity, and small envelope. The balls of the KC are set in UV curing adhesive while a vision system monitors the position of the fixture. The vision system commands a nanopositioner to move the fixture until the vision system confirms that it is properly aligned, at which point the fixture will be flooded with UV light and the balls set permanently in place.

A UV adhesive was selected from the Dymax fiber optical assembly OP-4-20632 series. It is an acrylate urethane adhesive with a reported 0.2% shrinkage after curing. The data sheet for the selected adhesive can be seen in Appendix D. This adhesive was selected based on its low growth of 600 nanometers over 48 hours, which was measured and compared with a variety of

other adhesives. This particular adhesive cures after approximately 20 seconds of light exposure, which is fast for a UV curing adhesive. The quick curing time is important for manufacturing applications such as this one. The results of the measurements are discussed in Chapter 4.

The light source for this application was selected based on the adhesive used. The light source selected is a combination of three small portable UV lights consisting of 21 LED's at a wavelength of 395 nanometers. The three UV lights are arranged such that each light hits the fixture from a different angle, thus maximizing the curing area.

The KC is kinematically constrained to the universal mount via the three points on the back of the groove mount. The back of the groove mount can be seen in Figure 5.10. The two radii along one side of the groove mount align the groove mount to the parallel edge on the universal mount, and the single radius on the perpendicular side aligns the groove mount to the perpendicular side of the universal mount (Figure 5.11). These three points of contact allow the groove mount to be perfectly constrained to the universal mount.

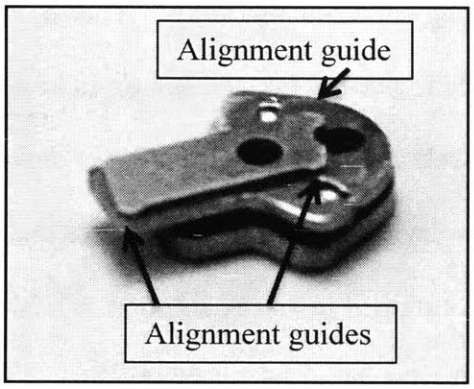

Figure 5.10: Alignment guides on the back side of the groove mount; three points kinematically locate the groove mount to the edges of the universal mount

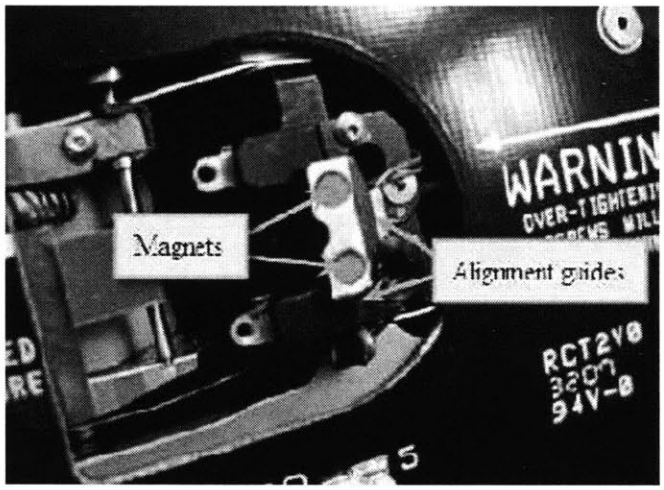

Figure 5.11: DPN 5000 universal mount magnets and alignment guides for mounting the tip

In designing this particular fixture, the conditions in which it was to be used were carefully considered. In the DPN processing environment the fixture would be exposed to various chemicals used for inking the tips, humidity, and heat. For writing with a single tip, the tip is dipped into a solution of the ink. The most common solvents used by NanoInk are methanol, ethanol, acetyl nitrile, isopropenol, DMF, DMSO, and dichloromethane. After dipping the tip the ink is then dried in ambient conditions or in a stream of inert gas, i.e., a nitrogen gun. Another tip inking process involves using universal ink wells. This is NanoInk's method of "controlled" dipping. Microwells are filled with the ink and the tip is lowered into the well for inking. The tip is then taken out of the well and used. Well inking is done on the machine itself, so there is no scope for using inert gas drying. If multiple tip arrays are being used, the inking process is quite different. The tip is not dipped in an ink solution, but is vapor coated with the ink. Vapor coating is done by heating the ink in an enclosed chamber and keeping the tip close to the ink. The temperature during vapor coating is upwards of 70 degrees Celsius and the tips are heated

for 30 minutes to one hour. The chamber during the writing process can get very humid because the ink flows better in humidity.

All of these things had to be considered when designing the fixture. It was important to select an adhesive that is not soluble in any of the solvents used by NanoInk. It was necessary to test iterations of the fixture design to make sure that increased temperatures, humidity, and inks would not negatively affect the performance of the fixture and that the added mass and stiffness that the fixture brings to the machine would not negatively affect the writing process.

The fixture can be seen in Figure 5.12.

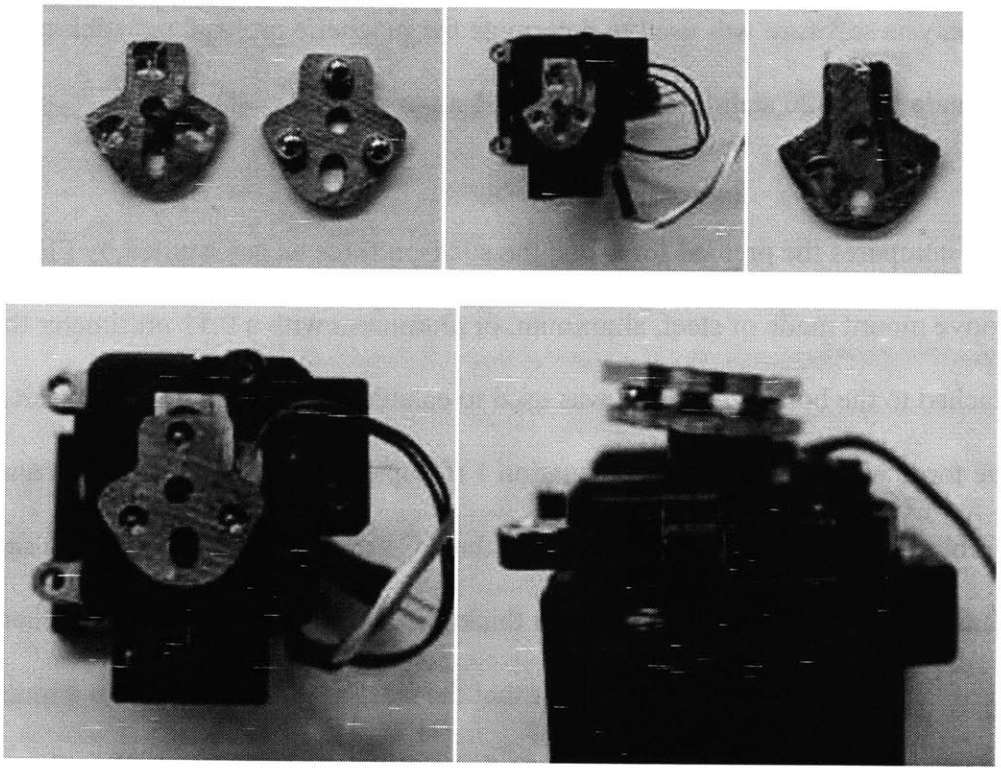

Figure 5.12: Fixture

5.3.3 Device Fabrication

The fixture was fabricated from 6061 aluminum. Material selection of the ball side of the fixture was based on cost, ease of manufacturing, and added mass to the machine. Aluminum best fulfilled these requirements. The two primary materials considered for the groove side of the KC were based on the magnetic circuit design, availability, ease of machining, and resistance to rust. The two materials compared were 420 stainless steel and 6061 aluminum. Aluminum adds less mass and allows for easier machining, which also means lower cost, but is not ferrous, which means the magnetic forces will be depleted as the flux travels through the aluminum. Steel is more difficult to machine, thus increasing cost, but is a ferrous material, therefore increasing both the magnetic preload and the holding force between the groove mount and universal mount. FEMM analysis software was used to determine the magnetic preload and stick-on forces for grooves made from 420 stainless steel and 6061 aluminum.

Table 5.2 compares the preload force and the stick-on force as determined by FEMM analysis for a groove mount made of steel, aluminum, or aluminum with a 0.51 millimeter thick strip of steel attached to the bottom. FEMM was used to calculate the magnetic flux density, *B,* and the attractive force was calculated using Equation 1 (Chapter 3). All of the scenarios analyzed estimate the shape of the universal mount and the KC as rectangular layers of the same thickness and include a stainless steel shim of correct thickness. Each model is identical, other than the material of the groove mount. It was found that the steel groove mount led to a much higher preload force than the aluminum groove model or the aluminum with a 0.51 millimeter thick steel shim, but the stick-on force was only slightly higher than that of the aluminum groove model and slightly less than that of the aluminum with thin steel. Additionally, in the steel

groove mount model, the preload force was more than double that of the stick-on force, which would lead to fixture dismounting. Thus the optimal material for the groove mount was determined to be aluminum, in terms of ease of manufacture, cost, and magnetic preload and stick-on force optimization.

Table 5.2: Preload force and stick-on force compared for steel grooves, aluminum grooves, and aluminum grooves with a steel shim

	Steel Grooves	Al Grooves	Al Grooves +0.51 mm Steel
Preload Magnetic Field (T)	0.60	0.42	0.45
Stick-on Magnetic Field (T)	0.43	0.43	0.44
μ_0	7.9E-08	7.9E-08	7.9E-08
A (m^2)	1.0E-05	1.0E-05	1.0E-05
Preload Force (N)	23.2	11.4	13.3
Stick-on Force (N)	11.9	12.0	12.5

The ball and groove sides of the fixture were cut on a three-axis CNC milling machine. The 2.1 millimeter (0.083 inch) diameter stainless steel balls were a commercially available product. The ball and groove sides of the fixture can be seen in Figure 5.13

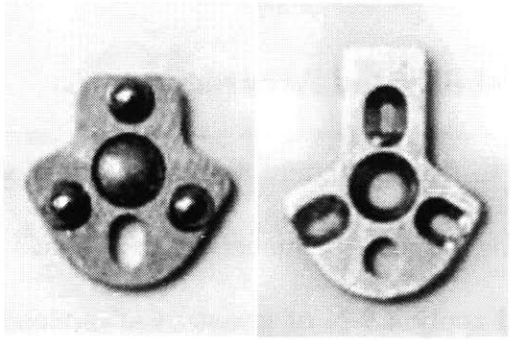

Figure 5.13: Ball and groove sides of the KC fixture

The shim was optimized by Corey Harris, undergraduate student in the Precision Compliant Systems Lab at MIT (41). It was cut from 17-7 precipitate hardened stainless steel due to its ferromagnetic properties, high strength, corrosion resistance, and formability. It was important to use a ferromagnetic material to strengthen the magnetic force between the universal mount and the fixture. The high ultimate tensile strength to yield strength ratio made it possible to bend the shim tabs up without material failure. The shim was cut from 0.41 mm (0.016 inch) 17-7 PH steel using a CNC milling machine and bent to the correct angle after manufacturing. The shim is shown in Figure 5.14.

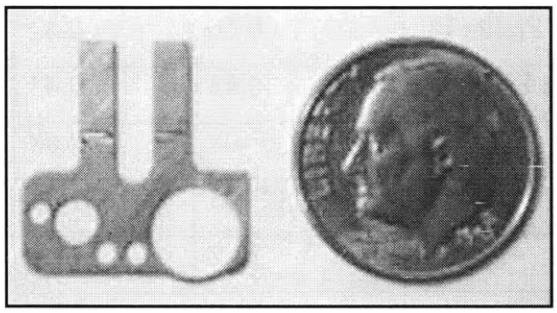

Figure 5.14: Magnetic shim cut from 0.41 mm 17-7 PH stainless steel

5.4 Validation

5.4.1 Measuring Repeatability and Accuracy

A test fixture was assembled so that the fixture repeatability and accuracy could be measured. Preload was achieved for testing purposes by mounting the ball side of the kinematic coupling to a large steel block that would apply 4.9 N of gravitational preload force to the coupling. The

groove side of the coupling was fixed to an aluminum plate that was bolted to an air table. The ball and groove sides of the coupling are pictured before testing in Figure 5.15.

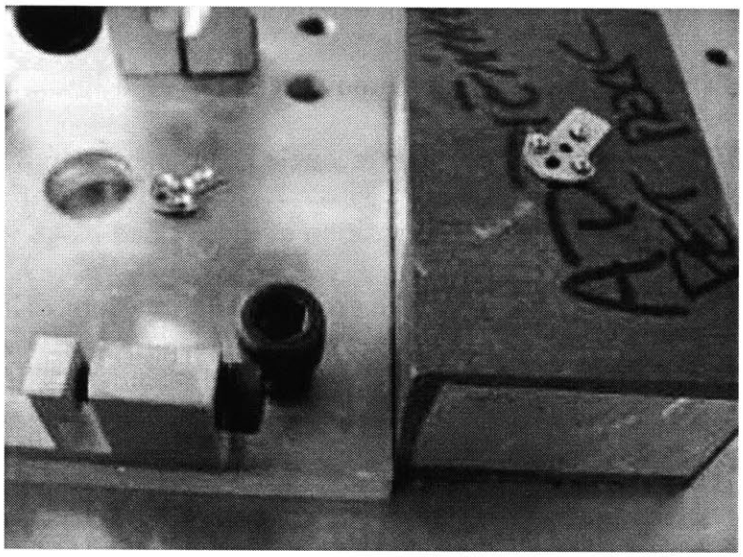

Figure 5.15: Fixture repeatability and accuracy validation set-up. The groove side of the KC is rigidly mounted to a plate that is bolted to an air table (left) and the ball side is rigidly mounted to a preload weight (right).

The system was bolted to an air table to eliminate vibrations. High pressure grease was used at the ball-groove interface to reduce friction and contact wear, allowing the ball to settle into its lowest energy state in the groove. Noise in the system was determined by measuring variations in position as the test system sat still; the noise measured to be on the order of 30 nanometers. In order to reduce the random noise, the system was grounded by attaching one end of a copper wire to the aluminum block and the other end to ground. The system was also surrounded by an aluminum foil cover to reduce any electrical noise. The grounding and aluminum foil cover reduced the noise in the system to the order of 10 nanometers.

Repeatability was measured by coupling and uncoupling the KC through 50 cycles and measuring the position of the ball side of the KC after each cycle. The ball mount was uncoupled and recoupled using a wooden dowel to lift the coupling so as not to allow any thermal energy to enter the system. The order of engagement of the ball and groove surfaces was kept constant: the balls were lifted off of the grooves and replaced in the same order for each testing cycle. The fixture was uncoupled and recoupled 50 times and allowed 60 seconds to settle between each measurement cycle. The position of the preload block was measured by six capacitance probes in order to measure motion in six degrees of freedom. The 200 point average displacement over a 10 second time period was measured and recorded. The capacitance probes were arranged as shown in Figure 5.16.

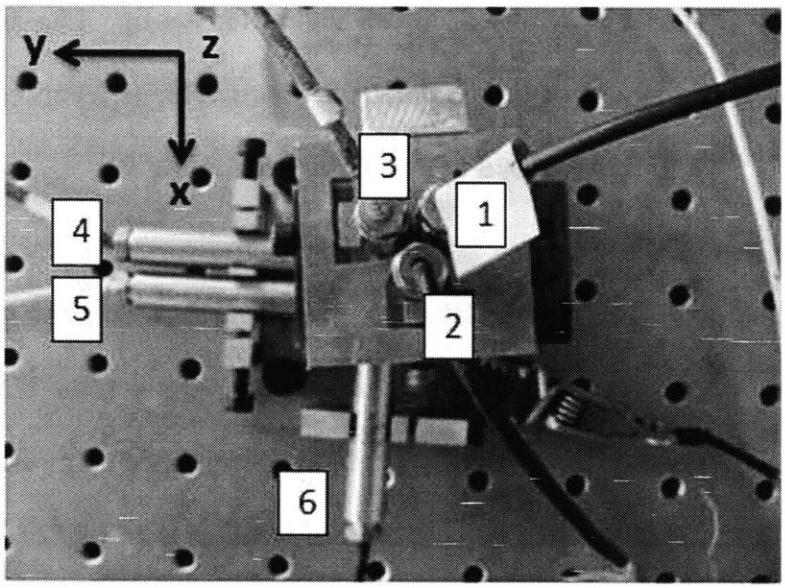

Figure 5.16: Capacitance probe arrangement for repeatability and accuracy validation

Probes 1, 2, and 3 were clamped by adjustable flexures to a plate above the KC, measuring the out of plane position of the coupling. Probes 4 and 5 were mounted to one side of the preload

block, measuring the in plane position, and probe 6 was secured at a 90 degree angle from probes 4 and 5, also measuring in plane position. The experimental set-up can be seen in Figure 5.17.

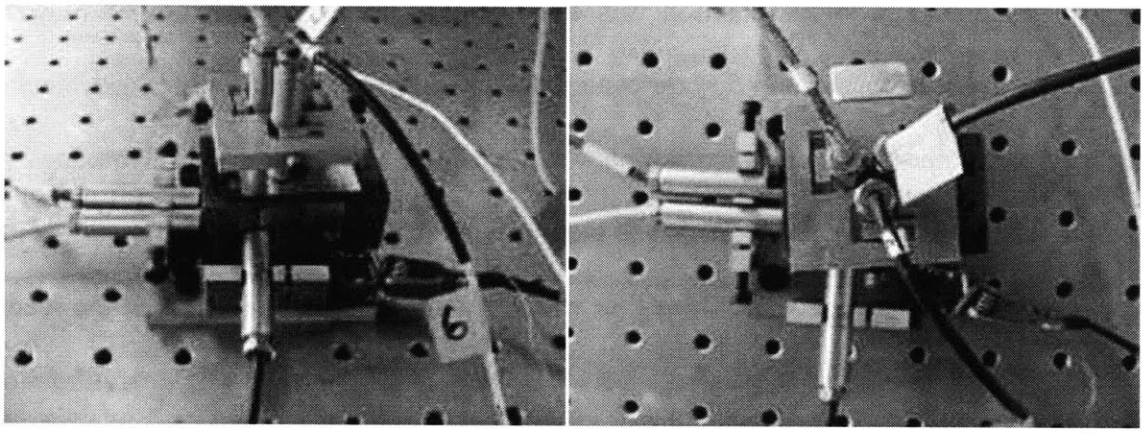

Figure 5.17: Experimental set-up

The coupling surfaces were thoroughly cleaned using compressed air and lubricated with grease/tap magic cutting fluid in order to reduce any additional friction on the coupling interface.

The accuracy was measured by monitoring the stability of the KC over time. The same capacitance probe and preload block set-up was used to measure the KC accuracy. The KC was coupled and measured for 48 hours with a measurement made every second.

The data was collected using LabView data acquisition software. The low resolution calibration of the capacitance probes is 12.5 microns/volt.

5.4.2 Experimental Results

The coupling repeatability in 6 degrees of freedom was calculated from the raw data collected from the six capacitance probes over 50 coupling cycles. The probes are numbered and arranged as shown in Figure 5.17. The x-axis position was obtained directly from the reading from capacitance probe 6. The y-axis position was calculated as the average of the readings from probes 4 and 5 since probes 4 and 5 were centered around the center of the preload block and parallel with each other. The z-axis position was calculated as the average of readings from probes 1, 2, and 3 since probes 1, 2, and 3 were arranged in an equilateral triangle centered around the center of the cube. The θ_x position was calculated by the difference in the readings from probes 3 and 1 divided by the distance between them, using a small angle approximation to approximate the tangent of the angle θ_x as θ_x. The θ_y position was calculated by the difference in the readings between probe 2 and the average reading of probes 1 and 3 divided by the distance between probe 2 and the center between probes 1 and 3. The θ_z position was calculated by the difference in the readings from probes 4 and 5 divided by the distance between probes 4 and 5.

The mean data values were calculated and the readings were normalized to the mean values. The displacements from the mean reading in six degrees of freedom were plotted. Results of the repeatability tests are summarized in Figures 5.18-5.23 with error bars according to the noise in the system. The three-dimensional repeatability in x, y, and z was also calculated by taking the square root of the sum of the squared x, y, and z displacements. The three-dimensional repeatability was normalized to the mean and plotted in Figure 5.24. The repeatability was measured by one standard deviation and three standard deviations from the mean of the data. The 1-σ and 3-σ repeatability in each degree of freedom is summarized in Table 5.3.

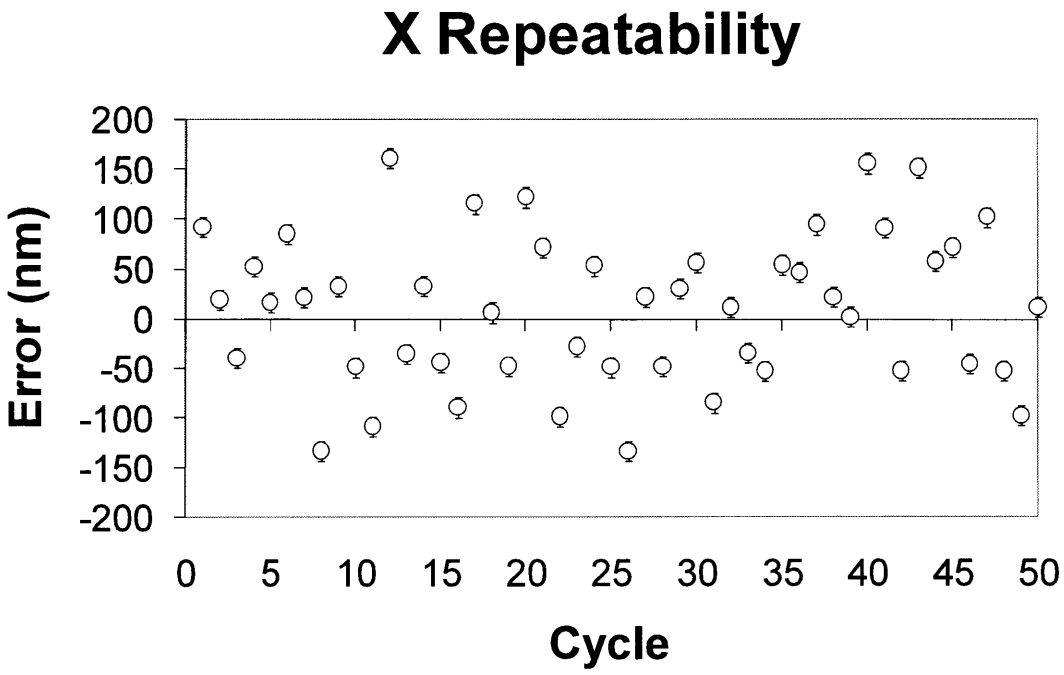

Figure 5.18: X-axis repeatability measurements

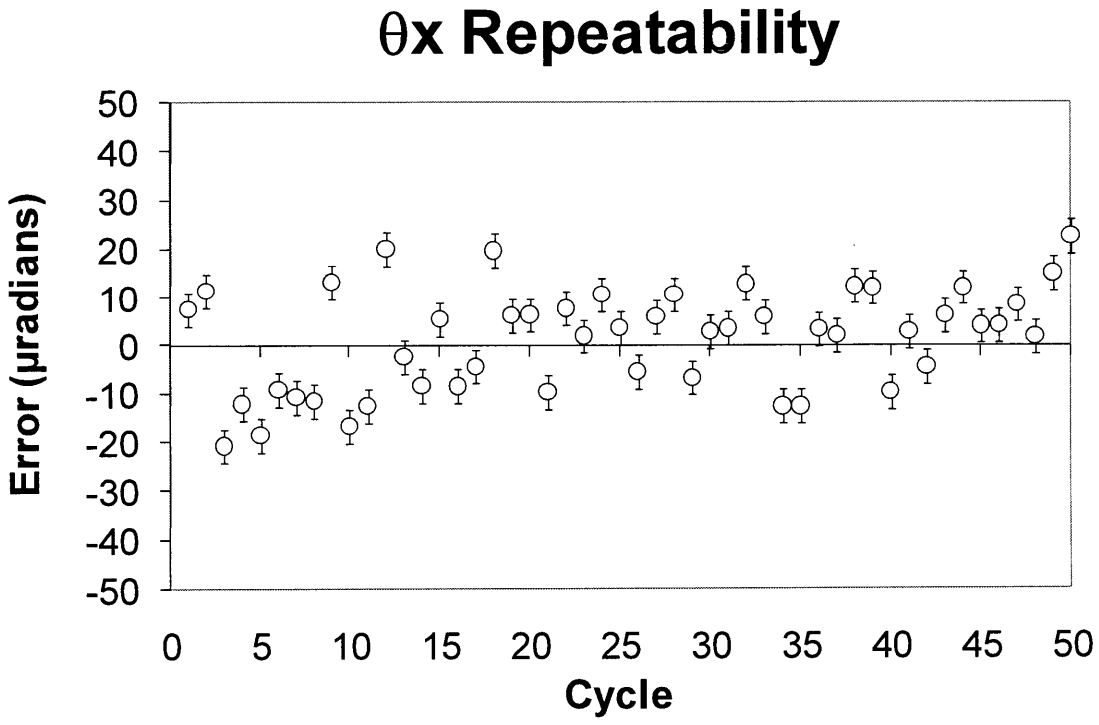

Figure 5.19: θ_x-axis repeatability measurements

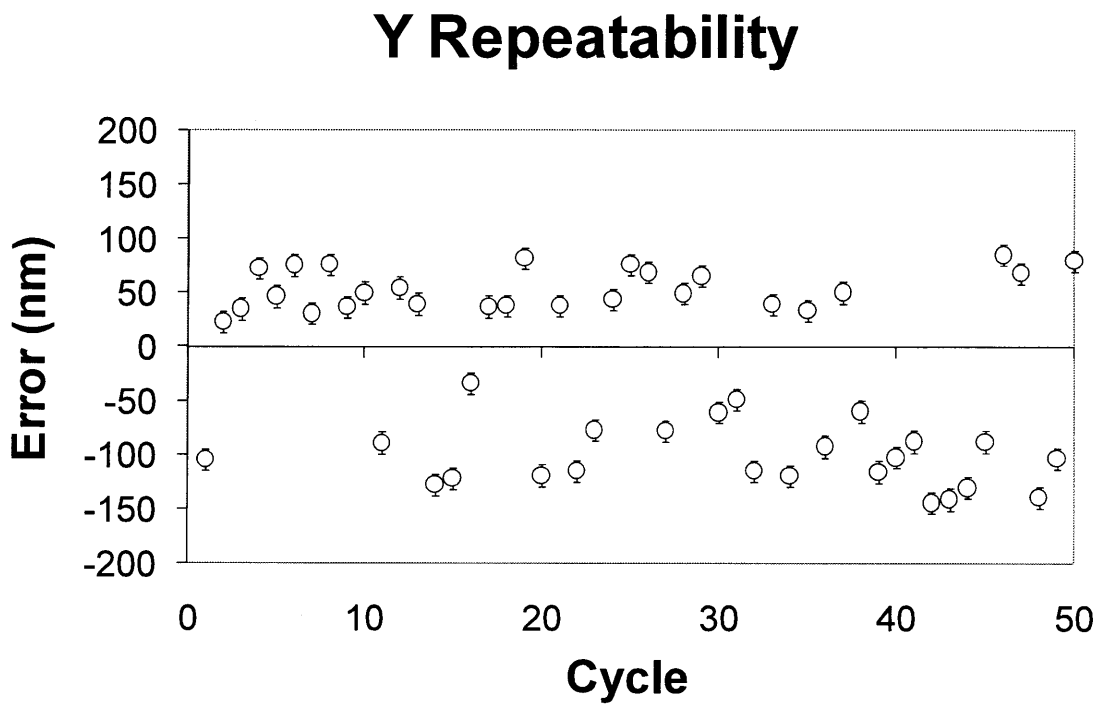

Figure 5.20: Y-axis repeatability measurements

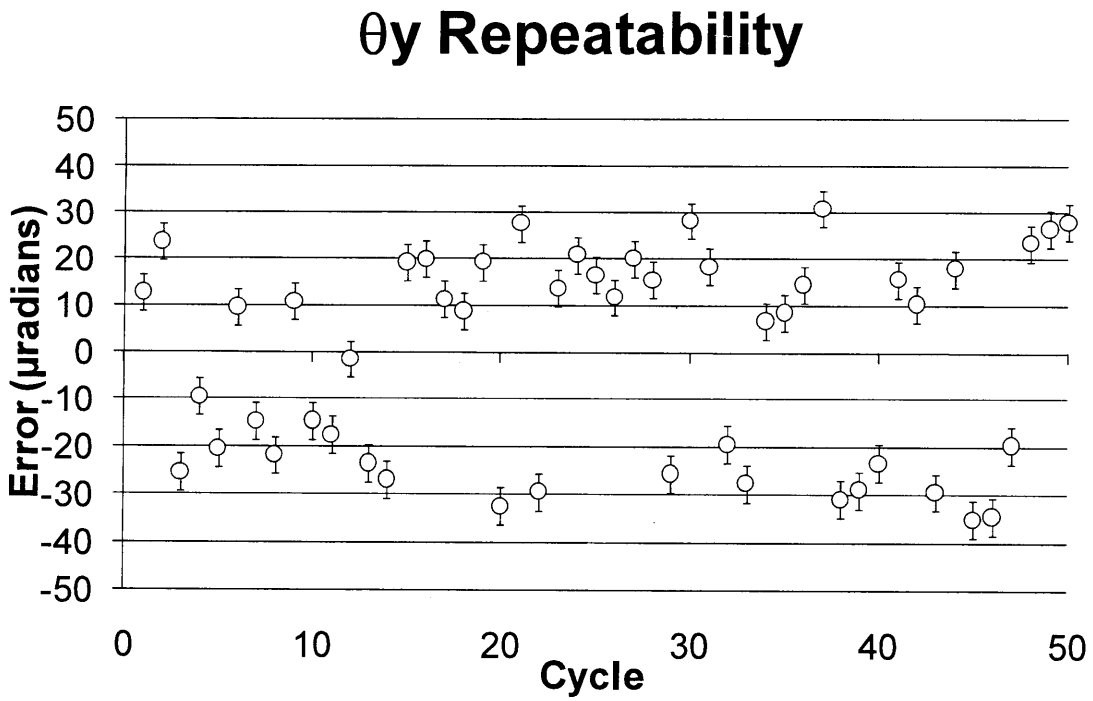

Figure 5.21: θ_y-axis repeatability measurements

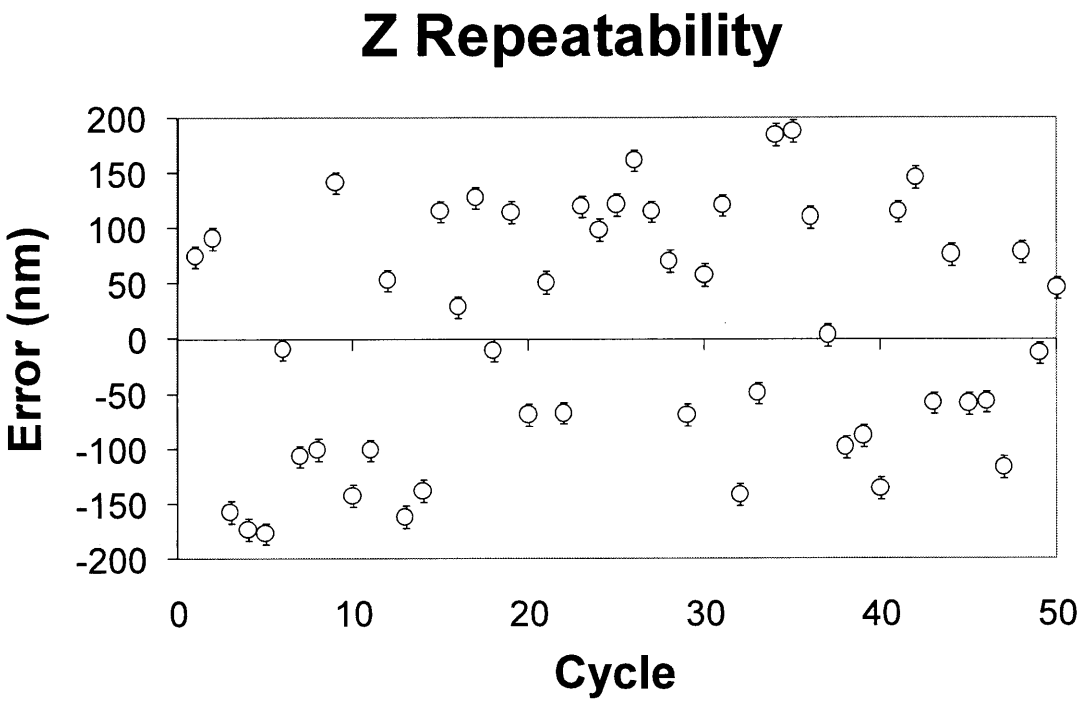

Figure 5.22: Z-axis repeatability measurements

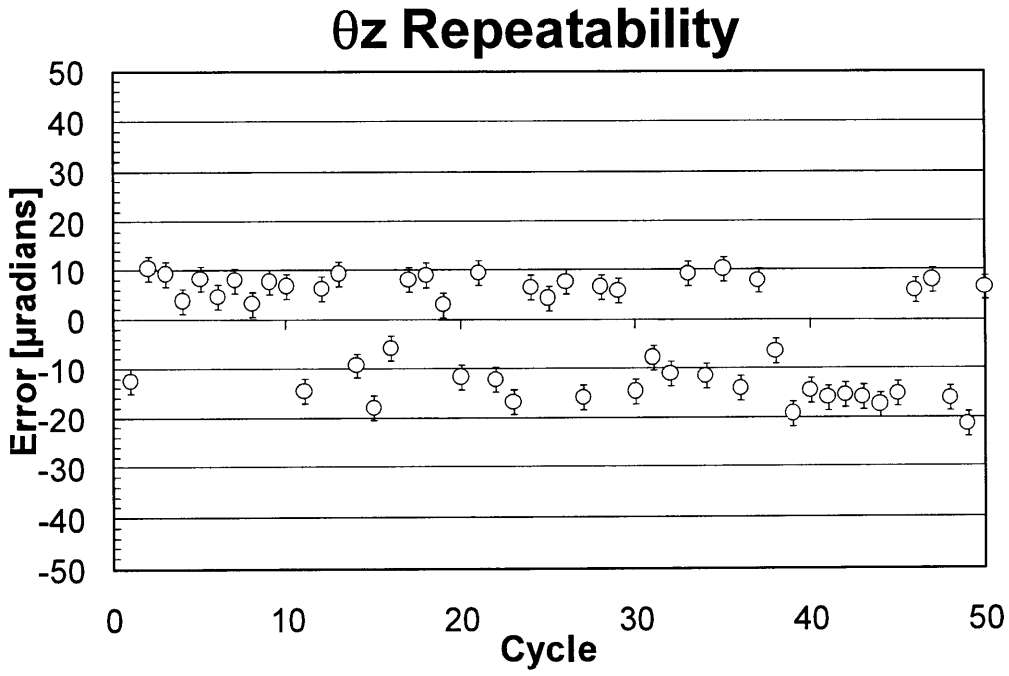

Figure 5.23: θ_z-axis repeatability measurements

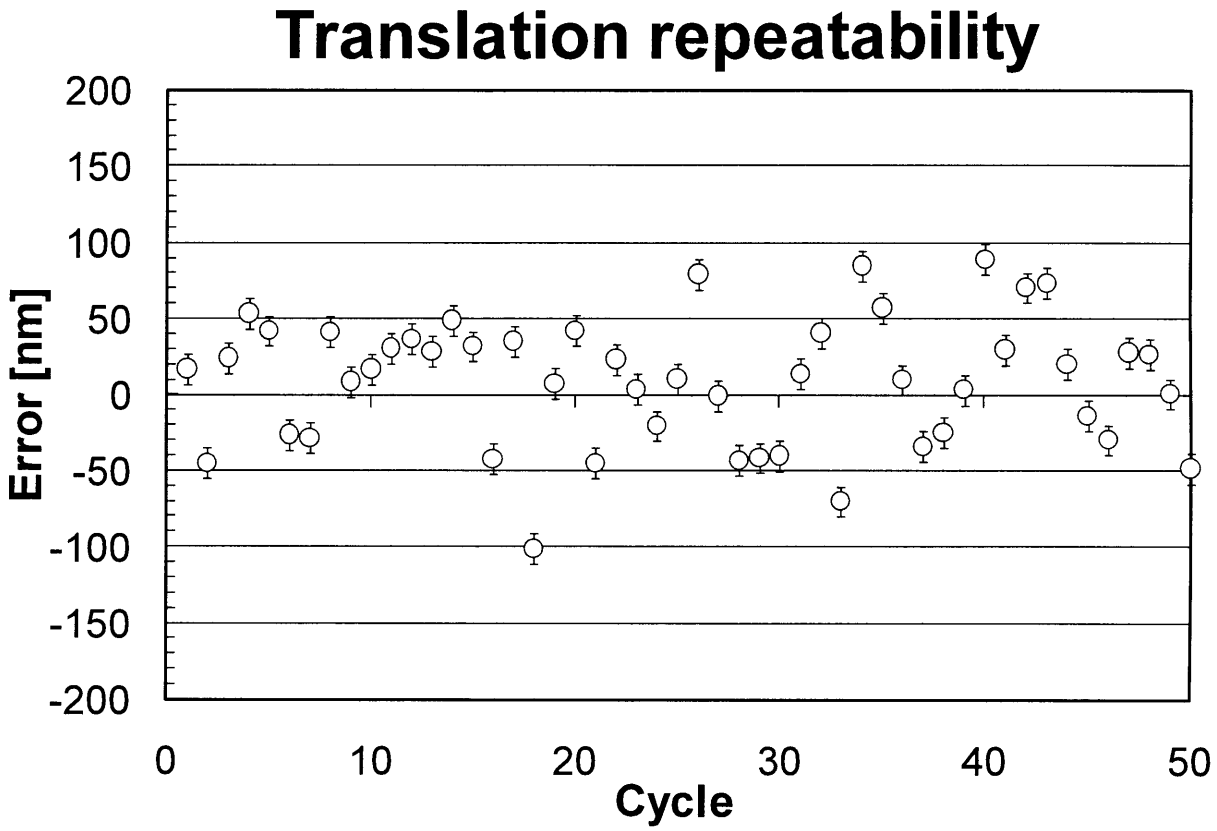

Figure 5.24: 3-D translation repeatability measurements

Table 5.3: 1-σ and 3-σ Repeatability Summary

	X(μm)	Y(μm)	Z(μm)	θ_x(μrad)	θ_y (μrad)	θ_z (μrad)	3D(μm)
σ	0.087	0.092	0.120	10.3	22.0	11.1	0.087
3σ	0.261	0.276	0.360	30.4	66.0	33.2	0.261

The KC stability is plotted over 48 hours in six degrees of freedom in Figures 5.25-5.30. The 3-dimensional translational stability was calculated to be 344 nanometers. The six-axis stability is summarized in Table 5.4.

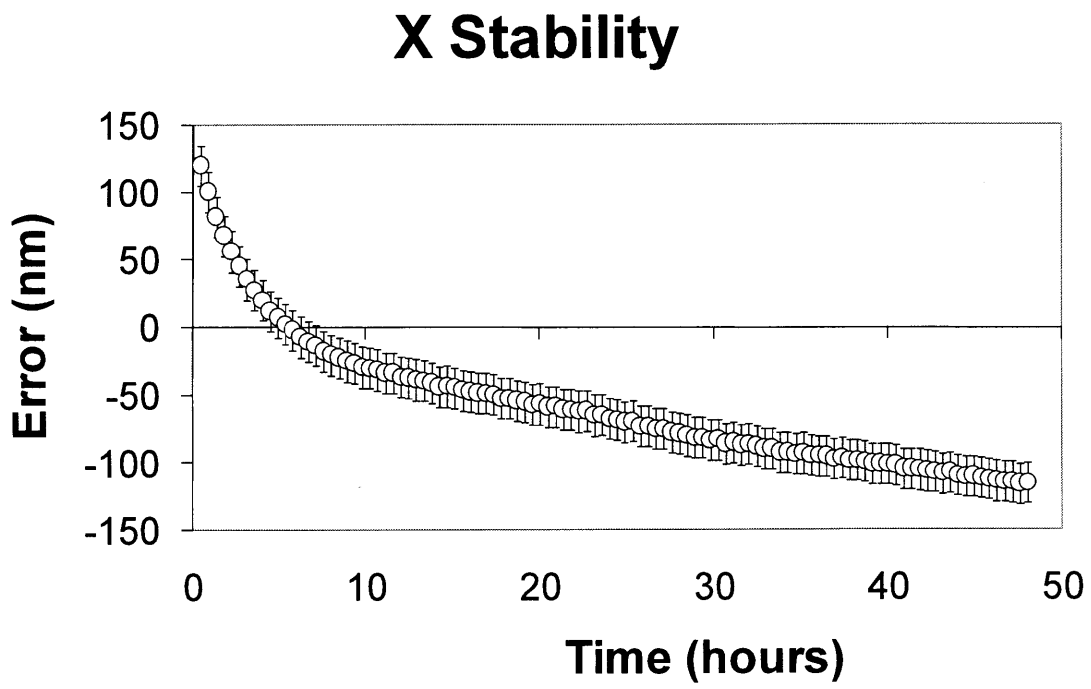

Figure 5.25: X-axis stability measurements

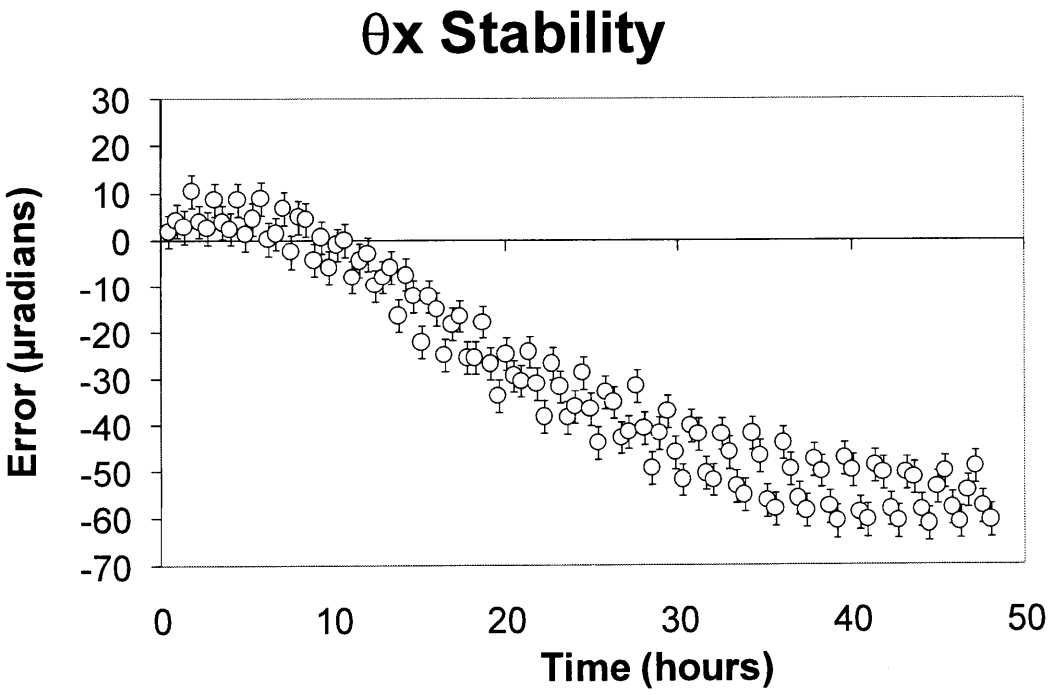

Figure 5.26: θ_z-axis stability measurements

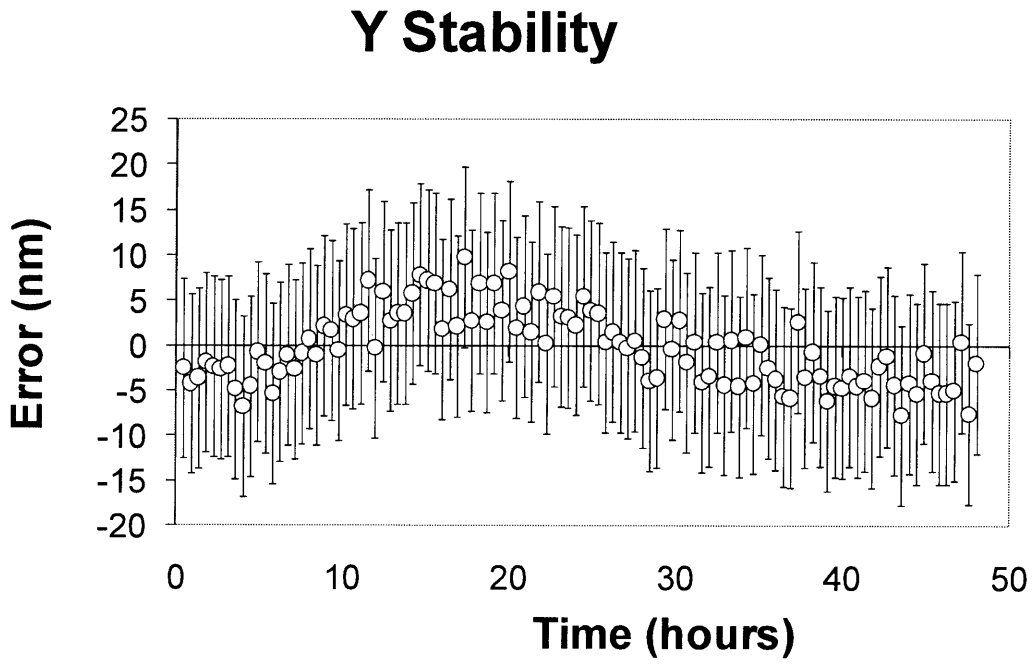

Figure 5.27: Y-axis stability measurements

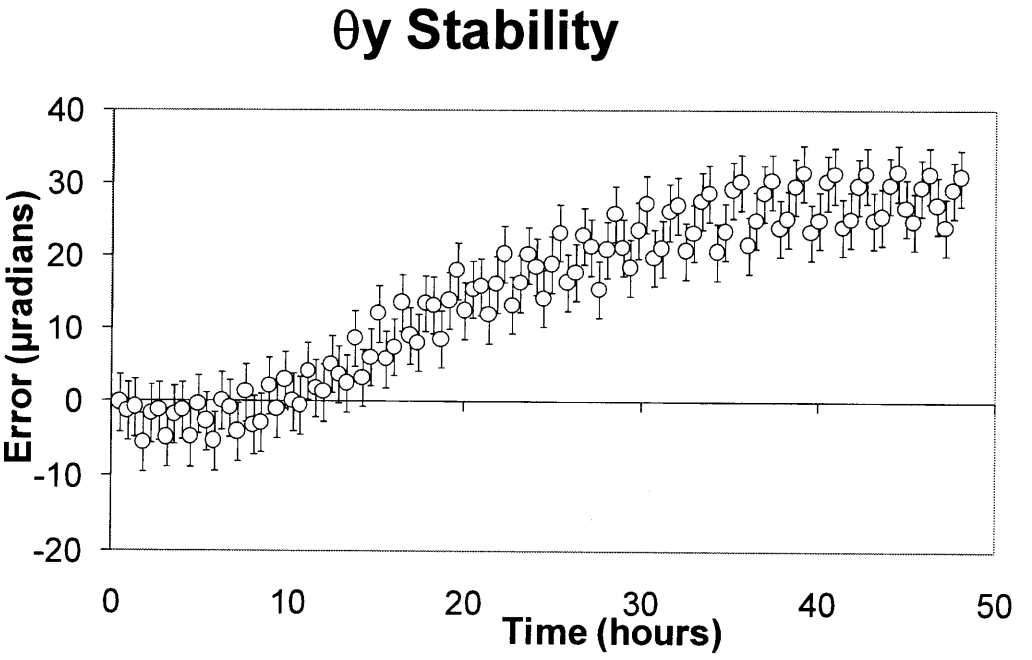

Figure 5.28: θ_y-axis stability measurements

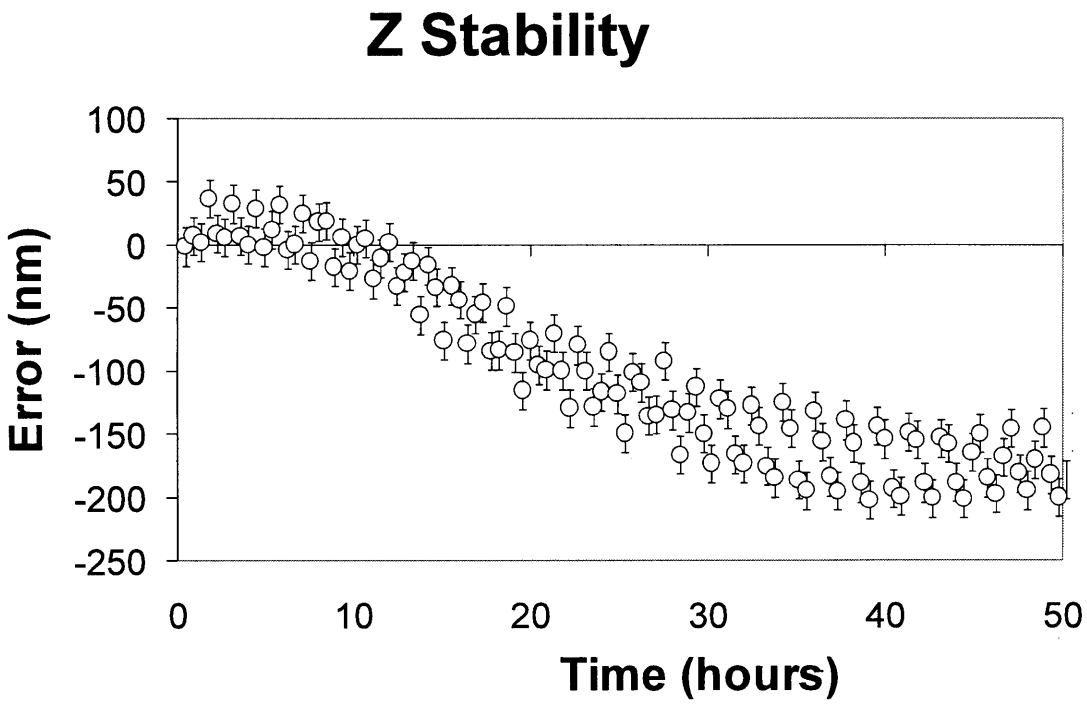

Figure 5.29: Z-axis stability measurements

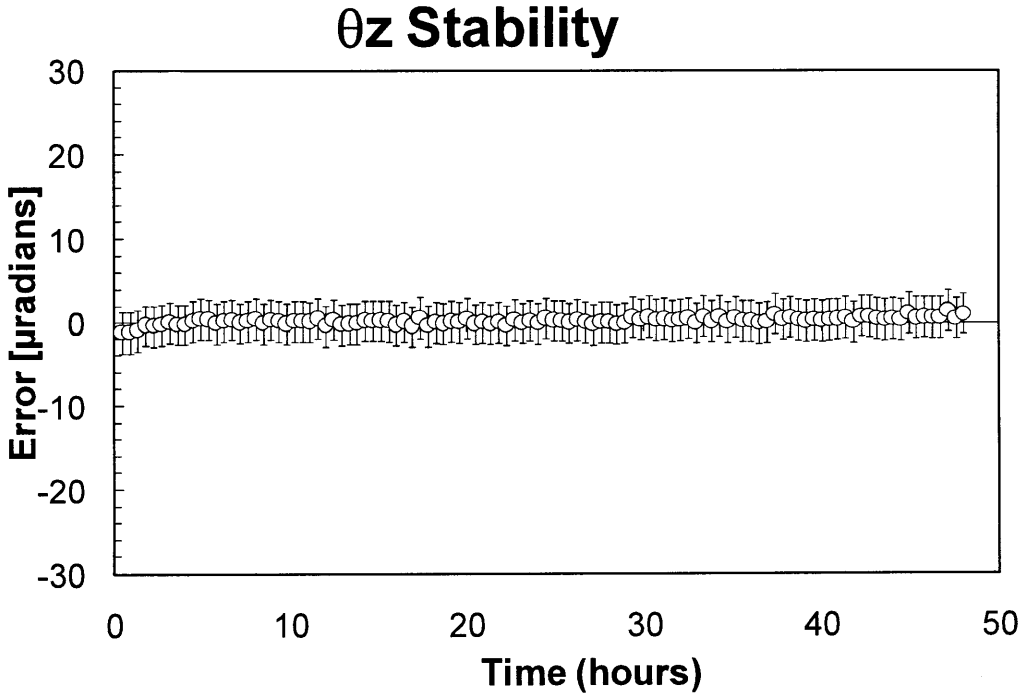

Figure 5.30: θ_z-axis stability measurements

Table 5.4: Stability Summary

	X(μm)	Y(μm)	Z(μm)	θ_x(μrad)	θ_y (μrad)	θ_z (μrad)	3D(μm)
Error	0.236	0.017	0.250	79.8	40.6	2.63	0.344

5.4.3 Discussion of Results

The repeatability measurements show a typical distribution. The 1-σ translational repeatability was approximately 100 nanometers, which meets the functional requirements of the fixture. The repeatability in the z-direction was the highest of the translational repeatabilities, at 120 nanometers. This is not problematic since the z direction is the least critical dimension for mounting the tools for NanoInk's DPN 5000 machine.

The 3-dimensional translational stability was measured to be approximately 350 nanometers, which exceeds the functional requirement for accuracy of the fixture. The displacement in all degrees of freedom had stabilized after 48 hours, so any instabilities were likely due to movement in the adhesive after curing. The z-direction had the greatest error, which makes sense because the adhesive was applied symmetrically around the balls and was constrained in the x and y directions by the edges of the holes. The z-direction was unconstrained and therefore the coupling was able to move in z. The error in the z direction was measured to be 250 nanometers in the negative direction. This does not agree with the measurement of the adhesive shrinkage presented in Chapter 4. The measurements of the adhesive bonding two metal plates described expansion of the adhesive, which was attributed to absorption of humidity from the environment. The expansion measured in Chapter 4 was approximately 600 nanometers, while the shrinkage measured by the stability of the fixture was 250 nanometers. The difference could

be attributed to the differences in set-up or environmental factors. The 4.9 N of preload added on top of the adhesive removed the degree of freedom in the positive z direction, so the adhesive expanded in the negative z direction; or the shrinkage of the adhesive may have been greater than the water absorption, causing the overall error to be in shrinkage.

The stability measurements in θ_x, θ_y, and z include a periodic cycling that is possibly caused by temperature cycling every 15 minutes in the room where the measurements were taken. This suggests that the fixture is most repeatable in a temperature controlled environment, such as NanoInk's DPN 5000 is.

CHAPTER 6

CONCLUSIONS

6.1 Recap of Research Objectives

The purpose of this research was to generate the knowledge, technology, and methods required to design and engineer small scale fixtures with 1 micron accuracy and 100 nanometer repeatability using potting and magnetic preload. This thesis includes the design and fabrication of the adjustable kinematic fixturing hardware, as well as the development of the UV cure potting process to set the fixture's position after being adjusted by a micro vision assembly station. The design rules outlined in this thesis can be applied to general fixture design for small scale accurate and repeatable kinematic fixtures.

The import of this work is that it produces a low-cost method of part and tool alignment in nano-scale manufacturing equipment. Accurate and repeatable fixturing technology helps enable a fabrication process to become a manufacturing process by improving the rate, cost, quality, and flexibility of the process.

The impact of this research is a general technology that improves (i) rate, cost, quality, and flexibility in nanomanufacturing & (ii) quality and speed of measurement in instruments and

research. This fixturing technology allows the adaptation of small scale fabrication equipment to manufacturing applications.

6.2 Research Accomplishments

The outcomes of this research include an optimized design and prototype of a centimeter-scale detachable kinematic fixturing system for probe-based nanomanufacturing equipment that has been measured to have 1 micron accuracy and 100 nanometer repeatability. The repeatability and accuracy achieved by the fixture enables quick and elegant precision alignment of nanomanufacturing tools with respect to parts and equipment, thus allowing fabrication to become probe-based nanomanufacturing. This fixture is a platform technology that can be implemented in numerous possible applications, including probe-based nanomanufacturing, optics, wafer processing, and small-scale machine design. The fabricated fixture is shown in Figure 6.1 mounted to the DPN 5000 machine universal mount. An exploded view of the fixture can be seen in Figure 6.2.

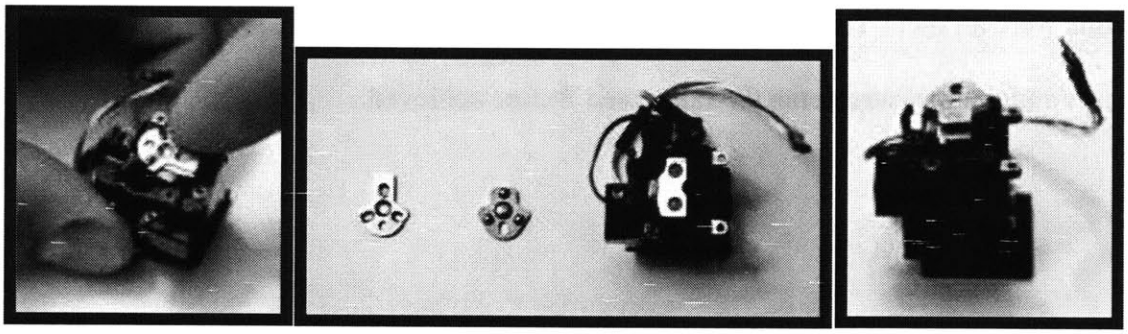

Figure 6.1: Accurate and repeatable kinematic fixture prototype mounted to a universal scanner mount of a DPN machine

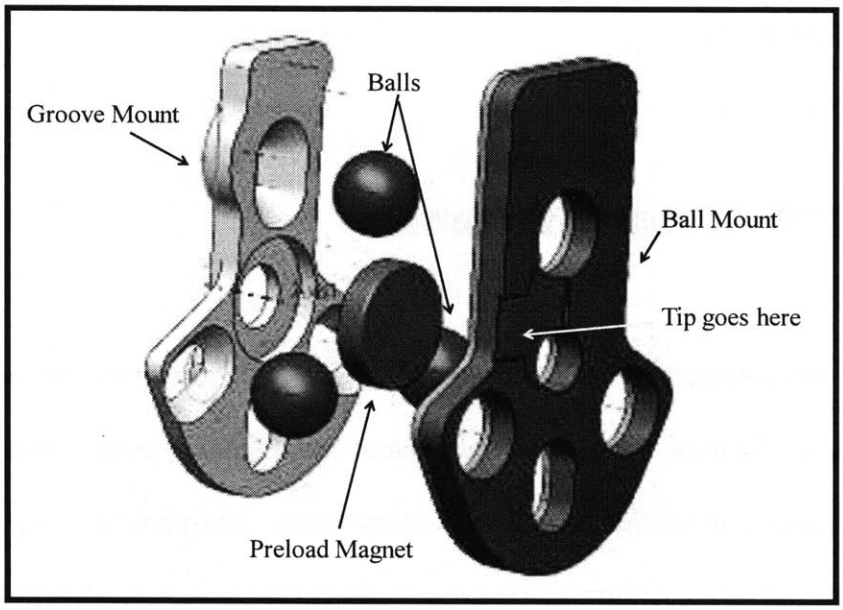

Figure 6.2: Accurate and repeatable kinematic fixture CAD model exploded view

The fixture was required to have an accuracy of 1 micrometer and a repeatability of 100 nanometers. The achieved accuracy was measured to be 344 nanometers and the achieved 3-dimensional translational repeatability was measured to be 87 nanometers. Both the accuracy and repeatability requirements were exceeded. The remaining functional requirements and constraints were all met. Table 6.1 summarizes the fixture functional requirements and constraints and the measurements the fabricated fixture achieved.

Table 6.1: Functional Requirements and Constraints

Functional Requirement or Constraint	Required	Achieved
Probe tip placement accuracy	1000 nm	**344 nm**
Fixture centroid repeatability	100 nm	**87 nm**
System incremental cost per probe or tool	$50	$50
Fixture load capacity	1 N	1 N
Fixture change-out time	15 s	15 s
Calibration time	60 s	60 s
Fixture envelope	1.5 x 1.5 x ¼ cm^3	1.5 x 1.5 x ¼ cm^3

Previous accurate and repeatable kinematic couplings that meet this cost requirement have achieved accuracy to approximately 2-3 micrometers and repeatability to approximately 300-500 nanometers. The fixture designed in this thesis was measured to be accurate to 344 nanometers, an order of magnitude improvement. The repeatability was measured to be 87 nanometers, which is 4 times more repeatable than previously achieved.

6.3 Future Work

6.3.1 Flexural Elements

The repeatability of small scale kinematic couplings can be improved dramatically by utilizing flexures. Flexures were not implemented in this thesis because the size constraints did not allow for low-cost easily manufacturable flexural elements to be made. A way to make low-cost flexures at this scale will be useful in improving upon the fixtures designed in this thesis.

6.3.2 Automation

Automating the visual inspection and positioning components of the assembly station will make the assembly process faster and more reliable. The vision system, nanopositioner, and adhesive dispensing can all be automated.

6.3.3 Modeling Shrinkage

The fixture accuracy could be improved if the shrinkage of the adhesive was properly compensated for. The shrinkage of the adhesive used in this thesis was measured with capacitance probes in six-degrees of freedom over a 48 hour time period. A model to determine the shrinkage without measuring would be useful in selecting the proper adhesive to use in specific applications as well as for being able to predict the motion of the fixture over time after the adhesive cures. This would allow for the shrinkage to be compensated for in the fixture design, thus improving the fixture accuracy.

6.3.4 Refine Magnetic Model

The magnetic model utilized in designing the fixtures for the purposes of this thesis is based on basic magnetic circuit design theory and FEMM software modeling. The model should be refined to incorporate more complex magnetic circuit design. A refined magnetic model would make the magnetic circuit design and magnetic preload calculations more accurate, thus making the repeatability of the fixture more predictable.

REFERENCES

1. **Gest, G, et al.** *Review of fast tool change systems.* 1995, Computer Integrated Manufacturing Systems, Vol. 8, pp. 205-210.

2. **Vallance, R, Morgan, C and Slocum, A.** *Precisely positinoing pallets in multi-station assembly systems.* 2004, Precision Engineering, Vol. 28, pp. 218-231.

3. **Culpepper, M.** *Design and Application of Compliant Quasi-Kinematic Couplings.* Department of Mechanical Engineering, Massachusetts Institute of Technology. 2000.

4. **Culpepper, M.**. ASPE 2007 Kinematic Coupling Tutorial.

5. **Schouten, CH and Rosielle, JN, Schellekans, PH.** *Design of a Kinematic Coupling for Precision Applications.* 1997, Precision Engineering, Vol. 20, pp. 46-52.

6. **Hale, LC and Slocum, AH.** *Optimal Design Techniques for Kinematic Couplings.* 2001, Precision Engineering, Vol. 20, pp. 114-127.

7. **Slocum, AH and Donmez, A.** *Kinematic Couplings for Precision Fixturing--Part I: Formulation of Design Parameters.* 1988, Precision Engineering, Vol. 10, pp. 85-91.

8. **Taylor, James and Tu, Jay.** *Precision X-Y microstage with maneuverable kinematic coupling mechanism.* 1996, Precision Engineering, Vol. 18, pp. 85-94.

9. **Culpepper, M, Kartik, M and DiBiasio, C.** *Design of integrated eccentric mechanisms and exact constraint fixtures for micron-level repeatability and accuracy.* 2005, Precision Engineering, Vol. 29, pp. 65-80.

10. **Slocum, AH.** *Design of three-groove kinematic couplings.* 1992, Precision Engineering, Vol. 14, pp. 67-76.

11. **Watral, Adrienne.** *Design of a Low-Cost, Meso-scale, Detachable Fixturing System for Probe-based Nanomanufacturing Equipment and Instruments.* Department of Mechanical Engineering, Massachusetts Institute of Technology. 2009.

12. **Hale, Layton.** *Principles and Techniques for Designing Precision Machines.* Department of Mechanical Engineering, Massachusetts Institute of Technology. 1999.

13. **Varadarajan, Kartik and Culpepper, Martin.** *A dual-purpose positioner-fixture for precision six-axis positioning and precision fixturing Part I. Modeling and design.* 2007, Precision Engineering, Vol. 31, pp. 276-286.

14. **Varadarajan, Kartik and Culpepper, Martin.** *A dual-purpose positioner-fixture for precision six-axis positioning and precision fixturing Part II. Characterization and calibration.* 2007, Precision Engineering, Vol. 31, pp. 287-292.

15. **Culpepper, Martin, Araque, Carlos and Rodriguez, Marcos.** *Design of Accurate and Repeatable Kinematic Couplings.*

16. **Piner, R.** *Dip-Pen Nanolithography.* 1999, Science, Vol. 283, pp. 661-663.

17. **NanoInk.** NanoInk. [Online] 2010. http://www.nanoink.net.

18. **Slocum, AH.** *Precision Machine Design.* Englewood Cliffs : Prentice-Hall, 1992. pp. 401-412.

19. **Precision Engineering Research Group, MIT.** Kinematic Couplings Website. [Online] http://pergatory.mit.edu/kinematiccouplings/index.htm.

20. **Taylor, John.** *An Introduction to Error Analysis: The Study of Uncertainties in Physical Measurements.* Sausalito : University Science Books, 1997.

21. **Oberg, et al.** *Machinery's Handbook 25th Edition.* s.l. : Industrial Press, 1997.

22. **Vallance, R, Morgan, C and Slocum, AH.** *Precisely positioning pallets in multi-station assembly systems.* 2004, Precision Engineering, Vol. 28, pp. 218-231.

23. **Goedertier, PV.** *Unitary Q-switch laser device. 3500234* US, 1966.

24. **Kindl, H and Westemeier, H.** *Gas Laser. 3826998* US, 1976.

25. **Knowles, KH.** *Laser components and fabrication method. 3978425* US, 1976.

26. **Van den Brink, HG.** *A method of adjusting gas laser mirror. 4217559* US, 1980.

27. **Conover, Steven, Murdza, Randal and Stern, Margaret.** *Optical component installation and train alignment process utilizing metrology and plastic deformation. 7124928* US.

28. **Heyler, R.** Package design considerations for automated assembly. [Online] www.newport.com/support/magazine_features/fpn01.asp.

29. **Shimaoka, M, et al.** *Optical coupling apparatus and manufacturing of the same and lens holder. 5195155* US, 1993.

30. **Verviell, J.** *Optical electronic assembly having a flexure for maintaining alignment between optical elements. 6207950B1* US, 2001.

31. **Masghati, M and Racz, LM.** *Re-entrant alignment features for optical components. US2002/0048446A1* US, 2002.

32. **Pan, J, et al.** *Fiber optic support clip. 5619609* US, 1997.

33. **Verviell, J.** *Opto-electronic assembly and method of making the same. 5977567* US, 1999.

34. **Jang, S and Heyler, R.** *Process for detecting and correcting a misalignment between a fiber cable and a light source within a fiber module. 6184987* US, 2001.

35. **Katagiri, T, Tachikura, M and Murakami, Y.** *Basic design for a stable fiber clamping in multi-fiber ribbon mechanical splice.* August 2001, IEICE Transactions of Communication, Vols. E84-B, pp. 2161-2196.

36.**Culpepper, ML, Slocum, AH and Shaikh, FZ.** *Quasi-kinematic couplings for low-cost precision alignment of high-volume assemblies.* Journal of Mechanical Design, Vol. 126(4), pp. 456-463.

37. **Culpepper, ML.** *Design of Quasi-Kinematic Couplings.*3, July 2004, Journal of Precision Engineering, Vol. 28, pp. 338-357.

38. **Chiu, Michael A.** *Roadmap of mechanical systems design for the semiconductor auto equipment industry.* Department of Mechanical Engineering, Massachusetts Institute of Technology. 1998.

39. **Hale, Layton.** *Adjustable link for kinematic mounting systems. 5642956* US, 1997.

40. [Online] http://www.astro.virginia.edu/class/skrutskie/images/light_em_spectrum.jpg.

41. **Harris, Corey.** *Design of a Shim for a Nanopositioner.* Department of Mechanical Engineering, Massachusetts Institute of Technology. 2010.

APPENDIX

A

KC DESIGN SPREADSHEET

The following pages include the spreadsheet used to optimize the kinematic coupling design and to calculate the contact forces, contact stresses, deflections at the contact points, and the error motions of any kinematic coupling. The user inputs the ball diameters, groove radii of curvature, contact point locations, contact force directions, preload force locations and magnitudes, applied force locations and magnitudes, and material properties.

Kinematic Coupling Design Spreadsheet

Authors:	Adrienne Wykol and Martin Culpepper
Created:	12/11/2009
Last updated:	01/06/2010
Version:	5
Instructions:	Only change cells in BLUE. Do not change cells in RED

Ball 1		
Minor Radius	0.0011	m
	0.0415	in
Major Radius	0.0011	m
	0.0415	in
Material Properties		
Yield Stress	1000000000	Pa
	145040	psi
Elastic Modulus	210000000000	Pa
	30457925	psi
Poisson Ratio	0.300	---
Position		
x	0.0000	m
	0.0000	in
y	0.0377	m
	1.4835	in
z	0.0000	m
	0.0000	in
Distance From Coupling Centroid		
$\|r_{b1}\|$	0.0377235	m

Ball 2		
Minor Radius	0.0011	m
	0.0415	in
Major Radius	0.0011	m
	0.0415	in
Material Properties		
Yield Stress	1000000000	Pa
	145040	psi
Elastic Modulus	210000000000	Pa
	30457925	psi
Poisson Ratio	0.300	---
Position		
x	-0.0500	m
	-1.9685	in
y	-0.0289	m
	-1.1365	in
z	0.0000	m
	0.0000	in
Distance From Coupling Centroid		
$\|r_{b2}\|$	0.0577235	m

Ball 3		
Minor Radius	0.0011	m
	0.0415	in
Major Radius	0.0011	m
	0.0415	in
Material Properties		
Yield Stress	1000000000	Pa
	145040	psi
Elastic Modulus	210000000000	Pa
	30457925	psi
Poisson Ratio	0.300	---
Position		
x	0.0500	m
	1.9685	in
y	-0.0289	m
	-1.1365	in
z	0.0000	m
	0.0000	in
Distance From Coupling Centroid		
$\|r_{b3}\|$	0.0577235	m

Groove 1		
Minor Radius	1.00E+98	m
	3.94E+99	in
Major Radius	1.00E+98	m
	3.94E+99	in
Half Angle	45.0	
	0.785	rad
	0.785	rad
Material Properties		
Tensile Yield Stress	1380000000	Pa
	200152	psi
Shear Yield Stress	796800000	Pa
	115578	psi
Elastic Modulus	200000000000	Pa
	29007548	psi
Poisson Ratio	0.248	---
Orientation Angle		
θ_{g1}	1.571	radians
	90.0	degrees
Contact Points		
A_{g1}	0.0000	m
A_{g1}	0.0377	m
A_{g1}	-0.0000	m
B_{g1}	-0.0000	m
B_{g1}	0.0377	m
B_{g1}	0.0000	m

Groove 2		
Minor Radius	1.00E+98	m
	3.94E+99	in
Major Radius	1.00E+98	m
	3.94E+99	in
Half Angle	45.0	
	0.785	deg
	0.785	rad
Material Properties		
Tensile Yield Stress	1380000000	Pa
	200152	psi
Shear Yield Stress	796800000	Pa
	115578	psi
Elastic Modulus	200000000000	Pa
	29007548	psi
Poisson Ratio	0.248	---
Orientation Angle		
θ_{g2}	3.665	radians
	210.0	degrees
Contact Points		
A_{g2}	0.0500	m
A_{g2}	0.0289	m
A_{g2}	-0.0000	m
B_{g2}	0.0000	m
B_{g2}	0.0289	m
B_{g2}	0.0000	m

Groove 3		
Minor Radius	1.00E+98	m
	3.94E+99	in
Major Radius	1.00E+98	m
	3.94E+99	in
Half Angle	45.0	
	0.785	deg
	0.785	rad
Material Properties		
Tensile Yield Stress	1380000000	Pa
	200152	psi
Shear Yield Stress	796800000	Pa
	115578	psi
Elastic Modulus	200000000000	Pa
	29007548	psi
Poisson Ratio	0.248	---
Orientation Angle		
θ_{g3}	5.760	radians
	330.0	degrees
Contact Points		
A_{g3}	0.0500	m
A_{g3}	-0.0289	m
A_{g3}	-0.0000	m
B_{g3}	0.0433	m
B_{g3}	-0.0250	m
B_{g3}	0.0000	m

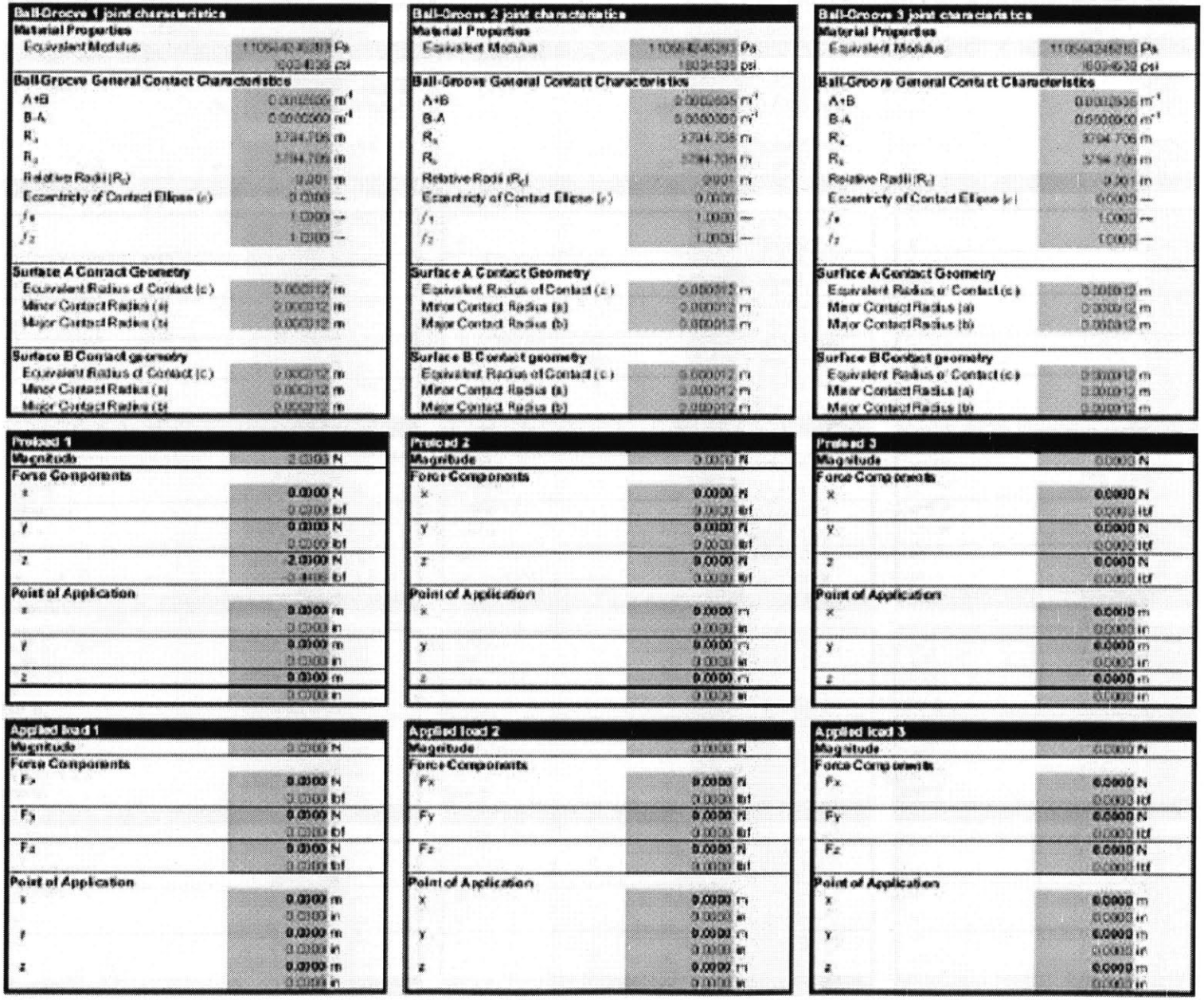

Ball-Groove 1 joint characteristics		
Material Properties		
Equivalent Modulus	1.10564E+11	Pa
	16034539	psi
Ball Groove General Contact Characteristics		
A+B	0.0002500	m^{-1}
B-A	0.0000000	m^{-1}
R_x	3794.706	m
R_y	3794.706	m
Relative Radii (R_r)	0.001	m
Eccentricity of Contact Ellipse (ε)	0.0000	--
f_1	1.0000	--
f_2	1.0000	--
Surface A Contact Geometry		
Equivalent Radius of Contact (c)	0.000312	m
Minor Contact Radius (a)	0.000312	m
Major Contact Radius (b)	0.000312	m
Surface B Contact geometry		
Equivalent Radius of Contact (c)	0.000312	m
Minor Contact Radius (a)	0.000312	m
Major Contact Radius (b)	0.000312	m

Ball-Groove 2 joint characteristics		
Material Properties		
Equivalent Modulus	1.10564E+11	Pa
	16034539	psi
Ball-Groove General Contact Characteristics		
A+B	0.0002500	m^{-1}
B-A	0.0000000	m^{-1}
R_x	3794.706	m
R_y	3794.706	m
Relative Radii (R_r)	0.001	m
Eccentricity of Contact Ellipse (ε)	0.0000	--
f_1	1.0000	--
f_2	1.0000	--
Surface A Contact Geometry		
Equivalent Radius of Contact (c)	0.000312	m
Minor Contact Radius (a)	0.000312	m
Major Contact Radius (b)	0.000312	m
Surface B Contact geometry		
Equivalent Radius of Contact (c)	0.000312	m
Minor Contact Radius (a)	0.000312	m
Major Contact Radius (b)	0.000312	m

Ball-Groove 3 joint characteristics		
Material Properties		
Equivalent Modulus	1.10564E+11	Pa
	16034539	psi
Ball-Groove General Contact Characteristics		
A+B	0.0002500	m^{-1}
B-A	0.0000000	m^{-1}
R_x	3794.706	m
R_y	3794.706	m
Relative Radii (R_r)	0.001	m
Eccentricity of Contact Ellipse (ε)	0.0000	--
f_1	1.0000	--
f_2	1.0000	--
Surface A Contact Geometry		
Equivalent Radius of Contact (c)	0.000312	m
Minor Contact Radius (a)	0.000312	m
Major Contact Radius (b)	0.000312	m
Surface B Contact geometry		
Equivalent Radius of Contact (c)	0.000312	m
Minor Contact Radius (a)	0.000312	m
Major Contact Radius (b)	0.000312	m

Preload 1		
Magnitude	2.0000	N
Force Components		
x	0.0000	N
	0.0000	lbf
y	0.0000	N
	0.0000	lbf
z	2.0000	N
	0.4496	lbf
Point of Application		
x	0.0000	m
	0.0000	in
y	0.0000	m
	0.0000	in
z	0.0000	m
	0.0000	in

Preload 2		
Magnitude	0.0000	N
Force Components		
x	0.0000	N
	0.0000	lbf
y	0.0000	N
	0.0000	lbf
z	0.0000	N
	0.0000	lbf
Point of Application		
x	0.0000	m
	0.0000	in
y	0.0000	m
	0.0000	in
z	0.0000	m
	0.0000	in

Preload 3		
Magnitude	0.0000	N
Force Components		
x	0.0000	N
	0.0000	lbf
y	0.0000	N
	0.0000	lbf
z	0.0000	N
	0.0000	lbf
Point of Application		
x	0.0000	m
	0.0000	in
y	0.0000	m
	0.0000	in
z	0.0000	m
	0.0000	in

Applied load 1		
Magnitude	0.0000	N
Force Components		
F_x	0.0000	N
	0.0000	lbf
F_y	0.0000	N
	0.0000	lbf
F_z	0.0000	N
	0.0000	lbf
Point of Application		
x	0.0000	m
	0.0000	in
y	0.0000	m
	0.0000	in
z	0.0000	m
	0.0000	in

Applied load 2		
Magnitude	0.0000	N
Force Components		
Fx	0.0000	N
	0.0000	lbf
Fy	0.0000	N
	0.0000	lbf
Fz	0.0000	N
	0.0000	lbf
Point of Application		
x	0.0000	m
	0.0000	in
y	0.0000	m
	0.0000	in
z	0.0000	m
	0.0000	in

Applied load 3		
Magnitude	0.0000	N
Force Components		
Fx	0.0000	N
	0.0000	lbf
Fy	0.0000	N
	0.0000	lbf
Fz	0.0000	N
	0.0000	lbf
Point of Application		
x	0.0000	m
	0.0000	in
Y	0.0000	m
	0.0000	in
z	0.0000	m
	0.0000	in

Direction Angle Cosines		
α_1	-0.7071	---
α_2	0.7071	---
β_1	0.0000	---
β_2	0.0000	---
γ_1	0.7071	---
γ_2	0.7071	---

Direction Angle Cosines		
α_3	0.3536	---
α_4	-0.3536	---
β_3	-0.6124	---
β_4	0.6124	---
γ_3	0.7071	---
γ_4	0.7071	---

Direction Angle Cosines		
α_5	0.3536	---
α_6	-0.3536	---
β_5	0.6124	---
β_6	-0.6124	---
γ_5	0.7071	---
γ_6	0.7071	---

Groove 1 Contact Forces		
Side A	0.4714	N
F_{1Ax}	-0.3333	N
F_{1Ay}	0.0000	N
F_{1Az}	0.3333	N
Side B	0.4714	N
F_{1Bx}	0.3333	N
F_{1By}	0.0000	N
F_{1Bz}	0.3333	N

Groove 2 Contact Forces		
Side A	0.4714	N
F_{2Ax}	0.1667	N
F_{2Ay}	-0.2887	N
F_{2Az}	0.3333	N
Side B	0.4714	N
F_{2Bx}	-0.1667	N
F_{2By}	0.2887	N
F_{2Bz}	0.3333	N

Groove 3 Contact Forces		
Side A	0.4714	N
F_{3Ax}	0.1667	N
$F3_{Ay}$	0.2887	N
F_{3Az}	0.3333	N
Side B	0.4714	N
F_{3Bx}	-0.1667	N
F_{3By}	-0.2887	N
F_{3Bz}	0.3333	N

Groove 1 Contact Stresses		
σ_A	1589211591	Pa
σ_B	1589211591	Pa
$\tau_{max\text{-}A}$	492655593	Pa
$\tau_{max\text{-}B}$	492655593	Pa
$Z_{max\text{-}1A}$	0.000006	m
$Z_{max\text{-}1B}$	0.000006	m

Groove 2 Contact Stresses		
σ_A	1589206864	Pa
σ_B	1589206864	Pa
$\tau_{max\text{-}2A}$	492654128	Pa
$\tau_{max\text{-}2B}$	492654128	Pa
$Z_{max\text{-}2A}$	0.000006	m
$Z_{max\text{-}2B}$	0.000006	m

Groove 3 Contact Stresses		
σ_A	1589206864	Pa
σ_B	1589206864	Pa
$\tau_{max\text{-}3A}$	492654128	Pa
$\tau_{max\text{-}3B}$	492654128	Pa
$Z_{max\text{-}3A}$	0.000006	m
$Z_{max\text{-}3B}$	0.000006	m

Joint 1 Ball Center Displacements		
δ_{1A}	0.000000	m
	0.269	µm
δ_{1B}	0.000000	m
	0.269	µm
δ_{1C}	0.000	m
	0.000	µm
δ_{1A}	0.000000	m
	0.000	µm
δ_{1Z}	0.000000	m
	-0.380	µm

Joint 2 Ball Center Displacements		
δ_{2A}	0.000000	m
	0.269	µm
δ_{2B}	0.000000	m
	0.269	µm
δ_{2C}	0.000	m
	0.000	µm
δ_{2A}	0.000000	m
	0.000	µm
δ_{2Z}	0.000000	m
	-0.380	µm

Joint 3 Ball Center Displacements		
δ_{3A}	0.000000	m
	0.269	µm
δ_{3B}	0.000000	m
	0.269	µm
δ_{3C}	0.000	m
	0.000	µm
δ_{3A}	0.000000	m
	0.000	µm
δ_{3Z}	0.000000	m
	-0.380	µm

Global Coupling Displacements, including Preload-induced Displacements					
Xo	0.000000	m	Yo	0.000000	m	Zo	0.000000	m
	0.000	µm		0.000	µm		-0.380	µm
θ_x	0.000000	radians	θ_y	0.000000	radians	θ_z	0.000000	radians
	0.000	µradians		0.000	µradians		0.000	µradians

Stiffness Calculation					
Incremental applied load	0.000	N	Incremental displacement	0.000001000	m	Stiffness	0.00E+00	N/m
							0.00	N/µm

WARNINGS - IF ANY CHECKS SAY 'NO' THERE IS A PROBLEM WITH DESIGN/USE		
Are all contact stresses OK?		FOS
τ_{max-1A}	YES	1.62
τ_{max-1B}	YES	1.62
τ_{max-2A}	YES	1.62
τ_{max-2B}	YES	1.62
τ_{max-3A}	YES	1.62
τ_{max-3B}	YES	1.62
Are all the contact forces positive?		
F_{1A}	YES	
F_{1B}	YES	
F_{2A}	YES	
F_{2B}	YES	
F_{3A}	YES	
F_{3B}	YES	
Are the balls in the correct relative location?		
Is ball 2 to the left of ball 1 (smaller x value)	YES	
Is ball 3 to the right of ball 1 (higher x value)	YES	

Nomenclature--INFORMATION ONLY

Title:	**Definition of Geometry and Contact Point Locations**
By:	Martin Culpepper
Created:	01/05/2010
Last update:	01/05/2010
Revison:	1

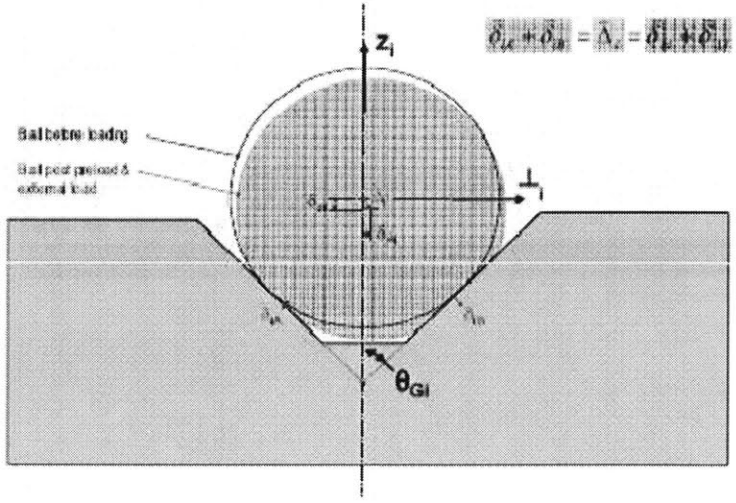

$$\delta_{i,e} + \delta_{i,0} = \Lambda_i = \delta_{i,L} + \delta_{i,U}$$

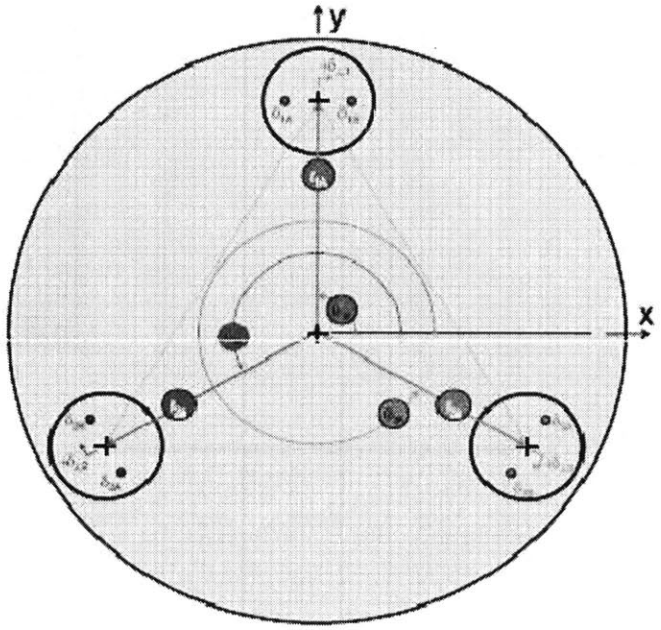

APPENDIX

B

FORCE AND DISPLACEMENT SOLUTIONS

The following pages contain the solvers used to calculate the contact forces and displacements in the KC design spreadsheet.

Solver sheet for kinematic coupling contact forces

DO NOT CHANGE ANY CELLS ON THIS SPREAD SHEET

Title: Solver sheet for kinematic coupling contact forces
By: Martin Culpepper
Created: 12/22/09
Last update: 12/23/09
Revision: 2

Matrices have been given variable names as follows:

A_{force}: Matrix that relates contact forces to applied and preload forces
B_{force}: Vector that contains force elements due to applied and contact forces
A_{force_inv}: Inverse of A_{force}
X_{force}: Contact force vector

Given system of linear equations

A_{force}							X_{force}		B_{force}	
0.707107	-0.707107	-0.353557	0.353557	-0.353557	0.353557		F_1A		0.000000	N
0.000000	0.000000	0.612371	0.612371	0.612371	0.612371		F_1B		0.000000	N
0.707107	0.707107	0.707107	0.707107	0.707107	0.707107	*	F_2A	=	2.000000	N
0.040825	0.040825	-0.020413	-0.020413	-0.020413	-0.020413		F_2B		0.000000	N-m
0.000000	0.000000	0.035355	0.035355	-0.035355	-0.035355		F_3A		0.000000	N-m
-0.040825	0.040825	-0.040825	0.040825	-0.040825	0.040825		F_3B		0.000000	N-m

Define array variables A_{force}, B_{force} and X_{force}

Calculate A_{force}^{-1} → Selected 6X6 cells and entered "=MINVERSE(A_{force})" followed by CTRL-SHIFT-ENTER

A_{force}^{-1}					
0.471403	0.000000	0.235704	8.164917	0.000000	-4.082495
-0.471403	0.000000	0.235704	0.164917	0.000000	4.082495
0.235702	0.408250	0.235702	4.082459	7.071068	4.082459
0.235702	-0.408250	0.235702	-4.082459	7.071068	4.082459
-0.235702	-0.408250	0.235702	-4.082459	-7.071068	-4.082459
0.235702	0.408250	0.235702	-4.082459	-7.071068	4.082459

Solve for X_{force} → Selected 6x1 cells and entered "=MMULT(A_{disp_inv})" followed by CTRL-SHIFT-ENTER

$A_{force}^{-1} * B_{force}$		
F_1A =	0.4714	N
F_1B =	0.4714	N
F_2A =	0.4714	N
F_2B =	0.4714	N
F_3A =	0.4714	N
F_3B =	0.4714	N

DO NOT CHANGE ANY CELLS ON THIS SPREAD SHEET

Title:	Solver sheet for kinematic coupling centroid displacements and required ball motions along grooves
By:	Martin Culpepper
Created:	12/23/09
Last update:	12/23/09
Revision:	2

Matrices have been given variable names as follows:

$A_{in\_plane\_disp}$	Matrix that relates ball center displacements to coupling centroid displacements
$B_{in\_plane\_disp}$	Vector that contains displacements due to ball center displacements
$A_{inv\_in\_plane\_disp}$	Inverse of $A_{in\_plane\_disp}$
$X_{in\_plane\_disp}$	Displacement vector containing in-plane displacements and ball displacements along grooves

Given system of linear equations:

$A_{in\_plane\_disp}$					
1.000000	0.000000	-0.057735	0.000000	0.000000	0.000000
0.000000	-1.000000	0.000000	1.000000	0.000000	0.000000
1.000000	0.000000	0.028868	0.000000	0.866023	0.000000
0.000000	-1.000000	0.050000	0.000000	-0.500004	0.000000
1.000000	0.000000	0.028868	0.000000	0.000000	-0.866023
0.000000	-1.000000	-0.050000	0.000000	0.000000	-0.500004

·

$X_{in\_plane\_disp}$
X_e
Y_e
qz_e
D_r1a
D_r2a
D_r3a

=

$B_{in\_plane\_disp}$	
0.000000	m
0.000000	m
0.000000	radians
0.000000	m
0.000000	m
0.000000	m

=

$B_{in\_plane\_disp}$	
0.000	µm
0.000	µm
0.000	µradians
0.000	µm
0.000	µm
0.000	µm

Define array variables $A_{in\_plane\_disp}$, $B_{in\_plane\_disp}$ and $X_{in\_plane\_disp}$

Calculate $A_{in\_plane\_disp}^{-1}$ --- Selected 6X6 cells and entered "=MINVERSE(Ain_plane_disp)" followed by CTRL-SHIFT-ENTER

$A_{in\_plane\_disp}^{-1}$					
0.666665	0.000000	0.166668	0.288673	0.166668	-0.288673
0.000000	0.000000	-0.288679	-0.500000	0.288679	-0.500000
-5.773520	0.000000	2.886760	4.999955	2.886760	-4.999955
0.000000	1.000000	-0.288679	-0.500000	0.288679	-0.500000
-0.577347	0.000000	0.866025	-0.500000	-0.288679	0.500000
0.577347	0.000000	0.288679	0.500000	-0.866025	-0.500000

Sove for $X_{in\_plane\_disp}$ --- Select 6x1 cells and enter"=MMULT(A_inv_in_plane_disp,B_in_plane_disp)", followed by CTRL-SHIFT-ENTER

$A_{in\_plane\_disp}^{-1} * B_{in\_plane\_disp}$		
X_e	0.000000000	m
Y_e	0.000000000	m
qz_e	0.000000000	radians
D_r1a	0.000000000	m
D_r2a	0.000000000	m
D_r3a	0.000000000	m

=

$A_{in\_plane\_disp}^{-1} * B_{in\_plane\_disp}$	
0.000000	µm
0.000000	µm
0.000000	µradians
0.000000	µm
0.000000	µm
0.000000	µm

APPENDIX

C

HERTZIAN CONTACT STRESS ANALYSIS

The following pages contain the equations used for the Hertzian contact stress analysis done for the kinematic couplings designed in this thesis. The pages were taken from pages 419-421 of Layton Hale's Ph.D. thesis, entitled *Principles and Techniques for Designing Precision Machines* (12).

C.2 Elliptical Contact

An elliptical contact area forms when two three-dimensional bodies, each described locally with orthogonal radii of curvature, come into contact. In addition, the orthogonal coordinate system of one body may be rotated relative to the other by an arbitrary angle α. Any radius may be positive (convex) or negative (concave) so long as all three relative radii (C.9) are positive. To first order. R_c represents an equivalent sphere in contact with a plane, while R_a and R_b represent an equivalent toroid in contact with a plane. The contact modulus remains unchanged from circular contact (C.1). Quite different sets of contacting surfaces behave identically if they have identical contact modulii and relative radii.

Relative Radii $$R_c = \sqrt{R_a R_b} \tag{C.9}$$

$$R_a = \frac{1}{(A+B)-(B-A)} \qquad R_b = \frac{1}{(A+B)+(B-A)}$$

$$A+B = \frac{1}{2}\left(\frac{1}{R_{1xx}}+\frac{1}{R_{1yy}}+\frac{1}{R_{2xx}}+\frac{1}{R_{2yy}}\right)$$

$$B-A = \frac{1}{2}\left\{\left(\frac{1}{R_{1xx}}-\frac{1}{R_{1yy}}\right)^2+\left(\frac{1}{R_{2xx}}-\frac{1}{R_{2yy}}\right)^2 \cdots \right.$$

$$\left. +2\left(\frac{1}{R_{1xx}}-\frac{1}{R_{1yy}}\right)\left(\frac{1}{R_{2xx}}-\frac{1}{R_{2yy}}\right)\cos(2\alpha)\right\}^{\frac{1}{2}}$$

The approximate expression for the eccentricity of the contact ellipse (C.10) is sufficient for practical geometries; however, the full solution is implemented in Section C.6. The radius of an equivalent circular contact (C.11) contains a correction factor F_1 that gradually decreases from one as the contact becomes more elliptical. The major and minor radii of the contact ellipse (C.12) follow from the eccentricity and the equivalent radius. The maximum pressure (C.13) differs from circular contact only in that the pressure profile is semiellipsoidal going to zero of course at the edge of the contact ellipse. The maximum shear stress and depth below the surface (C.14) are very similar to circular contact. The equations provided are curve fits to Table 4.1 in [Johnson, 1985]. The radially oriented tensile stress at the major and minor contact radii (C.15) becomes increasingly different from one another (and the tensile stress for circular contact) as the contact becomes more elliptical. The tensile stress at the major radius σ_a is maximum.

Eccentricity of Contact Ellipse

$$e^2 = 1 - \left(\frac{b}{a}\right)^2 \cong 1 - \left(\frac{R_b}{R_a}\right)^{\frac{4}{3}} \tag{C.10}$$

Equivalent Radius of Contact

$$c = \sqrt{ab} = \left(\frac{3PR_c}{4E_c}\right)^{\frac{1}{3}} F_1 \tag{C.11}$$

Major and Minor Contact Radii

$$a = c\left(1 - e^2\right)^{-1/4} \qquad b = c\left(1 - e^2\right)^{1/4} \tag{C.12}$$

Maximum Pressure

$$p = \frac{3P}{2\pi c^2} = \frac{3P}{2\pi ab} \tag{C.13}$$

Maximum Shear Stress

$$\tau \cong p\left\{0.303 + 0.0855\frac{b}{a} - 0.808\left(\frac{b}{a}\right)^2\right\} \qquad z \cong b\left\{0.7929 - 0.3207\frac{b}{a}\right\} \tag{C.14}$$

Tensile Stress at a and b

$$\sigma_a = p(1-2\nu)\frac{b}{ae^2}\left\{\frac{1}{e}\tanh^{-1}(e) - 1\right\} \qquad \sigma_b = p(1-2\nu)\frac{b}{ae^2}\left\{1 - \frac{b}{ae^2}\tan^{-1}\left(\frac{ea}{b}\right)\right\} \tag{C.15}$$

The normal displacement (C.16) and the normal stiffness (C.17) differ from circular contact only by the correction factors F_1 and F_2. Equation C.18 provides curve fits to the exact values as calculated in Section C.6.

Normal Displacement

$$\delta = \frac{c^2}{R_c}\frac{F_2}{F_1^2} = \frac{ab}{R_c}\frac{F_2}{F_1^2} \tag{C.16}$$

Normal Stiffness

$$k = \frac{2E_c c}{F_1 F_2} \tag{C.17}$$

$$F_1 \approx 1 - \left|\left(\frac{R_a}{R_b}\right)^{0.0602} - 1\right|^{1.456} \qquad F_2 \approx 1 - \left|\left(\frac{R_a}{R_b}\right)^{0.0684} - 1\right|^{1.531} \tag{C.18}$$

APPENDIX

D

DYMAX OP-4-20632 SERIES UV ADHESIVE DATA SHEET

The following pages contain the product data sheet for the selected adhesive for use with the fixture designed for NanoInk's DPN 5000 machine. The selected adhesive is an acrylate urethane adhesive from the Dymax fiber optical assembly OP-4-20632 series.

DYMAX CORPORATION

PRODUCT DATA SHEET

15 May 2006

HIGH T_g LIGHT PATH ADHESIVES
Fiber Optical Assembly
OP-4-20632 SERIES

INTRODUCTION

DYMAX high performance optical adhesives cure upon exposure to UV light in seconds and are designed to increase productivity, lower assembly cost and enhance worker safety. These results were obtained using very high speed DYMAX spot, beam and flood lamps. DYMAX lamps deliver optimum speed and performance for a variety of optical applications.

DESCRIPTION

Ultra Light-Weld® OP-4-20632 Series are clear, UV-curable adhesives designed for durable bonding of fiber optic couplings. OP-4-20632 Series were designed for maximum resistance to yellowing and maintain its dimensions when thermally cycled. OP-4-20632 Series have high bond strength to optical glass and most metals. Although the product fully cures in seconds upon UV or visible light exposure, heating the UV cured product to 150°C for 1 hour will increase the T_g to 100°C and may further improve bond strength.

FEATURES:	• Low Shrinkage UV Cure (<0.2%) With High Optical Clarity 300-1800 nm • High Strength Bond Resists Yellowing • High Glass Transition Temperature (Tg) • Good Thermal Cycling With Minimal Degradation of Optics or Strength
APPLICATIONS:	• Bonding, Fiber Optic Couplings and Prisms

TYPICAL UNCURED PROPERTIES (not specifications)

Solvent Content		None-100% Reactive Solids	
Composition		Acrylate	
Appearance		Optically Clear	
Solubility		Alcohols/Ketones/Chlorinated Solvents	
Toxicity		Low	
Flash Point		Over 93°C (>200°F)	
Refractive Index, n^{25}_D		1.522	ASTM D-1218
Viscosity, (Brookfield, 25°C, 20 rpm)	OP-4-20632	500 cP	ASTM D-1084
	OP-4-20632-GEL	50,000 cP (thixotropic gel)	ASTM D-2556
	OP-4-20632-H	500 cP	ASTM D-2556

TYPICAL CURED PROPERTIES (not specifications)

Linear Shrinkage, after UV cure	0.2%	ASTM D-2566
Refractive Index, n^{25}_D	1.554	ASTM D-1218
Glass Transition, T_g	100°C (UV cure and heat)	ASTM E-831
Glass Transition, T_g	50°C (UV cure without heat)	ASTM E-831
CTE α_1 (below T_g)	45 x 10^{-6} in/in/°C	ASTM E-831
CTE α_2 (above T_g)	110 x 10^{-6} in/in/°C	ASTM E-831
CTE (-50°C to 200°C)	91 x 10^{-6} in/in/°C	ASTM E-831
Durometer Hardness	D75	ASTM D-2240
Tensile at Break	8,900 psi	ASTM D-638
Modulus of Elasticity	800,000 psi	ASTM D-638
Elongation at Break	2%	ASTM D-638
Tensile Compression Shear, glass to glass	2,200 psi (exceeds glass strength)	DSTM D-250*
Thermal Range (brittle/degrades)	-55° to +200°C (-65 to 400°F)	DSTM D-200*
24 hr Water Absorption	1.0 %	ASTM D-570
2 hr Boiling Water Absorption	1.2%	ASTM D-570

*DSTM Refers to DYMAX Standard Test Method

Dymax Corporation - 51 Greenwoods Road - Torrington, CT 06790 - Phone: 860-482-1010 - Fax: 860-496-0608
E-mail: info@dymax.com - www.dymax.com

Dymax Europe GmbH - Trakehner Strasse 3 - D-60487 Frankfurt am Main - Germany - Phone: (49) 69-7165-3568
Fax: (49) 69-7165-3830 - E-mail: dymaxinfo@dymax.de

DYMAX CORPORATION

PRODUCT DATA SHEET

OP-4-20632 Series, 5/15/06

CURE DATA

Lamp	DYMAX® 2000-EC	DYMAX® 5000-EC	DYMAX® Bond Box	DYMAX® Blue Wave 50	ADAC 50
Light Type Lamp Type	UV/Visible 8" x 8" Flood	UV/Visible 5" x 5" Flood	UV/Visible 8" Rotating stage	UV/Visible 3/16" Spot	UV/Visible 3/16" Spot
Maximum Lamp Intensity @ 365 nm Intensity @ time of test @ 365 nm	50 mW/cm^2 20 mW/cm^2	300 mW/cm^2 150 mW/cm^2	150 mW/cm^2 50 mW/cm^2	4,000 mW/cm^2 2,500 mW/cm^2	4,000 mW/cm^2 2,500 mW/cm^2
Adhesive Absorption Range (nm) Equipment Output Range (nm)	300-400 300-500	300-400 300-500	300-400 300-500	300-400 300-500	300-400 300-500
Typical Cure speed (seconds) Fixture between glass slides Tack-free surface cure 1/16-inch bead	 1 1 3	 1 1 3	 1 1 3	 1 1 3	 1 1 3

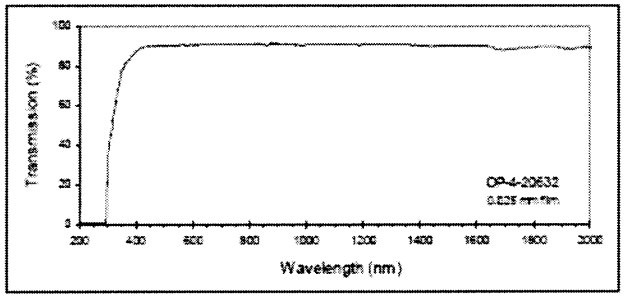

STORAGE & SHELF LIFE

Store material in a cool, dark place when not in use. Do not expose to UV light or sunlight. Material may polymerize upon prolonged exposure to ambient light. Product has a one-year shelf life when stored below 90°F in the original, unopened container.

DISPENSING & HANDLING ADHESIVE

DYMAX OP-4-20632 Series adhesives are available in 3-mL, 5-mL, 10-mL and 30-mL manual or machine ready syringes and 170-mL cartridges. Machine ready syringes may be dispensed from a variety of automatic bench-top syringe applicators or other equipment as required. Any questions relating to dispensing and curing systems for specific applications should be referred to the DYMAX Technical Center at (860) 482-1010.

SAFETY

Wear impervious gloves and/or barrier cream. Repeated or continuous skin contact with liquid adhesive will cause irritation and should be avoided. Do not wear absorbent gloves. Remove adhesive from skin with soap and water. Never use solvents to remove adhesive from skin or eyes.

CAUTION

For industrial use only. Avoid breathing vapors. Avoid contact with eyes and clothing. In case of contact, immediately flush with water for at least 15 minutes; for eyes, get medical attention. Wash clothing before reuse. Keep out of reach of children. Do not take internally. If swallowed, vomiting should be induced at once and a physician called. For specific information, refer to the Material Safety Data Sheet before use.

Dymax Corporation - 51 Greenwoods Road - Torrington, CT 06790 - Phone: 860-482-1010 - Fax: 860-496-0608
E-mail: info@dymax.com - www.dymax.com

Dymax Europe GmbH - Trakehner Strasse 3 - D-60487 Frankfurt am Main - Germany - Phone: (49) 69-7165-3568
Fax: (49) 69-7165-3830 - E-mail: dymaxinfo@dymax.de

APPENDIX

E

DPN 5000 SYSTEM DATA SHEET

The following pages contain the product data sheet for the DPN 5000 system made by NanoInk.

nanoINK
NanoFabrication Systems

DPN 5000 System

Desktop NanoFabrication System

NanoInk has developed the DPN 5000 System to have the standard controls and tools for all tip-based nanofabrication applications, while maintaining compatibility with a wide range of applications.

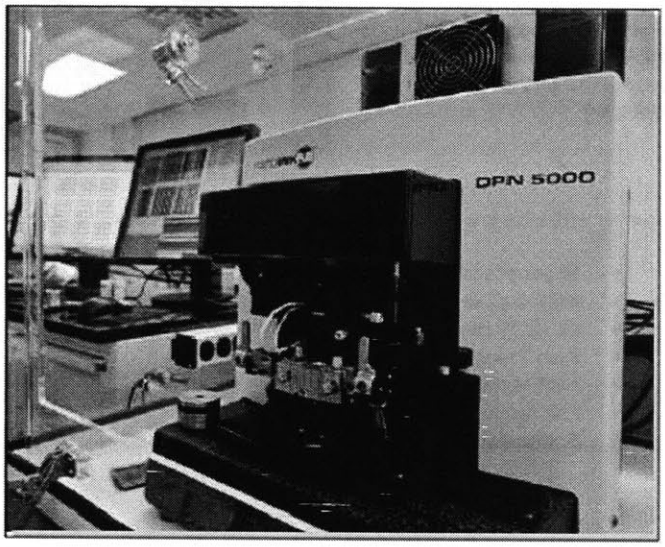

Standard features include:

- Custom DPN® Scanner
- InkCAD™ Version 4.0 Software
- Ultra-Low Noise LFM & AFM Imaging
- New DPN Stage & Optics
- Linux® DPN Controller
- E-Chamber Controller

The DPN 5000 System supports all of the following options:

- Customized Ink Library Option
- 2D nano PrintArray™ Kit
- Active Pen™ Array Kit
- AFM Imaging Modes
- Applications Support Package
- Extended Service Package

DPN 5000 System

NanoInk Inc.
NanoFabrication Systems

Custom DPN Scanner

NanoInk designed a custom scanner for DPN which allows for compatibility with a wide range of cantilever geometries, reflectivities, and ink coatings. Relevant features include:

- Compatible with NanoInk 1D & 2D pen arrays and ink protocols
- Sum signal switch for photo-detector adjustment, allowing maximum ink versatility and patterning control
- Extended laser and photo-detector working range to accommodate multiple cantilever array geometries
- Adjustable laser focus up to 2 mm for precise focal placement (advanced user)

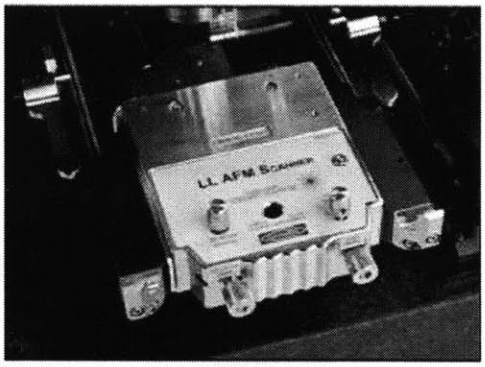

A new, closed loop flexure scanner with ultra-low noise inductive sensors allows for positional precision and accuracy.

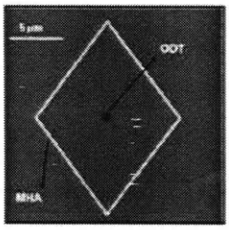

- 90 µm XY scan range with better than 0.5% linearity
- XYZ inductive calibration sensors resolution ~ 1 nm
- XY, XZ, YZ crosstalk < 1%
- 8 µm Z range
- Z out of plane motion +/- 30 nm over 90 microns
- Z bit resolution < 0.001 nm
- Z-noise 0.06 nm (in optimal vibration conditions)

Advanced LFM Imaging

NanoInk has specifically designed the DPN 5000 scanner to assure high quality lateral force microscopy (LFM) imaging for immediate detection of DPN patterned substrates. Relevant features include:

- A low coherence laser with 7 x 20 micron laser spot size
- A flip down mirror to facilitate laser alignment on cantilever

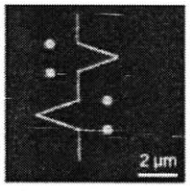

AFM Imaging & Analysis

For those users that need AFM functionality and control, NanoInk provides a research AFM software package (SPM Cockpit) and a comprehensive collection of SPIP™ modules for sophisticated image processing and measurement **all as standard equipment** with the system.

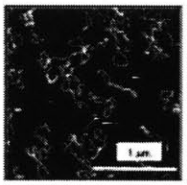

DPN 5000 System

NANOINK INC.
NanoFabrication Systems

InkCAD™ 4.0 Software

NanoInk's InkCAD 4.0 software is the user interface for driving the DPN 5000 system, providing full-featured, industrial-strength functionality. Supporting a true CAD capability, it goes well beyond what commercial AFM lithography packages can offer in terms of tip control. In addition, InkCAD software provides a comprehensive set of tools for tackling all DPN research experiments.

InkCAD 4.0 provides the following capabilities:

- Simple pattern creation routines for easy DPN experiments
- Layered structural hierarchy for sophisticated pattern design, with organizational tools for the individual design elements
- The ability to import and write complex CAD patterns from GDS II format files
- Automated alignment (NanoFind) and linearization routines for better DPN process control
- The ability to calibrate ink diffusion rates and by writing a prescribed pattern, and then use these diffusion rates to control patterned feature sizes

As well as the following **NEW** features:

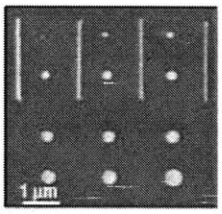

- **Advanced tip control** allowing for shorter dwell times and faster lines speeds, precise layer to layer alignment allows for multi-ink deposition using NanoFind, MicroMap and NanoMap.
- **User Profiles**, allowing the user to define and save all DPN lithography and AFM settings, so multiple users on the same system can save and load their own settings.
- **Advanced CAD capabilities**, including order of lithography previews, easy arrayer, and multi-layer, multi-ink capability.

For a detailed description of InkCAD 4.0 software, please consult the InkCAD data sheet at www.nanoink.net.

DPN 5000 System

DPN Stage

The DPN stage has all the features needed for tip sample leveling and easy tip exchange for rapid ink development experiments.

- Easy tip exchange (1 minute) independent of the sample stage, allowing for rapid ink development and more accurate lithography
- 3 independently adjustable Z motors serve to level the plane of the pen and scanner assembly with the substrate tip 3.5° (Z1 wrt Z2, Z3) and 7° tilt (Z2 wrt Z3, Z1 fixed)
- XY sample stage translator motors: min. 3 micron step size, 1" x 1" travel, max. 2.5 mm/sec slew rate XY stage stationary during tip exchange, allowing for more accurate substrate alignments with different tips
- Solid granite support base, size: 16" x 16" x 14", weight: 122 lbs (loaded)
- Sample holder is grounded, made of stainless steel disks with a central magnetic post
- Maximum sample size: 2" in diameter, < 1.5" thick, and can be attached to a magnetic central post
- Vacuum stage (optional) for holding 2" wafers for large area patterning.

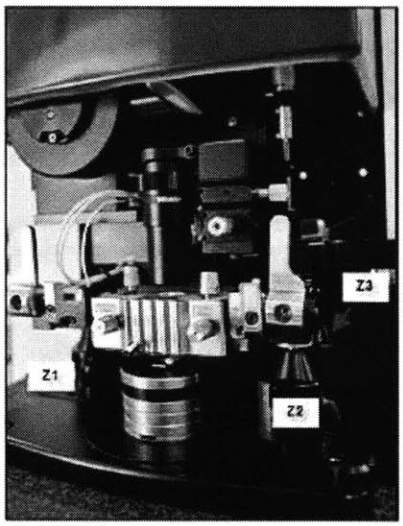

Optics

- Optical Stage registered to and overlaid with AFM images through InkCAD software (MicroMap) for easy relocation of any feature.
- Color CCD video camera with motorized zoom (4X) and focus capability.
- High-quality 10X long working distance (WD = 44 mm) Mitutoyo lens mounted on an adjustable collar that allows panning the field of view over 4 mm of viewable travel.
- Computer controlled focus and zoom.

Video magnification:

	Magnification	FOV
Min Zoom	365X	1050 µm x 820 µm
Max Zoom	1140X	340 µm x 260 µm

DATASHEET

DPN 5000 System

NanoInk 's MEMs, Accessories & Deposition Protocols

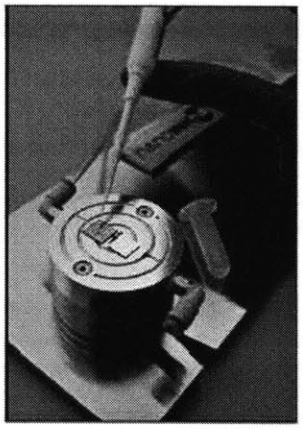

The DPN 5000 System comes complete with all of the tools you need to create nanostructures using DPN, from the simple to the complex. After careful study, NanoInk has developed the DPN 5000 System to have the standard controls and parts common to all tip based nanofabrication applications, while maintaining compatibility with a wide range of applications. As such, NanoInk provides a "Getting Started" kit—everything needed for additional DPN experimentation.

DPN® Getting Started Kit:

- MHA (Mercaptohexadecanoic acid) Pen Kit: Qty. 5 pens and 1 ink vial
- ODT (Octodecane Thiol) Pen Kit: Qty 6 pens and 1 ink vial
- DPN Single Pens: Qty. 20, 10 each of Type A & B
- DPN Passive, Multi-Pen Arrays: Qty. 20, 10 each of Types E & F
- AC Mode Pens: Qty. 10
- Probe Clip & Clip Mounting Block
- Universal Inkwell Array Chips: 1 tray of 10 inkwell chips
- DPN Patterned Sample Substrates: Qty. 16, 8 gold coated and 8 silicon oxide substrates

DPN Passive Pens: Single & Multi-Pen Arrays (standard)

NanoInk's passive single and multi-pen arrays allow for deposition of are produced at NanoInk's own MEMs facility in California. Features include:

- Silicon nitride pens
- Passive multi-pen arrays
- Large-area coverage and/or multi-ink patterning
- Arrays with both writing and reading pens
- A-frame or diving board shaped cantilevers

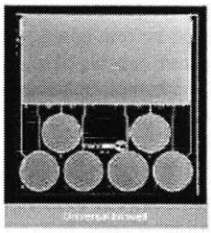

Inkwells (standard)

The Universal Inkwell solution was specifically designed to overcome the problem of delivering a solvent-based ink to one (or several) tips among a pen array without cross contamination.

- With Universal Inkwells, an ink/solvent solution is delivered to one of six inkwell reservoirs via a micropipette.
- Six unique molecular inks are possible on each inkwell chip.
- The ink is then guided through microchannels to the microwell, where the tip will dip and be coated with ink.

For more detailed information on these and other options, please visit www.nanoink.net for a corresponding datasheet.

DATASHEET

DPN 5000 System

NANOINK INC.
NanoFabrication Systems

Every customer has different DPN applications needs. Therefore, the system base price includes 2 of the following customer specified options.

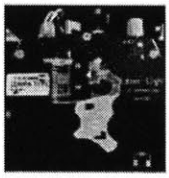

Active Pen™ Array Kit

Using thermal bimorph technology, individual cantilevers can be actuated to enable multi-ink writing without any cross-contamination or unintended surface patterning. Additionally, reader tips can be left clean to image surface patterns, or address specific surface structures without unintentional inking.

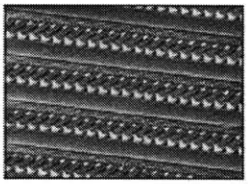

2D nano PrintArray™ Kit

The 2D nano PrintArray Chip provides a high-throughput solution to flexibly pattern nanoscale features. The 2D nano PrintArray retains the direct write, high resolution, ambient deposition, and chemical and material flexible attributes of DPN, while multiplying the desired pattern 55,000 times across a 1 cm^2 area.

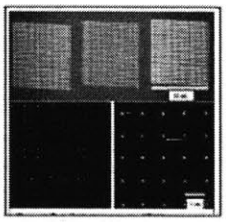

Customized Ink Library Option

This option allows NanoInk's customers access to our library of ink types and protocols. Examples include:

- Just Add DNA™
- Protein Inks
- Polyethylene Glycol Universal Carrier
- Thiols (MHA,ODT, etc.)
- Nanoparticle Inks

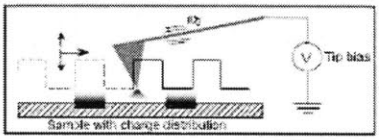

Advanced AFM Modes

An easy plug on bottom board, with fully integrated electronics, makes the DPN 5000 System capable of magnetic force microscopy, electric force microscopy, F-d curves, fluid imaging, and conductive mapping. Imaging and control are fully integrated in the software.

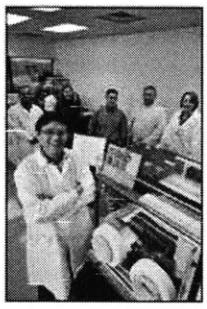

Extended Applications Support Package

NanoInk provides support to its customers with every sale, providing 5 standard training days with each system. Our applications and service team consists PhDs with extensive experience in nanotechnology, surface science, chemistry, and instrumentation. For those needing additional support, NanoInk offers and extended customer support package, up to 3 weeks a year. This is especially useful for large user facilities where there are multiple users with multiple applications.

Extended Service Package

Receive an additional 6 months service and warranty, beyond the standard 1 year warranty.

DPN 5000 System

nanoINK
NanoFabrication Systems

DPN Controller

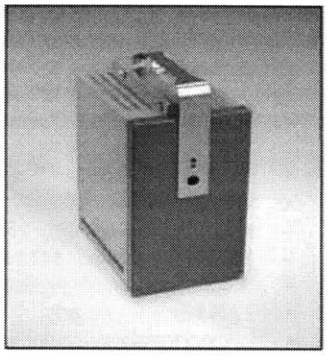

The controller includes all of the circuits required for controlling seven stepper motors as well as the piezoelectric flexure scanner.

- Pentium® IV microprocessor, controller software is written in C++ on a Linux® platform
- TCP/IP communications between controller and workstation
- Reliability is assured with the 16 bit input output cards from National Instruments

XYZ Board Scanner

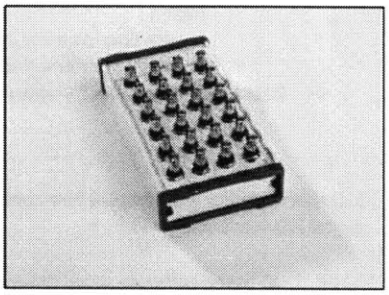

- Digital zoom/offset
- Analog zoom
- Z high voltage
- Z sample/hold
- GPID control
- Phase/amplitude
- XY high voltage
- XY sensor
- Phase/amplitude

Access to all internal controller signals is available through the Signal Access Console, which comes standard with the DPN 5000 System.

Workstation PC Configuration

- Pentium IV or latest equivalent architecture with minimum 3.0 GHz CPU with hyper threading technology for faster processing
- Minimum 1.0 GB RAM, 533 MHz DDR2 2x512
- 16X DVD+/- RW drive 48X/32X/48X
- 80 GB hard drive 8MB with data burst cache
- Dual video display card for dual LCD flat panel display configuration (19" and 19" display).

E-Chamber

NanoInk has integrated an environmental chamber as part of the DPN 5000 System, which controls the environmental conditions during DPN experiments. The chamber houses the entire DPN stage. Temperature and humidity sensors monitor the enclosed environment in real time, and both parameters are controlled by PID feedback loops. The system chamber is driven by a control module that is connected to the user PC. A PC-based software interface runs the E-Chamber from the PC.

- Box material: PolyCast™ cast acrylic with anti-static coating
- Weight: 180 lbs
- Inside dimensions: 28" x 23" x 29"
- Outside dimensions: 34" x 30" x 36"
- Hospital-grade multiple electric outlet strip (mounted on the interior left side)
- 2 gas valves for purging
- Latched front access door and side access door
  - 1 pair of bare-hand entry port conversions on front
  - Continuous stainless steel hinges (mounted on the top)
  - 2 stainless steel fastening clamps on each door access door opening on front is 24" wide x 20" high
  - Access door opening on side is 15" wide x 18" high
  - Specially mounted pressure relief valve (upper left hand side)
- Rear connector panel for easy feed-through of cables to the stage

External humidity and temperature control console, with dual digital PID feedback.

- PC-based software panel drives the power control console, connected via USB
- Inert gas hook-up and nebulizer (required for using the humidity control functions)
- Temperature control uses a 121-watt thermoelectric fan system for convective heating
- Sensor array components:
  - Humidity sensor (with 8' cable)
  - Temperature sensor (with 8' cable)
  - Pressure relief valve
  - Nebulizer on/off switch

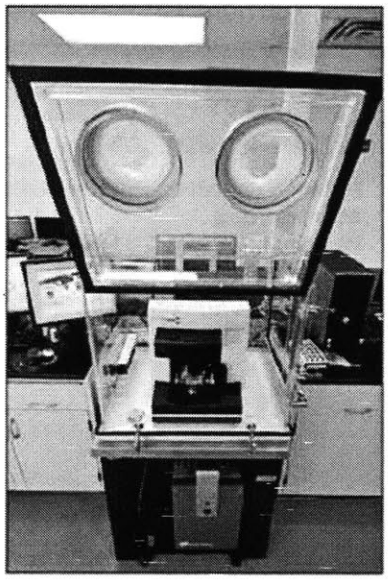

Humidity control performance specifications:

- Humidity range: Min. = 5% Rh, max. = 75% Rh (below dew point)
- Set point stability: ± 0.5 % Rh
- Sensor resolution: ± 2.0 % Rh
- Overshoot amplitude: 0.1 % Rh @ 60 % Rh from a 15% up-ramp
- Humidification ramp rate: 3% Rh/minute
- (> 15 % Rh range using a range > 15% Rh)
- Dehumidification ramp rate: -1% Rh/minute (over 20 % Rh) using an air compressor.

Temperature control performance specifications:

- Temperature range: Min. = 2°C less than room temperature max. = up to 10°C greater than room temperature
- Set point stability: ±0.2 °C (given a stable room temperature)
- Detection resolution: 0.1 °C for full scale
- Overshoot amplitude: 0.5°C
- Heating ramp rate: 0.26°C/minute without DPN stage
- Equilibrated heating ramp rate: 0.07°C/minute with DPN stage in chamber
- Programmability: Software stabilizes temperature to a desired set point

Learn more about NanoInk products and services at www.nanoink.net. Or call us at 847-679-NANO (6266).